

การพัฒนาวัสดุประกอบเต่งจากพอลิเอทิลีนชนิดความหนาแน่นสูงและแคลบ

นายสิริพัฒน์ ชนะกุล

วิทยานิพนธ์นี้เป็นส่วนหนึ่งของการศึกษาตามหลักสูตรปริญญาวิศวกรรมศาสตรมหาบัณฑิต

สาขาวิชาวิศวกรรมเคมี ภาควิชาวิศวกรรมเคมี

คณะวิศวกรรมศาสตร์ จุฬาลงกรณ์มหาวิทยาลัย

ปีการศึกษา 2550

ลิขสิทธิ์ของจุฬาลงกรณ์มหาวิทยาลัย

DEVELOPMENT OF HIGH DENSITY POLYETHYLENE / RICE HUSK
COMPOSITES

Mr. Sirapat Chanakul

A Thesis Submitted in Partial Fulfillment of the Requirements
for the Degree of Master of Engineering Program in Chemical Engineering
Department of Chemical Engineering
Faculty of Engineering
Chulalongkorn University
Academic Year 2007
Copyright of Chulalongkorn University

สิริพัฒน์ ชนะกุล: การพัฒนาวัสดุประกอบแต่งจากพอลิเอทิลีนชนิดความหนาแน่นสูงและ
 แกלב (DEVELOPMENT OF HIGH DENSITY POLYETHYLENE / RICE HUSK
 COMPOSITES) อ. ที่ปรึกษา: อ.ดร.สิริจุฑารัตน์ ไคววาริสารัช, 97 หน้า.

งานวิจัยนี้มีวัตถุประสงค์เพื่อพัฒนาวัสดุประกอบแต่งไม้พลาสติกที่เตรียมจากพอลิเอทิลีนชนิดความ
 หนาแน่นสูง (HDPE) และผงแกלב เพื่อใช้ทดแทนไม้ธรรมชาติ โดยศึกษาอิทธิพลของปริมาณ ขนาดอนุภาค
 แกלבและผลของการใช้สารประสานต่อสมบัติเชิงกล เชิงความร้อน และเชิงกายภาพของวัสดุประกอบแต่งไม้
 พลาสติก การศึกษาแปรปริมาณผงแกלבที่ร้อยละ 10 20 30 และ 40 โดยน้ำหนัก และขนาดอนุภาคของผง
 แกלבที่ขนาด 75 180 250 355 และ 500 ไมครอนตามลำดับ งานวิจัยนี้มีการใช้มาเลอิกแอนไฮไดรด์กราฟท์
 พอลิเอทิลีนเป็นสารประสานที่ความเข้มข้นร้อยละ 1 3 5 และ 7 โดยน้ำหนัก ผลการทดสอบสมบัติเชิงกลพบว่า
 การเพิ่มปริมาณแกלבมากขึ้น มีผลให้ค่ามอดูลัสภายใต้แรงดัดโค้ง แรงดึง และแรงกดของวัสดุประกอบแต่งไม้
 พลาสติกมีค่าเพิ่มขึ้น เนื่องจากแกלבมีความแข็ง และมีค่ามอดูลัสสูงกว่า HDPE ในขณะที่การทนต่อแรงดึง แรง
 ดัดโค้ง แรงกด และการทนต่อแรงกระแทกของวัสดุประกอบแต่งไม้พลาสติกมีค่าลดลง ทั้งนี้เป็นผลมาจากการ
 ยึดติดระหว่างเฟสของ HDPE และผงแกלבยังไม่สม่ำเสมอ มีช่องว่างระหว่างเฟส ส่งผลให้การถ่ายเทแรงที่
 ได้รับจาก HDPE ไปสู่ผงแกלבลดถอยลง ขนาดอนุภาคผงแกלבไม่มีผลต่อสมบัติแรงดึง แรงดัดโค้งและแรงกด
 แต่วัสดุประกอบแต่งไม้พลาสติกที่มีผงแกלבอนุภาคขนาดใหญ่สามารถทนแรงกระแทกได้สูงกว่าไม้พลาสติกที่
 มีผงแกלבอนุภาคขนาดเล็ก การศึกษาสมบัติเชิงความร้อนพบว่า การเพิ่มปริมาณของผงแกלב มีผลให้ค่า
 อุณหภูมิการหลอม และอุณหภูมิการดัดโค้งของวัสดุประกอบแต่งไม้พลาสติกมีค่าเพิ่มขึ้นเล็กน้อย แต่อุณหภูมิ
 การสลายตัวของวัสดุประกอบแต่งไม้พลาสติกลดลง ปริมาณของแข็งที่เหลือจากการเผาไม้พลาสติกมีปริมาณ
 สูงขึ้น ส่วนขนาดของผงแกלבไม่มีผลต่ออุณหภูมิเปลี่ยนสถานะคล้ายแก้ว อุณหภูมิการหลอม อุณหภูมิการดัด
 โค้งและอุณหภูมิการสลายตัวของวัสดุประกอบแต่งไม้พลาสติก การตรวจสอบสมบัติเชิงกายภาพ พบว่าความ
 หนาแน่นและอัตราการดูดซึมน้ำของวัสดุประกอบแต่งไม้พลาสติกมีค่าเพิ่มขึ้นเมื่อใส่ผงแกלבมากขึ้นในไม้
 พลาสติก การดูดซึมน้ำทำให้สีของไม้พลาสติกเข้มขึ้น ขนาดของผงแกלבมีผลต่อลักษณะปรากฏของไม้
 พลาสติกกล่าวคือ ไม้พลาสติกที่มีผงแกלבขนาดเล็กมีสีที่เข้มกว่าไม้พลาสติกที่มีผงแกלבขนาดใหญ่ การใช้
 สารประสานช่วยเพิ่มการยึดติดระหว่าง HDPE และผงแกלב เพิ่มสมบัติการทนต่อแรงดึง แรงดัดโค้ง แรงกด
 และการทนต่อแรงกระแทก และเสถียรภาพทางความร้อนของวัสดุประกอบแต่งไม้พลาสติก นอกจากนี้ยังพบว่า
 เมื่อเพิ่มปริมาณสารประสาน มีผลให้ค่าสมบัติเชิงกล อุณหภูมิการหลอม อุณหภูมิการดัดโค้งและอุณหภูมิการ
 สลายตัวของวัสดุประกอบแต่งไม้พลาสติกเพิ่มขึ้นเล็กน้อย แต่ไม่มีผลต่ออุณหภูมิเปลี่ยนสถานะคล้ายแก้ว

ภาควิชาวิศวกรรมเคมี..... ลายมือชื่อนิสิต.....
 สาขาวิชาวิศวกรรมเคมี..... ลายมือชื่ออาจารย์ที่ปรึกษา.....
 ปีการศึกษา2550.....

4970635021: MAJOR CHEMICAL ENGINEERING

KEY WORDS: HIGH DENSITY POLYETHYLENE/ RICE HUSK/ COMPOSITES
/ MECHANICAL PROPERT/ THERMAL PROPERTY

SIRAPAT CHANAKUL: DEVELOPMENT OF HIGH DENSITY
POLYETHYLENE / RICE HUSK COMPOSITES. THESIS ADVISOR:
SIRIJUTARATANA COVAVISARUCH, Ph.D., 97 pp.

This research aims to develop wood plastic composites (WPC) prepared from high density polyethylene (HDPE) and rice husk (RH) to be used as a substitution of solid wood. Investigation on the effects of RH contents, RH particle sizes and the maleic anhydride grafted polyethylene (MA-g-PE) on the mechanical, thermal and physical properties of the HDPE/RH composites was conducted. The contents of RH were varied at 10, 20, 30 and 40 % wt respectively. The RH was grinded and sieved to 75, 180, 250, 355 and 500 micron prior to the preparation of the HDPE/RH composites. The MA-g-PE was applied as a coupling agent at 1, 3, 5 and 7% by weight. The mechanical characterizations revealed that the increment of RH content led to an increase in the flexural, tensile and compressive modulus. This is because the RH possessed higher stiffness and modulus than the HDPE. But the tensile, flexural, compressive and impact strength were lowered due to the poor interfacial bonding between the HDPE and the RH. Furthermore, the RH particle sizes did not influence to the tensile, flexural and compressive properties. The HDPE/RH composites with larger RH particles yielded higher impact resistance. Thermal characterizations revealed that the melting temperature and the heat deflection temperature increased slightly with increasing RH contents. At high content of RH, the degradation temperature of the HDPE/RH composites was reduced and the amounts of solid residues were raised due to silica content and other inorganic compound in RH. The RH particle sizes did not influence the glass transition temperature, melting temperature, heat deflection temperature and degradation temperature of the HDPE/RH composites. The physical characterizations indicated the increment of both density and water absorption by raising the RH amount. The water absorption of the HDPE/RH composites induced darker color to the HDPE/RH WPC. The HDPE/RH composites with smaller RH appeared darker color than the larger ones. In addition, the utilization of MA-g-PE as coupling agent enhanced the interfacial adhesion between HDPE and RH, this initiated the higher mechanical properties and thermal stability of the HDPE/RH composites. With increasing in MA-g-PE contents, affected on the mechanical properties, the melting temperature, the heat deflection temperature and the degradation temperature of the HDPE/RH composites increased slightly, but it did not affect on the glass transition temperature.

Department.....Chemical Engineering... Student's signature.....

Field of study....Chemical Engineering... Advisor's signature.....

Academic year2007.....

ACKNOWLEDGEMENTS

I wish to express my sincerest gratitude and deep appreciation to my advisor, Dr. Sirijutaratana Covavisaruch for their kindness, invaluable supervision, invaluable guidance, advice, and encouragement throughout the course of this study and editing of this thesis.

I am also grateful to my committee members, who provided constructive and scientific advices for the completion of this thesis. This includes, Asst. Prof. Dr. Vichitra Chongvisal, Chairman, from the Department of Chemical Engineering, Faculty of Engineering, Chulalongkorn University, Assoc. Prof Dr. Siriwan Srisorachatr from Department of Chemical Engineering, Faculty of Engineering, Srinakharinwirot University and Dr. Ruengsak Thitiratsakul from the Petroleum Institute of Thailand (PTIT).

Gratefully thanks to Center of Excellence in Particle Technology and Center of Excellence in Catalysis and Catalytic Reaction, Faculty of Engineering Chulalongkorn University, Thailand, for supporting ball mill, sieves and SDT analyzer respectively.

Furthermore, thanks are due to BPE Company LTD., Thailand, Sookchareon Rice Mill, Ayutthaya, Thailand and Dupont Company LTD., Thailand, for their raw material support.

Additionally, many thank everyone in the Polymer Engineering Laboratory, Chulalongkorn University, especially Mr. Nawadon Petchwattana, for their discussion and friendly encouragement. Moreover, I would like to thank everyone here. I feel so fortunate having a chance to learn here.

Finally, I would like to affectionately give all gratitude to the members of my family for their wholehearted understanding, encouragement, and patient support throughout my entire study.

CONTENTS

	PAGE
ABSTRACT (THAI)	iv
ABSTRACT (ENGLISH)	v
ACKNOWLEDGEMENTS	vi
CONTENTS	vii
LIST OF TABLES	xi
LIST OF FIGURES	xii
LIST OF SCHEMES	xvi
CHAPTER I INTRODUCTION	1
1.1 General Introduction	1
1.2 Objectives of the Present Study	3
1.3 Scopes of the Present Study	3
CHAPTER II THEORY	4
2.1 Composite Materials	4
2.1.1 Classification of Composite Materials.....	4
2.1.1.1 Particulate Composites	4
2.1.1.2 Fibrous Composites	5
2.1.1.3 Laminate Composites.....	5
2.1.2 Types of Behaviour of Composite	5
2.1.3 Properties of Filled and Reinforced Plastic	7
2.2 Bonding Mechanisms.....	8
2.2.1 Interdiffusion.....	8
2.2.2 Electrostatic Attraction	8
2.2.3 Chemical Bonding	8
2.2.4 Mechanical Keying	9
2.3 Polymer Matrix	10
2.3.1 Polyethylene (PE)	10

	PAGE
2.4 Filler.....	11
2.4.1 Rice husk (RH)	12
2.5 Modification Interfaces.....	13
2.6 Polymer Processing.....	15
2.6.1 Extrusion Compounding	15
2.6.2 Injection Molding.....	16
2.7 Wood Composites Characterization	16
2.7.1 Mechanical Characterization	16
2.7.1.1 Tensile Test.....	16
2.7.1.2 Flexural Test	17
2.7.1.3 Compressive Test.....	18
2.7.1.4 Impact Test.....	19
2.7.2 Thermal Characterization.....	20
2.7.2.1 Differential Scanning Calorimetry (DSC)	20
2.7.2.2 Dynamic Mechanical Analysis (DMA)	21
2.7.2.3 Thermogravimetric Analysis (TGA).....	21
2.7.2.4 Heat Deflection Temperature (HDT).....	22
2.7.3 Interfacial Bonding Characterization.....	22
2.7.3.1 Scanning Electron Microscope (SEM)	22
2.7.3.2 Attenuated Total Reflectance (ATR-IR).....	23
CHAPTER III LITERATURE REVIEWS	24
CHAPTER IV EXPERIMENTS	31
4.1 Materials	31
4.2 Experimental Procedure.....	32
4.2.1 Preparation of Rice Husk (RH).....	32
4.2.2 Preparation of HDPE/RH Composites.....	32
4.3 Characterizations of HDPE/RH Composites	33
4.3.1 Mechanical Properties.....	33
4.3.1.1 Tensile Test.....	33
4.3.1.2 Flexural Test	34

	PAGE
4.3.1.3 Notched Izod Impact Test.....	36
4.3.1.4 Compressive Test.....	36
4.3.2 Thermal Properties.....	37
4.3.2.1 Thermogravimetric Analysis (TGA) and Differential Scanning Calorimetry (DSC).....	38
4.3.2.2 Dynamic Mechanical Measurement (DMA)	38
4.3.2.3 Heat Deflection Temperature (HDT).....	39
4.3.3 Physical Characterization.....	40
4.3.3.1 Density	40
4.3.3.2 Water Absorption.....	41
4.3.3.3 Natural Outdoor Weathering.....	42
4.3.4 Interfacial Adhesion.....	43
4.3.4.1 Scanning Electron Microscope (SEM)	43
4.3.4.2 Attenuated Total Reflectance (ATR-IR).....	44
CHAPTER V RESULTS AND DISCUSSION.....	45
5.1 Mechanical Characterization of the HDPE/RH Composites	45
5.1.1 Flexural Properties	45
5.1.2 Tensile Properties.....	50
5.1.3 Impact Properties	53
5.1.4 Compressive Properties	59
5.2 Thermal Characterization of the HDPE/RH Composites	62
5.2.1 Thermogravimetric Analysis (TGA).....	62
5.2.2 Glass Transition Temperature (T_g) and Melting Temperature (T_m) Measurement.....	66
5.2.3 Heat Deflection Temperature (HDT).....	67
5.3 Physical Characterization of the HDPE/RH Composites	69
5.3.1 Density Measurement	69
5.3.2 Water Absorption Measurement	71
5.3.3 Visual Appearance	75
5.3.4 Natural Weathering Test.....	75

	PAGE
5.4 Interfacial Characterization of the HDPE/RH Composites	75
5.4.1 Morphological Characteristics	75
5.4.2 Attenuated Total Reflectance (ATR-IR) Analysis.....	78
5.5 Cost Analysis of the HDPE/RH Composites	80
CHAPTER VI CONCLUSIONS AND RECOMMENDATIONS	82
REFERENCES.....	84
APPENDICES	89
APPENDIX A Mechanical Characterizations	90
APPENDIX B Physical Characterizations.....	96
VITA.....	97

LIST OF TABLES

TABLE	PAGE
2.1 Properties of high density polyethylene (HDPE) and other polyolefin	11
2.2 The chemical constituents of rice husk compared with soft and hardwood	13
5.1 Glass transition temperature (T_g) and melting temperature (T_m) of the HDPE/RH composites with different RH contents and particle sizes	66
5.2 Glass transition temperature (T_g) and melting temperature (T_m) of the HDPE/RH composites treated with MA-g-PE from 1 to 7% by weight	67
5.3 The raw materials cost of the HDPE/RH composites	81

LIST OF FIGURES

FIGURE	PAGE
2.1 Type of behaviour commonly observed for variation of a property P with composition for a two component system	6
2.2 Interfacial bonds formed by (a) Molecular entanglement following Interdiffusion, (b) Electrostatic Attraction, (c) Chemical Reaction, (d) Mechanical Keying	9
2.3 Chain structures of different types of polyethylene	10
2.4 Chemical coupling mechanisms of Maleated polyolefins in wood fiber-composites	14
2.5 A simplified extruder diagram	15
2.6 Stress-strain curve of tensile properties	17
2.7 The modes of deformation in compression testing	19
2.8 A schematic DSC curve demonstrating the appearance of several common features	20
4.1 (a) HDPE, (b) Rice husk and (c) MA-g-PE	31
4.2 (a) Ball mill and (b) Vibrational sieve analyzer	32
4.3 (a) Twin screw extruder and (b) Injection molding	33
4.4 (a) A dumbbell shape of the test specimens and (b) The tensile test	34
4.5 (a) Flexural test specimen and (b) Flexural test	35
4.6 Notched Izod impact strength test specimen	36
4.7 (a) Compressive test specimen and (b) The compressive test	37
4.8 (a) Thermogravimetric analyzer and (b) The HDPE/RH composite sample	38
4.9 (a) Dynamic mechanical analyzer and (b) The test specimen	39
4.10 Heat deflection temperature test specimen	40
4.11 Density measurement equipment	41
4.12 (a) The test specimen and (b) Water absorption test	42
4.13 Natural weathering test	43
4.14 Scanning electron microscope (SEM)	44
4.15 Attenuated total reflectance (FTIR-ATR)	44

FIGURE	PAGE
5.1 The flexural modulus of the HDPE/RH composites filled with different particle sizes of rice husk at 10 (●), 20 (■), 30 (◆) and 40% by weight (▲).....	46
5.2 The flexural strength of the HDPE/RH composites filled with different particle sizes of rice husk at 10 (●), 20 (■), 30 (◆) and 40% by weight (▲)	47
5.3 The SEM micrograph of the HDPE/RH composites with 40% of rice husk by weight at (a) 180µm and (b) 500µm	48
5.4 The flexural modulus and flexural strength of the HDPE/RH composites at 30% by weight of 500µm RH particle treated with MA-g-PE from 1 to 7% by weight	49
5.5 The SEM micrograph of the HDPE/RH composites at 30% by weight, 500µm treated with MA-g-PE at 5% by weight.....	50
5.6 The tensile modulus of the HDPE/RH composites filled with different particle sizes of rice husk at 10 (●), 20 (■), 30 (◆) and 40% by weight (▲).....	51
5.7 The tensile strength of the HDPE/RH composites filled with different particle sizes of rice husk at 10 (●), 20 (■), 30 (◆) and 40% by weight (▲)	52
5.8 The tensile modulus and tensile strength of the HDPE/RH composites at 30% by weight of 500µm RH particle treated with MA-g-PE from 1 to 7% by weight	53
5.9 The impact strength of the HDPE/RH composites filled with different particle sizes of rice husk at 10 (●), 20 (■), 30 (◆) and 40% by weight (▲).....	55
5.10 The impact value of the HDPE/RH composites filled with different particle sizes of rice husk at 10 (●), 20 (■), 30 (◆) and 40% by weight (▲)	56
5.11 The SEM micrograph of the HDPE/RH composites with 40% of rice husk by weight at (a) 75µm and (b) 180µm.....	57

FIGURE	PAGE
5.12 The impact strength of the HDPE/RH composites at 30% by weight of 500 μ m RH particle treated with MA-g-PE from 1 to 7% by weight	58
5.13 The compressive modulus of the HDPE/RH composites filled with different particle sizes of rice husk at 10 (●), 20 (■), 30 (◆) and 40% by weight (▲).....	60
5.14 The compressive strength of the HDPE/RH composites filled with different particle sizes of rice husk at 10 (●), 20 (■), 30 (◆) and 40% by weight (▲).....	61
5.15 The compressive modulus and compressive strength of the HDPE/RH composites at 30% by weight of 500 μ m RH particle treated with MA-g-PE from 1 to 7% by weight	62
5.16 TGA thermograms of the pure HDPE (●), RH (■) and the HDPE/RH composites: 10 %wt 75 μ m (◆), 40 %wt 75 μ m (▲), 10 %wt 500 μ m (▼) and 40 %wt 500 μ m (▲).....	64
5.17 TGA thermograms of the pure HDPE (●), RH (■) and the HDPE/RH composites treated with MA-g-PE at 1%wt (▲), 3%wt (▼), 5%wt (▲) and 7%wt (▲)	65
5.18 The heat of deflection temperature of the pure HDPE, the HDPE/RH composites with different RH contents and particle sizes	68
5.19 The heat deflection temperature of the HDPE/RH composites treated with MA-g-PE at 1 to 7% by weight	69
5.20 The density of the HDPE/RH composites filled with different particle sizes of rice husk at 10 (●), 20 (■), 30 (◆) and 40% by weight (▲).....	70
5.21 The water absorption behavior of the pure HDPE (●) and the HDPE/RH composites filled with different RH contents of 10 wt% (■), 20 wt% (◆), 30 wt% (▲) and 40 wt% (×) at (a) 75 μ m, (b) 180 μ m, (c) 250 μ m, (d) 355 μ m and (e) 500 μ m.....	71
5.22 The water absorption of the HDPE/RH composites filled with different particle sizes of rice husk at 10 (●), 20 (■), 30 (◆) and 40% by weight (▲) after 60 days of immersion in water.....	73

FIGURE	PAGE
5.23 The water absorption of the HDPE/RH composites treated with MA-g-PE at (a) 1%, (b) 3%, (c) 5% and (d) 7% by weight.....	74
5.24 The appearance property of the HDPE/RH composites at 40% by weight: (a) 75 μ m, (b) 180 μ m, (c) 250 μ m, (d) 355 μ m and (e) 500 μ m.....	75
5.25 Visual appearances of HDPE/RH composites at 40 %wt, (a) 75 μ m, (b) 180 μ m, (c) 250 μ m, (d) 355 μ m, (e) 500 μ m, (f) pure HDPE before and after natural UV-weathering testing for 60 days.....	76
5.26 The SEM micrograph of the HDPE/RH composites filled with different contents and particle sizes: (a) 10%, 75 μ m (b) 40%, 75 μ m (c) 10%, 500 μ m (d) 40%wt, 500 μ m	78
5.27 The SEM micrograph of the composites treated with MA-g-PE at (a) 1%, (b) 3%, (c) 5% and (d) 7% by weight	79
5.28 The ATR-IR spectra of the pure HDPE, MA-g-PE, untreated and treated HDPE/RH composites with 7% by weight (30% by weight of 500 μ m in RH size)	80

LIST OF SCHEMES

SCHEME	PAGE
2.1 Classification of fillers in polymer compound.....	12

CHAPTER I

INTRODUCTION

1.1 General Introduction

In the few years ago, the worldwide industries of wood plastic composites (WPC) are highly growth because of their several advantages over natural wood, such as low density and cost, abundant availability, biodegradability, and their high specific strength and modulus. [1] The market demand for wood plastic composites in North America and Europe is increasing every year. [2] In 2005, nearly 85% of the WPC market is in North America, primarily due to success in building product applications. [3] This is caused why many recent researches point to develop WPC substitute the natural wood. The main consistencies of WPC are polymer matrix, lignocellulose filler (such as wood flour) and some additives. This consistence are molded under high pressure and temperature. Examples of the WPC product such as decking boards, interior automotive panels, the parts of window and door and the outdoor furniture.

In Thailand, some government and private sectors have prioritized WPC as one of their research frontiers towards innovations. The most commonly used matrices for WPC manufacture are thermoplastics such as polyethylene (PE), polypropylene (PP), polyvinyl-chloride (PVC). The WPC produced in Thailand mostly used polyvinyl-chloride (PVC) as the matrix and wood flour as the filler. Western and European countries concentrated on utilizing recycled polyethylene (PE), polypropylene (PP) rather than PVC. In this research, HDPE was selected as the matrix because of its various applications and good processability. It is tough and flexible, also nontoxic and odorless. [4] In 2004, the family of polyethylene was used for wood plastic composites over 83% compared with those from other plastics. [5]

Nowadays, development of wood plastic composites using agricultural residues such as hemp, jute, bamboo, corn straw, corncobs and rice husk (RH) as reinforcing fillers is gaining extensive attention. This has prompted some researchers to utilize rice husk in the production of WPC. The fact that rice is cultivated not only for

domestic consumption but also for export has motivated Thai researchers to explore utilization of rice husk discarded from rice milling process in many application. Several million tons of rice husk is obtained every year. Moreover, only a minor quantity of these materials is reserved for animal feed or production of energy and a major portion is burned in the field creating environmental pollution. The conversion of these materials into useful industrial products leads to decreasing waste disposal problems. [28] So in the present study, rice husk was chosen as filler replacing the conventional wood flour to prepare wood composites. Chemical analysis reveal rice husk to possess chemical constituents closed to those of wood. The rice husk is also biodegradable, inexpensive and has low density makes it an attractive filler for wood plastic composites (WPC). This using of rice husk as filler in WPC has many advantages such as to reduce cost of WPC and increase value of agricultural waste. It is known that there are many factors are influence to the mechanical and physical properties of WPC products such as the volume fraction, aspect ratio of fiber, fiber orientation, dispersion level, fiber–polymer adhesion, mixing time and processing temperature. [6] The most important role on the mechanical properties of the composites is the incompatibility between the hydrophobic polymeric matrix and the hydrophilic rice husk. It is viewed that the problem can be alleviated by incorporation of an appropriate compatibilizer which is capable of enhancing the interfacial adhesion between the polymeric matrix and the rice husk.

The present study focused on the effects of content of rice husk, its particle sizes and the amount of MA-g-PE as compatibilizer on the mechanical properties, thermal properties, physical properties and morphology of HDPE/RH composites.

1.2 Objectives of the Present Study

This present study is aimed as follow.

- i) To develop wood plastic composites prepared from HDPE and rice husk.
- ii) To investigate the effects of RH contents and its particle sizes on the physical, mechanical and thermal properties of HDPE/RH composites.
- iii) To enhance better interfacial adhesion between the HDPE and RH by application of a compatibilizer.

1.3 Scopes of the Present Study

The scopes of the present study are listed as shown below.

- i) Wood plastic composites are prepared from HDPE filled with RH particles at various amounts namely 10, 20, 30 and 40% by weight. The RH was grinded sieved to fine particles of 75, 180, 250, 355 and 500 μm .
- ii) The WPC is selected for further investigation on the use of a compatibilizer.
- iii) The compatibilizer selected for the HDPE/RH wood plastic composites prepared in the present study is maleic anhydride grafted polyethylene (MA-g-PE). It is applied at 1, 3, 5 and 7% by weight.
- iv) Investigation on the properties for wood plastic composites includes mechanical, thermal and physical testing.

CHAPTER II

THEORY

2.1 Composite Materials

Composite is a material composed of two or more distinct phases and having bulk properties significantly different from those of any of its constituents. The primary phase, known as the matrix, is the continuous phase. It is usually more ductile and lower in hardness. The matrix holds the dispersed phase and shares a load with it. The second phase (or phases) is imbedded in the matrix in a discontinuous form, it is called the dispersed phase. It is usually stronger than the matrix, therefore it is sometimes called the reinforcing phase. [45] The dispersed phase can be organic, inorganic or metallic (synthetic and naturally occurring) in the form of the particles, rods, fibers, plates, foams, etc. [8]

2.1.1 Classification of Composite Materials

Composites can be divided into classes at various manners. One of them is based on their structure as follow;

2.1.1.1 Particulate Composites

Particulate composites consist of a matrix reinforced with a dispersed phase in form of particles. Reinforcement is considered to be a “Particle” if all of its dimensions are roughly equal. Thus, particle-reinforced composites include those reinforced by spheres, rods, flaked, and many other shapes of roughly equal axes. There are also materials, usually polymers, which contain particles that extend rather than reinforce the material. These are generally referred to as “filled” systems. Because filler particles are included for the aim of cost reduction rather than

reinforcement, these composites are not generally considered to be particulate composites. Nonetheless, in some cases the filler will also reinforce the matrix material. [8]

2.1.1.2 Fibrous Composites

Fibrous composites have the dispersed phase in form of fibers which are generally stronger than the matrix phase. So they improve strength, stiffness and fracture toughness of which material. Increase of strength becomes much more significant when the fibers are arranged in a particular direction (preferred orientation) and a stress is applied along the same direction. The strengthening effect is higher in long-fiber (continuous fiber) reinforced composites than in short-fiber (discontinuous fiber) reinforced composites. Short fiber reinforced composites, consists of a matrix reinforced with discontinuous fibers (length $< 100 \times$ diameter). The short fibre dispersing phase has a limited ability to share load. While long fibers carry most of the load. The matrix in which materials serves only as a binder of the fibers, keeping the fibres in a desired shape and protecting them from mechanical or chemical damages. [46]

2.1.1.3 Laminate Composites

Laminate composites consist of composite layers with different anisotropic orientations or of a matrix reinforced with a dispersed phase in form of sheets. When a fiber reinforced composite consists of several layers with different fiber orientations, it is called multilayer composite. Laminate composites provide increased mechanical strength, perpendicular to the preferred orientations of the fibers or sheet, mechanical properties of the material are low.

2.1.2 Types of Behaviour of Composite

The properties of multicomponent systems are rarely simple averages of those of the base component. The range of relationships between a given property P and composition is enormous. An excellent example is the variation of behaviour of viscosities of two phase blends. These have been reported to go through maxima or

minima or to be monotonic. Schematic diagrams of types of behaviour typical of two component systems are given in Figure 2.1[10]

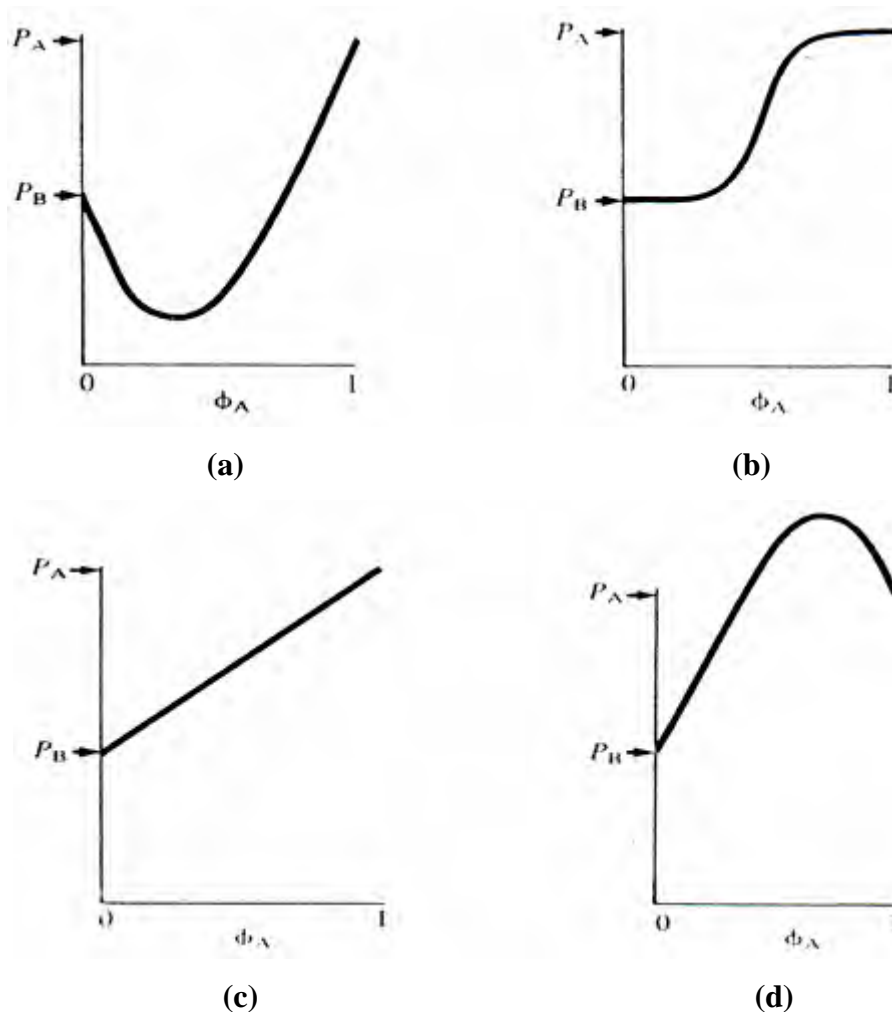


Figure 2.1 Type of behaviour commonly observed for variation of property P with composition for a two component system.

From Figure 2.1 (a) is the case where components contribute to the property in question more or less in proportion to composition. Positive or negative deviation from simple additivity can occur depending on the interaction between the components. For instance the specific volume of a mixture will generally obey this type of relationship. Strong favourable interaction between components will in this case lead to a negative deviation from additivity. Absolute maxima or minima as shown in Figure 2.1 (b,c) are not uncommon. Thus, emulsions are usually very much more viscous than either component and this can still hold when one or both liquids

are polymeric. Mechanical properties of a mixture can, on the other hand, be very much lower than those of either component. The dependence of P on composition in Figure 2.1 (d) is typical of a system for which property P is dominated by the continuous phase.

2.1.3 Properties of Filled and Reinforced Plastic

The main difference between inactive and active or reinforcing fillers is their influence on physical and mechanical properties. Modulus of elasticity and stiffness are increased to some extent by all fillers, even by the spherical types such as calcium carbonate or glass spheres. On the other hand, tensile strength can only be appreciably improved by fiber reinforcement. Also the temperature of deflection under load cannot be increased by spherical fillers to the same extent as by fiber reinforcement. Fillers in flake form, such as talc or mica, likewise produce a marked improvement in this property. [11]

The use of extender fillers can produce in the following changes in the properties of thermoplastics:

- Increase in density.
- Increase in modulus of elasticity, as well as in compressive and flexural strength (stiffening).
- Lower shrinkage.
- Increase in hardness and improvement in surface quality.
- Increase in heat deflection temperature.
- Less temperature dependence of mechanical and physical properties.
- Cost reduction.

Reinforcing fillers produce the following improvements in thermoplastics:

- Increase in tensile stress and tensile strength at break, as well as in compressive, shear and flexural strength.
- Increase in modulus of elasticity and stiffness of the composite material.
- Increase in heat deflection temperature and lowering of the temperature dependence of mechanical properties.
- Lower shrinkage.

- Improvement in creep behavior and apparent modulus, reduction in the viscoelastic yield under load; there is also a partial improvement in impact strength.

2.2 Bonding Mechanisms

To control the interface which can provide the composite with improved mechanical performance and structural integrity, it is essential to understand the mechanism of adhesion. Adhesion can be attributed to four main mechanisms, which can occur at the interface either in isolation or in combination to produce the bond [12].

2.2.1 Interdiffusion

It is possible to form a bond between two polymer surfaces by the diffusion of polymer molecules on one surface into the molecular network of the other surface, as shown in Figure 2.2(a) shows the diffusion of free chain ends at the interface between two polymers, which leads to chain entanglements and a rise in the adhesive strength. The bond strength will depend on the amount of molecular entanglement and the number of molecules involved.

2.2.2 Electrostatic Attraction

Forces of attraction occur between two surfaces when one surface carries a net positive charge and the other surface a net negative charge as in the case of acid-base interactions and ionic bonding and coupling agents laid down on the surface of the fillers, as shown in Figure 2.2(b).

2.2.3 Chemical Reaction

A chemical bond is formed between a chemical grouping on the filler surfaces and a compatible chemical group in the matrix as seen in Figure 2.2(c). The strength of the bond depends on the number and type of bonds and interface failure

must involve bond breakage. The chemical bonds maybe covalent, metallic, ionic, ect., and in many cases are very strong. There are many examples of the interfacial bond strength being raised by localized chemical reactions, but it is often observed that a progressive reaction occur which results in the formation of a brittle product.

2.2.4 Mechanical Keying

There may be contribution to the strength at the interfaces form the surface roughness of the fiber is possible if good wetting has occurred, as illustrated in Figure 2.2(d). The effects are much more significant under shear loading than for decohesion as a result of tensile stresses. Improved resistance to tensile failure may be achieved if re-entrant angles are present. Strength under all types of loading can be increased as a consequence of the increased area of contact.

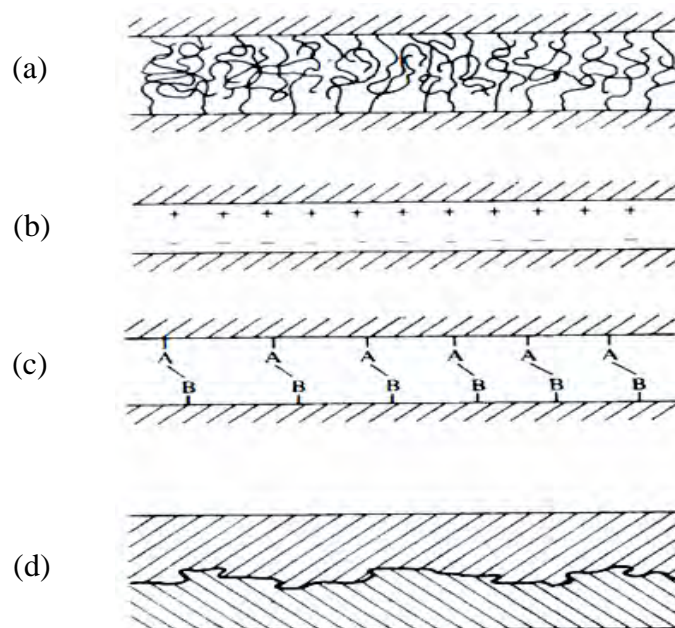


Figure 2.2 Interfacial bonds formed by Molecular entanglement following:
 (a) Interdiffusion, (b) Electrostatic Attraction, (c) Chemical Bonding, and (d) Mechanical Keying

2.3 Polymer Matrix

The purpose of using polymer as a matrix is to hold the fibers together so that mechanical loads may be transferred from the weak matrices to the higher strength fibers. In addition, polymer matrix protecting the fibers from handling damages and environmental degradation and in many cases contributing some needed properties such as ductility, toughness, or electrical insulation. Service temperature is often the main consideration in the selection of a matrix material as well as processing temperature during fabrication.

2.3.1 Polyethylene (PE)

Polyethylene (PE) is the one of the most commodity thermoplastic. It has a relative low-melting temperature (typically between 106 and 130 °C, depending on density/branching of PE). PE is manufactured by polymerization of ethylene monomer under pressure and temperature and can be produced in a very wide range of viscosity of its melts. PE is a semicrystalline polymer. It means that at ambient temperatures the polymer consists of phase-crystalline and amorphous. The glass transition point of PE varies from low to low (from -130 to -20 °C), thus making the plastic ductile at common temperature. [13] The main types of PE are high-density polyethylene (HDPE), low-density polyethylene (LDPE), and linear low-density polyethylene (LLDPE). From Figure 2.3 shows chain structures of different types of polyethylene.

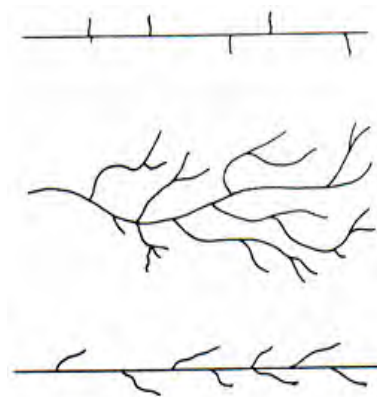


Figure 2.3 Chain structures of different types of polyethylene

(a) high-density, (b) low-density, (c) linear-low-density.

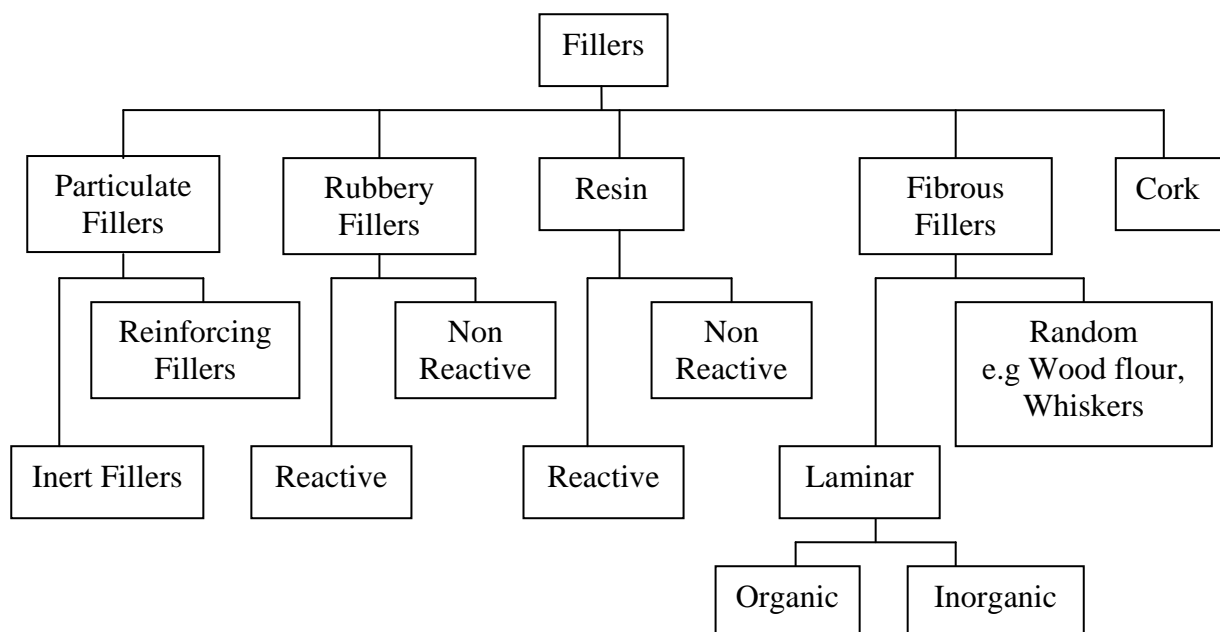
The characteristic that distinguish polyethylene from other polymer systems are very high resistance to chemicals, low cost, easy processability, excellent electrical insulation properties, toughness, flexibility, nontoxicity and odorlessness. [14] It is used in products and packaging such as packaging films, heavy duty shrink film, pipes, containers, bags, blown bottles. High density polyethylene is used as the polymer matrix in this study. It is produced in a low-pressure process either by Ziegler-Natta catalysis or by metal-oxide catalysis. It is essentially linear, having much less branching than LDPE, and has a melting range from 130 to 138 °C. HDPE is defined by a density of greater or equal to 0.941 g/cm³. Table 2.1 shows the properties of high density polyethylene (HDPE) compared with Polypropylene and low density polyethylene (LDPE).

Table 2.1: Properties of high density polyethylene (HDPE) and other polyolefin. [15]

Properties	ASTM	PP	LDPE	HDPE
Specific gravity	D792	0.90-0.91	0.91-0.93	0.94-0.97
Crystallinity (%)	-	82	50-70	80-95
Melting temperature (°C)	-	165-171	98-120	127-135
Tensile strength (Mpa)	D638	31-41	4.1-16	21-38
Tensile modulus (Gpa)	D638	1.10-1.55	0.1-0.26	0.41-1.24
Elongation-to-break (%)	D638	100-600	90-800	20-130
Impact strength Notched Izod (J/m)	D256	21-53	No break	27-1068
Heat deflection temperature at 455 Kpa (°C)	D648	115-125	38-49	60-88

2.4 Filler

The term filler is usually applied to solid additives incorporated into the polymer to modify its physical (usually mechanical) properties. Fillers and reinforcements are added to polymer matrix in order to reduce costs or enhance mechanical properties. A number of types of filler are generally recognized in polymer technology and these are summarized in Scheme 2.1. [16]



Scheme 2.1 Classification of fillers in polymer compound.

Usually the reinforcement is defined in terms of a particular property of interest. Particulate fillers are divided into two types: (1) inert fillers, and (2) reinforcing fillers. The term inert filler is something of a misnomer as many properties may be affected by incorporation of such a filler. Inert fillers will also usually substantially reduce the cost of the compound. Furthermore, filler- reinforcing ability depend on particle size, shape, size/shape distribution, method of compounding, processing, etc. A great variety of natural and synthetic material has been used as fillers in thermoset and thermoplastic matrices, e.g. wood fibres, or flour, synthetic fibres, ground nut shells or corncobs etc. [10]

2.4.1 Rice husk (RH)

Recent development of wood composites using agricultural residues as reinforcing fillers is gaining extensive attention because of stiffness, renewable, biodegradable, low cost and density and abundant. In this research, rice husk is chosen as a filler replacing the conventional wood flour. It was selected for two reasons. Firstly, Chemical analysis revealed RH to possess chemical constituents closed to those of wood as shown in table 2.2. And secondly, the fact that rice husk is one of

the major residues after rice production which accumulates in large volumes means that it is abundantly, available and renewable every year. So, rice husk can be the most interesting filler for both cost reduction and reinforcing HDPE matrix

. **Table 2.2:** The chemical constituents of rice husk compared with soft and hardwood. [57]

Compounds	Composition (%)		
	Softwood	Hardwood	Rice husk
Cellulose	42±2	44±3	38±8
Hemicellulose	26±3	32±5	25±3
Lignin	29±4	18±4	14±2
Silica	0.2-0.8	0.2-0.8	19

2.5 Modification Interfaces

Most polymers were used in the WPCs, especially thermoplastics, are non-polar (hydrophobic), which are not compatible with polar (hydrophilic) wood fibers. Therefore, the poor adhesion between polymer and wood filler is a main problem. One way of improving the adhesion between polymer and wood filler is to improve the level of wetting of the wood filler by the polymer. One approach, which has been used for many years, is to coat the filler with an additive that may be considered to have two active parts. One part is compatible with the filler, the other with the polymer. A much more attempt to increase the adhesion between polymer and filler by using coupling agents which are molecular ‘bridges’ at interface between substrates. Their function is to improve the bond between the two, to the benefit of the overall properties of the composite. [16] The maleated polyolefins are possibly the largest group of coupling agents for polyolefins. They contain two function domains: one, a polyolefin (typically high density polyethylene or polypropylene) which is able to form entanglements with the polymer matrix, to build into the matrix. The second group, maleic anhydride which is strongly interacts with cellulose fiber. However, when high density polyethylene was used as matrix in WPCs, the use of maleated polyethylene which contains ethylene blocks is chosen as coupling agent in this

research. Figure 2.4 represented the coupling mechanisms of maleated polyolefin in wood fiber-polymer composites. Grafting is done with peroxide reagents and takes place at tertiary carbons in the polymer chain or at terminal olefinic groups. When the grafted polyolefins are melted with polymers of similar composition and then cooled, they crystallize into the base polymers, while the maleic anhydride groups react with the hydroxyl groups on the surface of wood fiber to form strong covalent ester linkages. The reaction between wood fiber and maleated polyolefins may result in two products. One is the copolymer with diester bonds, whereas another has the half-ester structure. Secondary bonding is also involved in wood-polymer composites. [18]

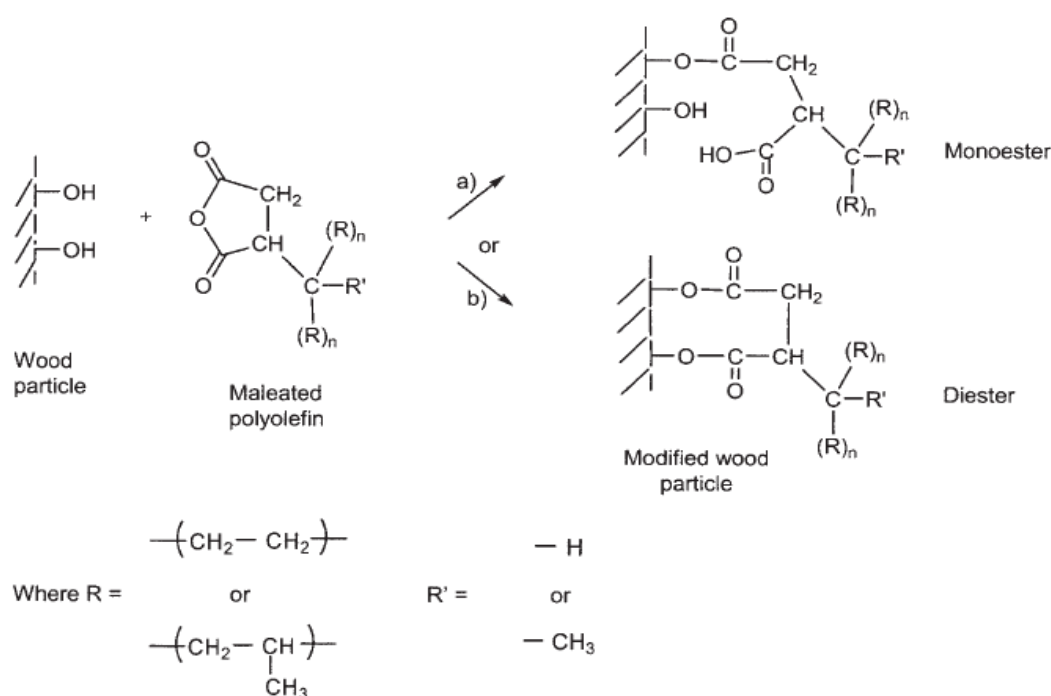


Figure 2.4 Chemical coupling mechanisms of maleated polyolefins in wood fiber-composites. [17]

2.6 Polymer Processing

The manufacture of wood plastic composites is usually a two-step process consisting of compounding and forming. In the compounding step, wood flour or wood fiber and additives are combined with molten thermoplastic to produce a homogeneous composite material and the compounded material is then formed into a product by using many different processes such as the extruder and injection molding.

2.6.1 Extrusion Compounding

The polymer is plasticized in a single or twin screw extruder and blended with the filler. Polymer granules and filler are dry blended in the appropriate proportions and then charged into the feed hopper of the extruder. The blend is melted and mixed, and then possibly passed through a decompression zone where volatiles are removed by application of a vacuum. The compound is then extruded through a die to form thin rods which are air or water cooled and then cut into pellets. A simplified extruder diagram is shown in Figure 2.5.

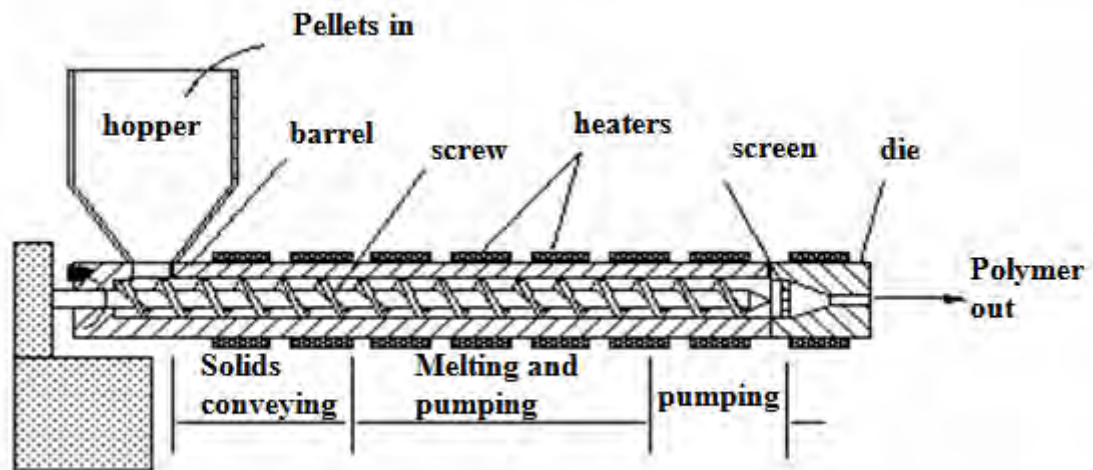


Figure 2.5 A simplified extruder diagram. [56]

2.6.2 Injection Molding

The compounded granules are charged into the feed hopper. The solid charge is moved forward by the rotation of the screw into the heated barrel, where the charge is melted, by conduction from the hot barrel wall, and mixed by the action of the screw. The plasticized charge is transported forward through the compression and metering stages of the screw towards the nozzle which, at this stage, is closed by a valve. Here the charge sets up a back pressure which forces the screw to retract against a controlled hydraulic pressure in the main cylinder. This continues until a sufficient quantity of the charge has been built up in the nozzle region. At this stage the screw rotation is stopped. The carriage is moved forward to engage the nozzle in the mold, which is held closed by a hydraulic or mechanical locking device. The nozzle valve is opened and the charge forced into the mold cavity by the action of the main ram pushing the (non-rotating) screw forward. A considerable pressure is built up in the cavity and is maintained until the charge has frozen in the feed gate. This is the point at which the charge cannot flow out of the mold when the pressure is relaxed. At this time the carriage can be retracted and the next plasticization cycle initiated. Meanwhile the charge in the mold continues to cool. When it has cooled the mold is opened, the part ejected and the mold then closed again for the next injection cycle.

2.7 Wood Composites Characterization

2.7.1 Mechanical Characterization

2.7.1.1 Tensile Test

Tensile test is probably the most fundamental type of mechanical test. The material will react to forces being applied in tension. As the material is being pulled and then its strength along with how much it will elongate. As continue to pull on the material until it breaks. As shows in Figure 2.6, a curve will result showing how it reacted to the forces being applied. The point of failure is of much interest and

is typically called the ultimate strength. For most tensile testing of materials, the initial portion of the test, the relationship between the applied force, or load, and the elongation the specimen exhibits is linear. In this linear region, the line obeys the relationship defined as "Hooke's Law" where the ratio of stress to strain is a constant, or $E = \sigma / \epsilon$. E is the slope of the line in this region where stress (σ) is proportional to strain (ϵ) and is called the Modulus of Elasticity or Young's Modulus. One of the properties you can determine about a material is its ultimate tensile strength (UTS). This is the maximum load the specimen sustains during the test. The UTS may or may not equate to the strength at break. This all depends on what type of material you are testing such as brittle, ductile, or a substance that even exhibits both properties. [41]

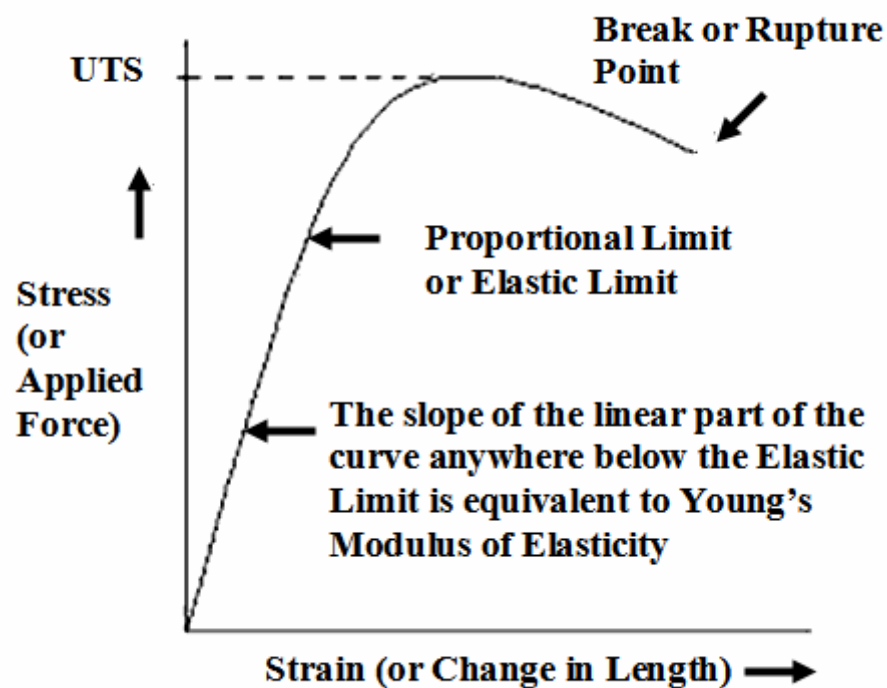


Figure 2.6 Stress-strain curve of tensile properties.

2.7.1.2 Flexural Test

The flexure test method measures behavior of materials subjected to simple beam loading. It is also called a transverse beam test with some materials. Maximum fiber stress and maximum strain are calculated for increments of load.

Results are plotted in a stress-strain diagram. Flexural strength is defined as the maximum stress in the outermost fiber. This is calculated at the surface of the specimen on the convex or tension side. Flexural modulus is calculated from the slope of the stress vs. deflection curve. If the curve has no linear region, a secant line is fitted to the curve to determine slope. A flexure test produces tensile stress in the convex side of the specimen and compression stress in the concave side. This creates an area of shear stress along the midline. To ensure the primary failure comes from tensile or compression stress the shear stress must be minimized. This is done by controlling the span to depth ratio; the length of the outer span divided by the height (depth) of the specimen. For most materials $S/d=16$ is acceptable. Some materials require $S/d=32$ to 64 to keep the shear stress low enough. Flexure testing is often done on relatively flexible materials such as polymers, wood and composites. There are two test types; 3-point flex and 4-point flex. In a 3-point test the area of uniform stress is quite small and concentrated under the center loading point. In a 4-point test, the area of uniform stress exists between the inner span loading points (typically half the outer span length). [42]

2.7.1.3 Compressive Test

A compression test determines behavior of materials under crushing loads. The specimen is compressed and deformation at various loads is recorded. Compressive stress and strain are calculated and plotted as a stress-strain diagram which is used to determine elastic limit, proportional limit, yield point, yield strength and, for some materials, compressive strength. Figure 2.7 illustrates the modes of deformation in compression testing. (a) Buckling, when $L/D > 5$. (b) Shearing, when $L/D > 2.5$. (c) Double barreling, when $L/D > 2.0$ and friction is present at the contact surfaces. (d) Barreling, when $L/D < 2.0$ and friction is present at the contact surfaces. (e) Homogenous compression, when $L/D < 2.0$ and no friction is present at the contact surfaces. (f) Compressive instability due to work-softening material.

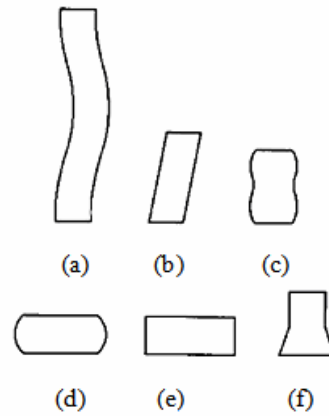


Figure 2.7 The modes of deformation in compression testing. [43]

2.7.1.4 Impact Test

Notched izod impact is a single point test that measures a materials resistance to impact from a swinging hammer. Izod impact is defined as the kinetic energy needed to initiate fracture and continue the fracture until the specimen is broken. [44] Izod specimens are notched to prevent deformation of the specimen upon impact. This test can be used as a quick and easy quality control check to determine if a material meets specific impact properties or to compare materials for general toughness. The specimen is clamped into the impact test fixture with the notched side facing the striking edge of the hammer. The hammer is released and allowed to strike through the specimen. The result of the Izod test is reported in energy lost per unit of specimen thickness at the notch (such as ft-lb/in or J/cm) or the results may be reported as energy lost per unit cross-sectional area at the notch (ft-lb/in² or J/m²). [45]

2.7.2 Thermal Characterization

2.7.2.1 Differential Scanning Calorimetry (DSC)

DSC is a technique in which the difference in the amount of heat required to increase the temperature of a sample and reference are measured as a function of temperature. Both the sample and reference are maintained at nearly the same temperature throughout the experiment. A sample of 10 to 20 mg. in an aluminum sample pan is placed into the differential scanning calorimeter. The sample is heated at a controlled rate (usually $10^{\circ}/\text{min}$). The difference in heat flow between the sample and reference, differential scanning calorimeters are able to measure the amount of heat absorbed or released during transitions. A plot of heat flow versus temperature is produced. The resulting thermogram is then analyzed. DSC may also be used to observe more subtle phase changes, such as glass transitions (T_g), crystallization temperature (T_c) and melting temperature (T_m) as shows in Figure 2.8

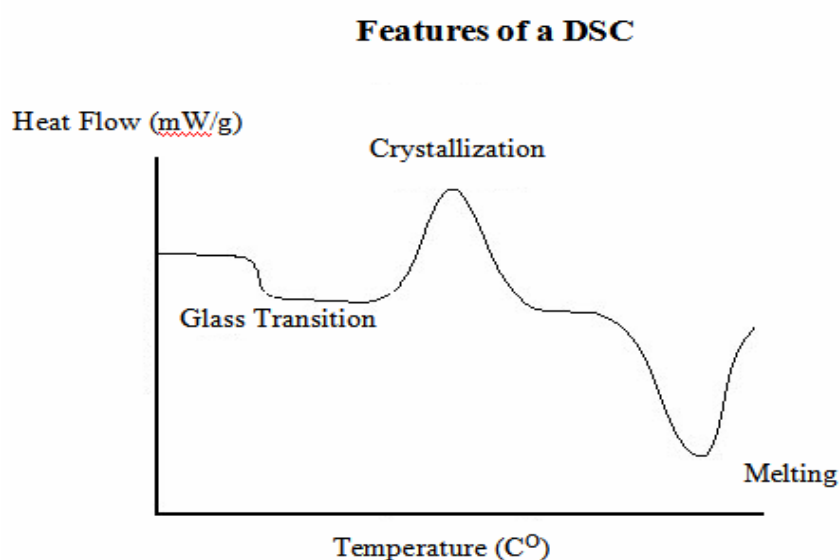


Figure 2.8 A schematic DSC curve demonstrating the appearance of several common features. [47]

2.7.2.2 Dynamic Mechanical Analysis (DMA)

DMA is a technique used to study and characterize materials. It is most useful for observing the viscoelastic nature of polymers. Two methods are currently used. One is the decay of free oscillations and the other is forced oscillation. Free oscillation techniques involve applying a force to a sample and allowing it to oscillate after the force is removed. Forced oscillations involve the continued application of a force to the sample. An oscillating force is applied to a sample of material and the resulting displacement of the sample is measured. [48] The test specimen is clamped between the movable and stationary fixtures, and then enclosed in the thermal chamber. Frequency, amplitude, and a temperature range appropriate for the material being tested are input. The elastic modulus (or storage modulus, G'), viscous modulus (or loss modulus, G'') and damping coefficient (Tan D) is determined as a function of temperature, frequency or time.

2.7.2.3 Thermogravimetric Analysis (TGA)

TGA is a type of testing that is performed on samples to determine changes in weight in relation to change in temperature. The analyzer usually consists of a high-precision balance with a pan loaded with the sample. The sample is placed in a small electrically heated oven with a thermocouple to accurately measure the temperature. The atmosphere may be purged with an inert gas to prevent oxidation or other undesired reactions. A computer is used to control the instrument. The percent weight loss of a test sample is recorded while the sample is being heated at a uniform rate in an appropriate environment. The loss in weight over specific temperature ranges provides an indication of the composition of the sample, including volatiles and inert filler, as well as indications of thermal stability. TGA is commonly employed in research and testing to determine characteristics of materials such as polymers, to determine degradation temperatures, absorbed moisture content of materials, the level of inorganic and organic components in materials, decomposition points of explosives, and solvent residues. It is also often used to estimate the corrosion kinetics in high temperature oxidation. [49]

2.7.2.4 Heat Deflection Temperature (HDT)

HDT is the temperature at which a polymer or plastic sample deforms under a specified load. This property of a given plastic material is applied in many aspects of product design, engineering, and manufacture of products using thermoplastic components. The test specimen is loaded in three-point bending in the edgewise direction. The specimens are then lowered into a silicone oil bath where the outer fiber stress used for testing is either 0.455 MPa or 1.82 Mpa and the temperature is raised at 2° C per minute until they deflect 0.25 mm. The value obtained for a specific polymer grade will depend on the base resin and on the presence of reinforcing agents. [50]

2.7.3 Interfacial Bonding Characterization

2.7.3.1 Scanning Electron Microscope (SEM)

SEM is a type of electron microscope that creates various images by focusing a high energy beam of electrons onto the surface of a sample and detecting signals from the interaction of the incident electrons with the sample surface. [51, 52] The surface of the sample is sputter coated in a vacuum with an electrically conductive layer of gold. The coated dry sample is now placed in a vacuum so that the electron beam can move without interference. Electricity is passed through the wire and then focused by magnets onto the sample. When the electrons from the gun strike the surface coating of gold, electrons are reflected back off the specimen to a detector, this is transmitted to a TV screen where the image is viewed and photographed. [53] The SEM is used to examine biological materials (such as micro-organisms and cells), a variety of large molecules, metals and crystalline structures, and the characteristics of various surfaces.

2.7.3.2 Attenuated Total Reflectance (ATR)

ATR is a sampling technique used in conjunction with infrared spectroscopy which enables samples to be examined directly in the solid or liquid state without further preparation. ATR uses a property of total internal reflection called the evanescent wave. A beam of infrared light is passed through the ATR crystal in such a way that it reflects at least once off the internal surface in contact with the sample. This reflection forms the evanescent wave which extends into the sample, typically by a few micrometres. The beam is then collected by a detector as it exits the crystal. In the case of a solid sample, it is pressed into direct contact with the crystal. Because the evanescent wave into the solid sample is improved with a more intimate contact, solid samples are usually firmly clamped against the ATR crystal, so that trapped air is not the medium through which the evanescent wave travels, as that would distort the results. Typical materials for ATR crystals include germanium, KRS-5 and zinc selenide, while silicon is ideal for use in the Far-IR region of the electromagnetic spectrum. The excellent mechanical properties of diamond make it an ideal material for ATR, particularly when studying very hard solids, but its much higher cost means it is less widely used. [54]

CHAPTER III

LITERATURE REVIEW

In recently years, the use of WPC are growing rapidly because they offer several advantage over natural wood and that are generating the interest in many applications. Therefore, many researches aim to report about innovation and development the properties of WPC. In literature survey, related research a papers concerning about natural fiber plastic composites is summarized as follow.

Hee-Soo Kim *et al.* [2007] studied the effects of the type pf MAPP on the interfacial adhesion properties of bio-flours/polypropylene composites. They used rice husk and wood flour as a filler at 30% by weight, polypropylene as the matrix and a fixed amount at 3% by weight of five types of MAPP as the compatibilizing agents (Epolene G-3003), E-43, Polybond3150, Polybond3200 and Bondyram1004). The compounds were mixed by using a twin-screw extruder and shaped to samples by an injection molding machine. The results indicated that the tensile, impact and flexural strengths of MAPP-treated composites were affected by the M_w and the MA graft (%) of MAPP. The sufficient polymer backbone M_w and MA graft (%) of MAPP is more easily diffused into the PP matrix, which indicating easier entanglement with the PP matrix and provide enough sites for attachment to the polar bio-flour. MAPP with lower M_w and higher MA graft (%) content showed higher MFI. The T_g and T_m did not show significant change with the MAPP type. The crystallinity of MAPP and treated composites were slightly higher than of the PP and the untreated composites. The interfacial adhesion of the PP matrix with the bio-flour was confirmed by the SEM micrographs and by the FTIR-ATR spectral results for the stretching vibration of the ester carbonyl groups (C=O) such as at 1741 cm^{-1} (PP-RHF) and a 1739 cm^{-1} (PP-WF) [20]

Han-Seung Yang *et al.* [2006] studied the effects of compatibilizers on the mechanical properties of lignocellulosic material filled polyethylene bio-composites. They used rice husk (RH) and wood flour (WF) as fillers at 10, 20, 30, 40 and 60% by

weight in low and high-density polyethylene matrix and a fixed amount of the two different compatibilizers (MAPE and MAPP) at 3% by weight. Each compound was mixed by twin-screw extruder and shaped into test specimens by an injection molding machine. The results indicated that the tensile and Izod impact strengths of the composites decreased as the filler loading increased, but they were significantly improved by adding the compatibilizer. The WF/LDPE composites showed higher strength and modulus than the RH/LDPE composites. The properties of the composites incorporating MAPE were better than those with MAPP. The SEM micrographs revealed strong interfacial bonding between the filler and the polymer matrix when MAPE or MAPP was added as the compatibilizer. [21]

Mohd Suzeren Jamil *et al.* [2006] studied the effects of rice husk filler on the mechanical and thermal properties of liquid natural rubber compatibilized high-density polyethylene/natural rubber blends. The HDPE/NR matrix was prepared and were mixed with RH at various contents. The composites were hot pressed into sheet for preparing test samples. The results showed that the mechanical properties of the composites were improved by adding of NR or LNR into the matrix. The tensile and impact strengths decreased with RH loading in matrix, while the tensile modulus and hardness increased. The storage modulus increased with the presence of RH in the matrix due to the rigidity of the filler in matrix. The transition temperature (T_g) decreased to a lower temperature when the RH was added. The SEM micrographs showed better dispersion and compatibility between RH and matrix when LNR was used as the compatibilizer. [22]

Smita Mohanty *et al.* [2006] studied the mechanical and viscoelastic behavior of jute fibre reinforced high-density polyethylene (HDPE) composites. The sample preparation was carried out in two stages. In the first stage, the untreated fibers along with HDPE were premixed at 10, 15, 30 and 45% by weight. In the second stage, the maleic grafted polyethylene (MAPE) treated fibers (at 30% by weight of the fiber) of variable concentrations (0.3, 0.5, 1, and 2%) were mixed with HDPE. The compounds were prepared by melt blending in a mixing chamber and pressed into test specimens. The results showed that the tensile, flexural and impact strengths increased with an increase in the fiber loading upto 30%. The treated composites showed improved

mechanical properties. Composites prepared at 30% fiber loading and 1% MAPE concentration showed optimum mechanical strengths. The modulus of pure HDPE increased with the of jute fiber. The FTIR spectra detected an ester group in the treated composites, was confirming the covalent linkage between the maleic anhydride group of the MAPE and the hydroxyl groups of the jute fiber. TGA thermograms displayed that the thermal stability of the HDPE increased with the addition of the jute fiber and the MAPE. The SEM micrographs showed improved adhesion between the jute fiber and the HDPE matrix in the treated composites. [23]

H. C. Chen *et al.* [2006] studied wood plastic composites prepared from wood waste flour and recycled HDPE. Factors affecting the properties of the composite were investigated, they included particle sizes at 16-32 mesh (1.18-0.59 mm), wood waste flour content at 50, 60, 70 and 75% by weight. The compounds were premixed in a plowshare adhesive-spraying machine between hot-pressed into test specimens. The results showed that the composites with a mixing ratio of 70:30 needed the shortest time to reach the target temperature when heating the composites during hot pressing. The bending strength of the composites increased with larger sized particles, while the density of composites decreased. Moisture content, thickness-swelling and water absorption of the composites increased as wood flour content increased, but the bending strength and density increased. The bending strengths in wet condition were lower than the bending strengths in normal condition. Based on the manufacturing time and the strength vantage, the composites with the mixing ratio of 70:30 of wood particle/HDPE was found to exhibit the optimum properties. [24]

John Z. Lu *et al.* [2005] studied the efficiency of coupling agents on wood plastic composites (WPC). They used pulp as a filler at 10, 30, 50 and 70% by weight for all the untreated composites and all modified composites with 50% pulp. The used coupling agents, they included MAPE copolymers (100D, 226D, Epolenes C16), Epolenes E-43(MAPP), oxidized polyethylene (Epolenes E17 and E20 were oxidized LDPE and HDPE respectively) and pure polyethylene (C10) was pure LDPE. The coupling agents were used at 0, 1, 3, 5 and 10% by weight. The compounds were prepared by melt blending in Haake Rheomix 600 blender and were hot-pressed to prepare test specimens. The results showed that the tensile strengths, flexural modulus and other mechanical properties of the composites were improved by adding the

coupling agents. Optimum mechanical properties were achieved at 3% by weight of wood flour. Maleated polyethylene (MAPE) led to WPC with better performance in mechanical properties than the oxidized polyethylene (OPE) and pure polyethylene (PPE). The coupling agents with a high molecular weight, moderate acid number and low concentration level improved the interfacial bonding in the WPC. At the same or close acid number and molecular weight, there was not significant difference between the MAPEs with LDPE backbone and those with HDPE backbone. According to the statistical analysis, it was found that 226D and 100D were the best among the seven coupling agents studied. [25]

Han-Seung Yang *et al.* [2005] studied the effects of compatibilizing agents on rice-husk flour-reinforced polypropylene composites. The filler used was rice husk at 10, 20, 30 and 40% by weight, MAPP was used as a compatibilizer at 1, 3 and 5% by weight. Tensile test was performed at various test temperatures of -30, 0, 20, 50, 80 and 110 C^o, The tests were conducted at five different crosshead speeds of 2, 10, 100, 500 and 1500 mm/min. The compounds were mixed by using a twin-screw extruder and shaped into test specimens by an injection molding machine. The results indicated that the tensile and Izod impact strengths of the composites decreased as the filler content increased, but mechanical properties were significantly improved by adding the compatibilizer. Optimum properties of the composites were found at 3% MAPP. The composites showed plastic matrix deformation when the test temperature increased. The SEM micrographs showed strong interfacial bonding between the rice husk filler and polymer matrix when the compatibilizer was used. [26]

John Z. Lu *et al.* [2005] studied the effects of the compounding conditions on the properties of composites prepared from pulp fibers and HDPE. They used pulp fibers at 50% by weight, oxidized polyethylene (Epolene E20) was applied as coupling agent at 5% by weight,. The compounds were prepared by melt blending in the Haake Rheomix 600 blender and hot-pressed to test specimens. The results showed that the blending torque increased when HDPE pellets were added. After HDPE melted, the melt torque decreased, so the actual torque values varied with the amount of HDPE. Furthermore, the melt torque and blend temperature rapidly decreased with the addition of wood fibers. The melt torque and compounding time decreased when the concentration of the coupling agent increased. The compatibility

between the wood fiber and the HDPE were improved upon addition of the coupling agent. At 50% wood fiber, the optimum compounding at 90 rpm were found to be at the temperature of 165 C° and mixing time of 10 min. [27]

X. Colom *et al.* [2003] studied the effects of different treatments on the interface of wood plastic composites prepared from HDPE and lignocellulosic fiber. They used Populus fibers as filler at 10, 20, 30 and 40% by weight. Two compatibilizers were used, silane and maleated polyethylene. The compounds were prepared by melt blending in C.W Brabender roll mill and pressed to form test specimens. The results showed that the tensile strengths, the % elongation at break and the toughness decreased when fiber content was increased. The tensile modulus increased with the fiber content. The composites treated with silane showed higher tensile strengths while their toughness slightly decreased. The FTIR spectra of the treated composites indicated an ester group which confirmed the esterification reaction between the populus fibers and the compatibilizers. The SEM micrographs showed better dispersion and compatibility between the fibers and the HDPE matrix when any of the compatibilizers was used. However, Silane was a more effective compatibilizer than MAPE. [28]

J. Ithipol *et al.* [2002] studied wood plastic composites from chemical-treated water hyacinth fibers and low density polyethylene (LDPE). They used water hyacinth as a filler at 10, 20 and 30 phr. The fiber sizes ranged from 35-50, 50-80 and >80 mesh and MAPE was applied as a compatibilizer at 2, 3 4% and 5% by weight. The compounds were mixed by a single-screw extruder and shaped to samples by an injection molding machine. The results indicated that the tensile strengths, modulus, hardness and % crystallinity of the composites increased with the fiber loading but the % elongation at break and impact strengths decreased. The properties of the composites were improved by adding MAPE as a compatibilizer. Optimum properties of the composites were found at 3% MAPE concentration and for the fiber lengths of 50-80 mesh (180-300 μm). The water absorption increased with fiber loading but decreased when the compatibilizer was used. The SEM micrographs showed that using the MAPE as a compatibilizer improved the interfacial bonding between the fibers and the LDPE matrix. [29]

S. Panthapulakkal *et al.* [2002] studied the effect of coupling agent and processing aid on the properties of RH/HDPE composites. The filler used was rice husk at 65% by weight and with different ratios of coupling agent (ethylene–acrylic ester–maleic anhydride) and processing aid (metallic stearate). The compounds were mixed by using a single-screw extruder and pressed to test specimens. The results showed that ethylene–acrylic ester–maleic anhydride as coupling agent improved the tensile, flexural strengths, but water absorption was decreased. The addition of a processing aid indicated a reduction of the strengths and stiffness, but water absorption and the thickness swelling of the composites were increased. Moreover, it was found that the extrusion rate of the composites improved by incorporating of processing aid. The density of the composites was not affect by the coupling agent nor the processing aid. The composites with coupling agent to processing aid ratio of 0.73 : 0.59 had optimum properties with enhanced processability of the composites. [30]

M.N. Ichazo *et al.* [2001] studied the effects of the treatments on the properties of PP/wood flour. Wood flour was used at 10, 20, 30 and 40% by weight. The filler was treated with sodium hydroxide and vinyl-tris-(2-metoxietoxi)-silane. Maleate polypropylene(MAPP) was also used as compatibilizer. The compounds were mixed by using a twin-screw extruder and shaped to samples by an injection molding machine. The results indicated that all treatments led to an increase in the tensile modulus and the tensile strengths of the composites, but they did not affect their MFI. The use of silane and MAPP improved the adhesion and dispersion between the filler and PP matrix, and resulted in lower water absorption when compared with the untreated composites. The alkaline treatments improved only the dispersion of the wood particles. The addition of untreated and treated fillers increased the crystallization temperature of the PP composites. The SEM micrographs showed better dispersion and adhesion between the fibers and the matrix when compatibilizers were used. [31]

J. J. Robin *et al.* [2001] studied the reinforcement of the recycled HDPE with heat-treated wood fibers. The filler was as spruce wood chips at 10, 20 and 30% by weight. The modified wood was heat-treated up the temperature of 230 C^o under inert atmosphere. The compounds were mixed in an industrial mill and shaped to samples by an injection molding machine. The results showed that the modulus of the

composites increased with the addition of the filler. The incorporation of the filler into recycled HDPE increased the stiffness of the matrix, but the tensile and impact strengths decreased. This was due to the poor adhesion between the HDPE matrix and the wood fibers. When using heat-treated wood fibers, the mechanical properties of the composites, mainly in flexural modulus and strengths were increased. The better adhesion of the matrix and the heat-treated filler was confirmed by SEM micrographs. Heat treatment of wood fibers improved mechanical properties of wood fibers/PE composites. [32]

CHAPTER IV

EXPERIMENTAL

4.1 Materials

High density polyethylene (HDPE) grade HJ 1100 was selected as polymer matrix. It was obtained from BPE Company Limited, Thailand. It has a melt flow index of 18 g/10 min and a density of 0.958 g/cm³. Maleic anhydride-grafted polyethylene (MA-g-PE) (Fusabond[®] W PC-576D) was used as compatibilizer. It was produced by Dupont Company Limited. It has a melt flow index of 25 g/10min and a density of 0.941 g/cm³. The filler used to produce wood plastic composite was rice husk. It was grinded and sieved to fine particles with average particle size of 75, 180, 250, 355 and 500 μm. Rice husk is agricultural waste materials. It was obtained from Sookchareon Rice Mill, Ayutthaya, Thailand. The appearances of HDPE, rice husk and PE-g-MA are shown in Figures 4.19(a), (b) and (c) respectively.



Figure 4.1 (a) HDPE, (b) Rice husk and (c) MA-g-PE.

4.2 Experimental Procedure

4.2.1 Preparation of Rice Husk (RH)

Rice husk was obtained mostly in shape of full grains discarded from rice-milling process. It was grinded to fine particles using a ball mill (Figure 4.2a). Rice husk flour was sieved to fine particles of 75, 180, 250, 355 and 500 μm by using a vibrational sieve analyzer (Figure 4.2b). Each of size of the rice husk particles was dried in an oven at 105°C for 24 hours prior to the production of wood plastic composites (WPCs) from HDPE and rice husk.



(a)



(b)

Figure 4.2 (a) Ball mill and (b) Vibrational sieve analyzer.

4.2.2 Preparation of HDPE/RH Composites

The experimental study was carried out in two steps. In the first step, the high density polyethylene was mixed with various contents of oven-dried rice husk at 10, 20, 30 and 40% by weight. In the second step, MA-g-PE was used as the compatibilizer at 1, 3, 5 and 7% by weight of rice husk. It was dried mixed with HDPE and RH. The WPCs were prepared by using a twin screw extruder (Rheocord 300p of Haake Inc., Figure 4.3a). The temperatures of the different zones used during compounding were set as 140/160/160/160/150 °C, the die temperature at 150 °C and

the screw speed of 50 rpm. The compound was obtained in a pellet form and dried at 105°C for 1 hour prior to injection molding (Figure 4.3b) at temperature of 190°C to form specimens for evaluation of the properties composites.



Figure 4.3 (a) Twin screw extruder and (b) Injection molding.

4.3 Characterizations of HDPE/RH Composites

4.3.1 Mechanical Properties

4.3.1.1 Tensile Test

The tensile test of HDPE/RH composites and those modified with MA-g-PE were conducted according to ASTM D638-03 by using a Universal Testing Machine (INSTRON Instrument, model 5567). The test specimens were a dumbbell shape as shown in Figure 4.4 (a). The dimensions of each test specimen was 115 mm x 13 mm x 3 mm as illustrated in Figure 4.4 (b). The test was performed at a crosshead speed of 50 mm/min and a gage length of 48 mm. Only the average results of five tested samples were reported. [33]

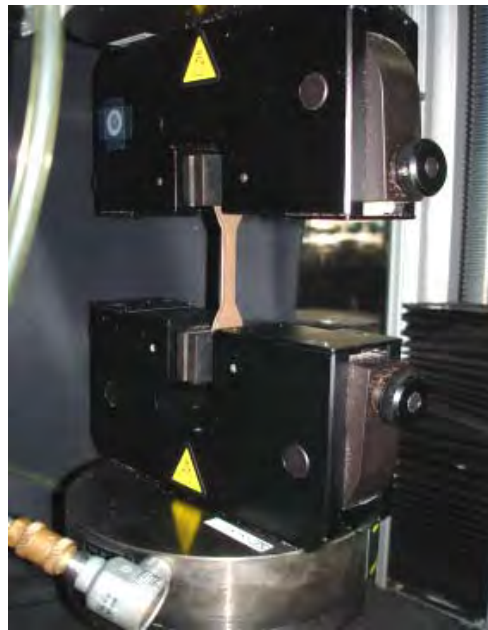
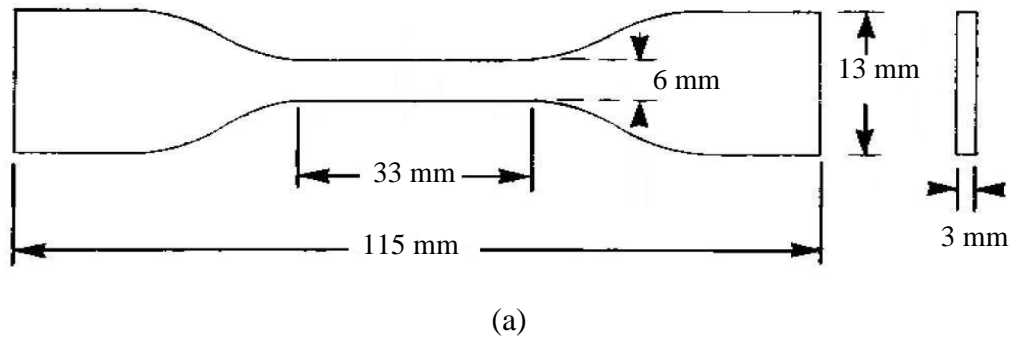
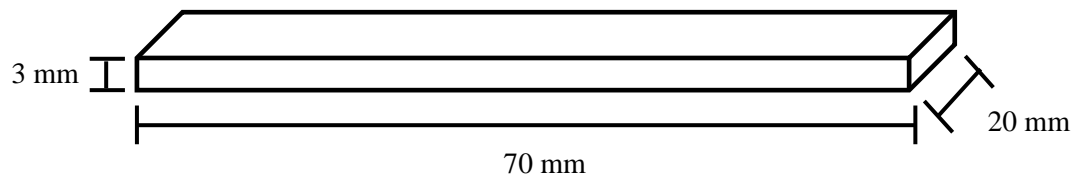


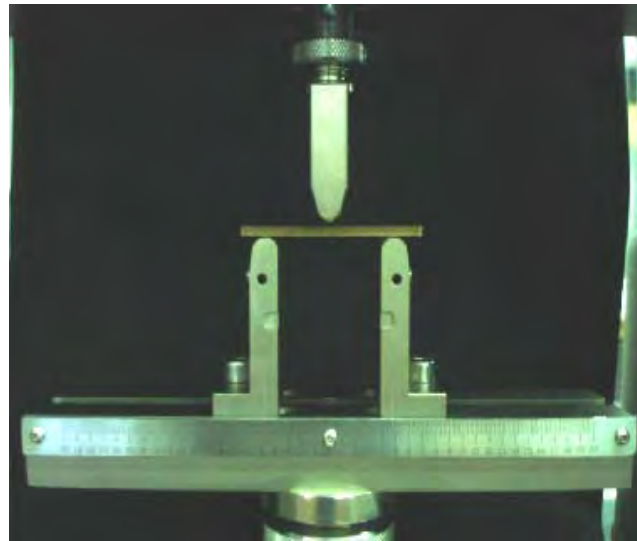
Figure 4.4 (a) A dumbbell shape of the test specimens and (b) The tensile test.

4.3.1.2 Flexural Test

The HDPE/RH composites and those modified with MA-g-PE of dimensions 20 mm×70 mm×3 mm as shown in Figure 4.5 (a) were prepared for flexural test according to ASTM D790-03. A three-point bending test with the support span of 48 mm was carried out by using a Universal Testing Machine (INSTRON Instrument, model 5567) at room temperature as demonstrated in Figure 4.5 (b). The crosshead speed was 1.2 mm/min. Results reported were average of five tested samples. [34]



(a)



(b)

Figure 4.5 (a) Flexural test specimen and (b) Flexural test.

4.3.1.3 Impact Test

The impact strength was determined from the HDPE/RH composites and those modified with MA-g-PE specimens having dimensions of 64 mm x 12.7 mm x 3 mm as performed in Figure 4.6. The tests were carried by using an Izod impact tester (Yasuda Impact Tester) according to ASTM D256-06. All test specimens were notched at an angle 45°. Impact strength reported was average of five tested samples. [35]

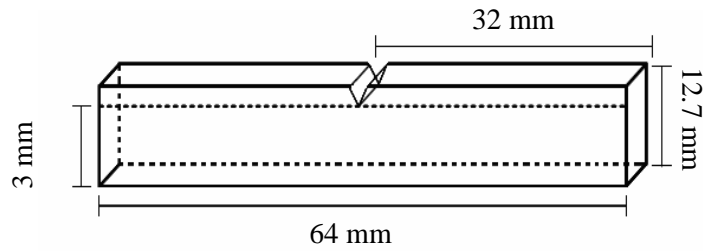


Figure 4.6 Notched Izod impact test specimen.

4.3.1.4 Compressive Test

The compressive properties of the HDPE/RH composites and those modified with MA-g-PE specimens were calculated by using a Universal Testing Machine (INSTRON Instrument, model 5567) according to ASTM D695-02 with the speed of compression at 1.3 mm/min as shown in Figure 4.7 (a) and (b). The dimensions of the test specimen were 12.7 mm x 12.7 mm x 5 mm. Compressive properties reported represented the average of five tested samples. [36]

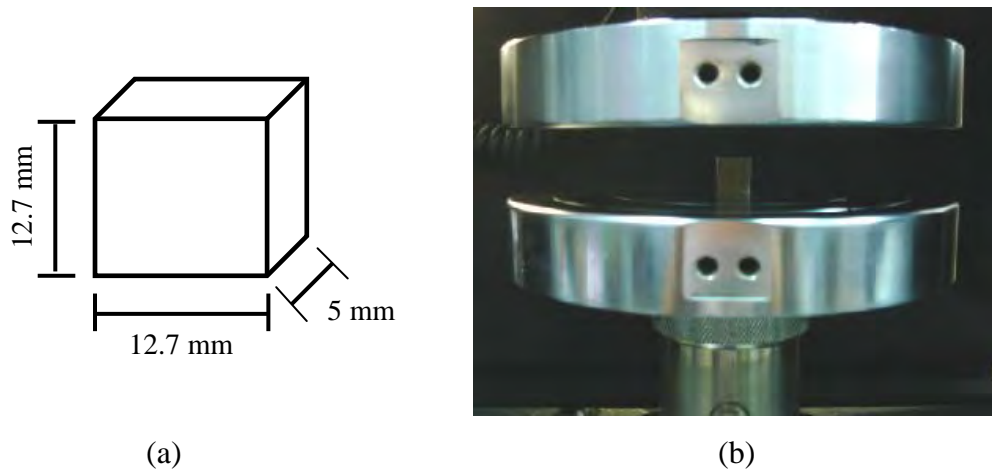


Figure 4.7 (a) Compressive test specimen and (b) The compressive test.

4.3.2 Thermal Properties

4.3.2.1 Thermogravimetric Analysis (TGA) and Differential Scanning Calorimetry (DSC)

The thermal behaviors of all the composites were characterized by using a DSC-TGA (TA instruments, SDT Q600) as shown in Figure 4.8 (a). The TGA simultaneously detected both the DSC and the TGA signals. The weight of each of the composites was 5-10 mg. The composites were heated at a controlled rate of 10°C/min from 30 °C-900 °C under nitrogen atmosphere. Figure 4.8 (b) demonstrates the HDPE/RH composite sample. The TGA was conducted to study the decomposition behavior of the pure HDPE, pure rice husk, the HDPE/rice husk composites and the MA-g-PE modified ones. The DSC was performed to measure the glass transition temperature (T_g) and melting temperature (T_m).

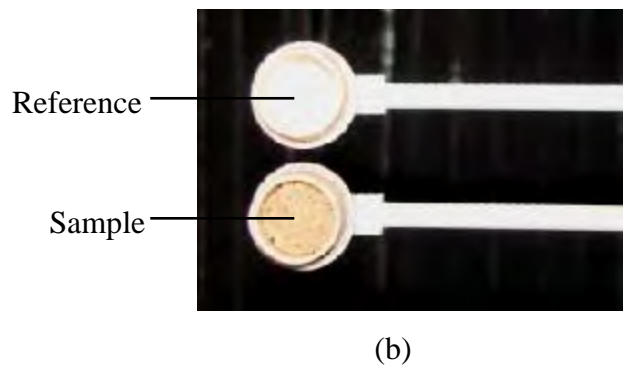
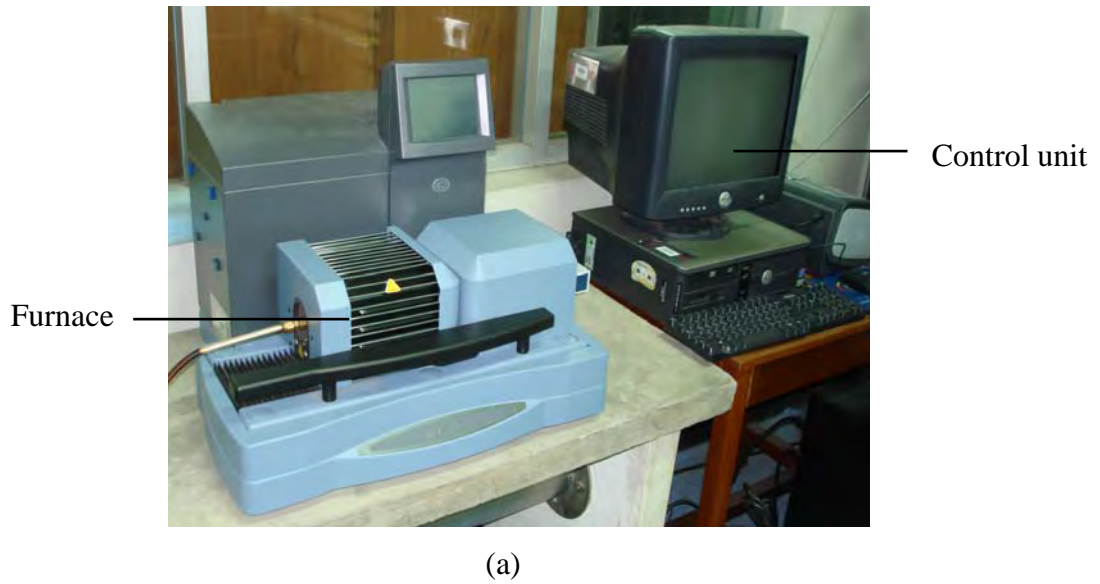


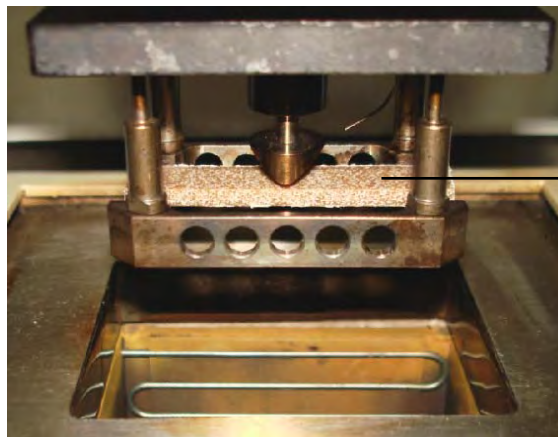
Figure 4.8 (a) Thermogravimetric analyzer and (b) The HDPE/RH composite sample.

4.3.2.2 Dynamic Mechanical Analysis (DMA)

The glass transition temperature, the storage modulus (G'), the loss modulus (G''), and loss tangent ($\tan \delta$) of the composites were obtained by Dynamic Mechanical Analysis, DMA (Model DMA 242C, NETZSCH) as illustrated in Figure 4.9 (a). The dimensions of the specimens were about 10 mm x 50 mm x 2 mm as shown in Figure 4.9 (b). The measurements were carried out in bending mode with a constant frequency of 1 Hz. The specimens were heated at a rate of 2 °C/min from -180 °C to 0 °C.



(a)



(b)

Figure 4.9 (a) Dynamic mechanical analyzer and (b) The test specimen.

4.3.2.3 Heat Deflection Temperature (HDT)

The heat deflection temperature (HDT) is the temperature at which a polymer deforms under a specified load. It was determined by following the procedure described in ASTM D648. The dimensions of the HDPE/RH composites and those modified with MA-g-PE specimens were 120mm x 10mm x 4mm as shown in Figure 4.10. It was loaded under three-point bending in the edgewise direction. The load used for this test was 0.455 MPa and the temperature was increased at 2 °C/min

until the specimen deflects to 0.25 mm. Each reported HDT represented the average of two tested samples. [37]

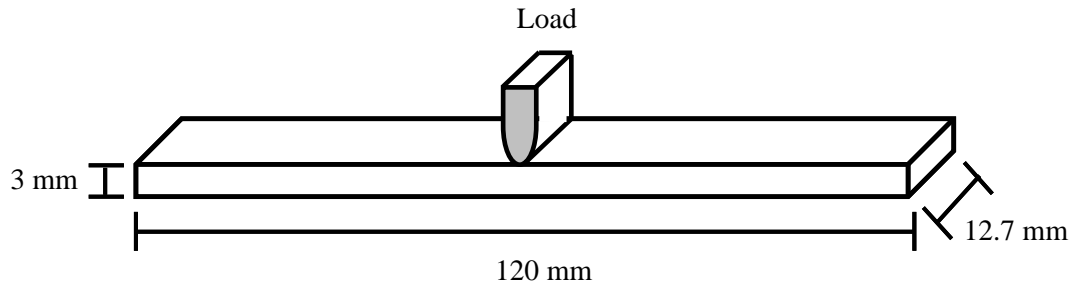


Figure 4.10 Heat deflection temperature test specimen.

4.3.3 Physical Characterization

4.3.3.1 Density

Density determination was performed by applying Archimedes' principle. The principle states that every solid body immersed in a fluid apparently loses weight by an amount equal to that of the fluid it displaces. Each specimens of the pure HDPE, HDPE/RH composites and those modified with MA-g-PE for determination of density was firstly weighed in air and then it was weighed again after immersion in water. Figure 4.11 shows density measurement equipment. The density can be calculated from the two weights as follow: [38]

$$\rho = \left[\frac{A}{(A - B)} \right] \times \rho_0 \quad (4.1)$$

ρ is the density of the solid (g/cm^3)

A is the weight of the solid in air (g)

B is the weight of the solid in water (g)

ρ_0 is the density of water at the given temperature (g/cm^3)

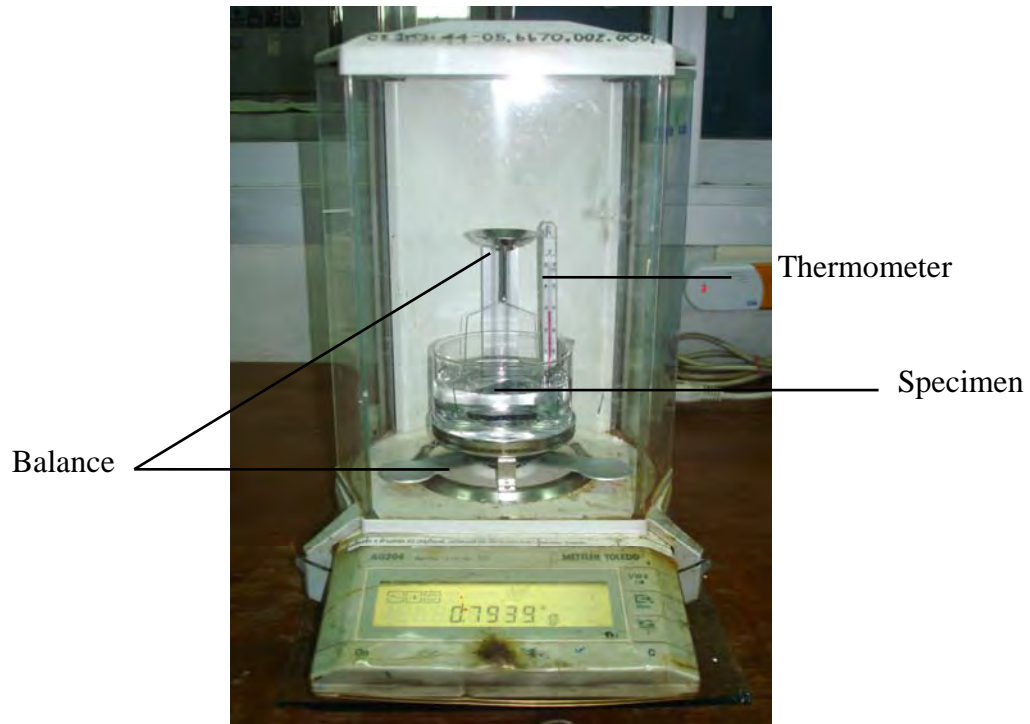
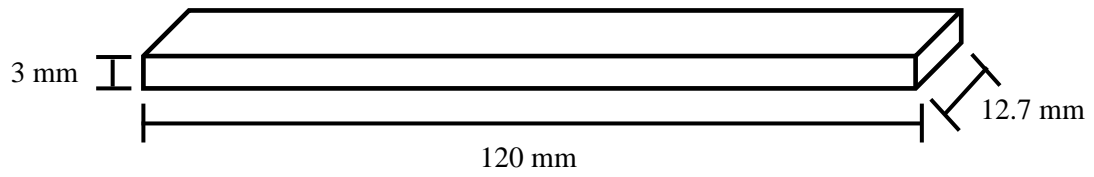


Figure 4.11 Density measurement equipment.

4.3.3.2 Water Absorption

Water absorption is used to determine the amount of water absorbed under specified conditions. The water absorption behaviours of the pure HDPE, HDPE/RH composites and those modified with MA-g-PE were investigated. It was conducted according to ASTM D-570. The composites were weighed, immersed in water for two months and reweighed every 7 days as illustrated in Figure 4.12 (a) and (b). The water absorption can be calculated according to Equation (4.2). Only the average obtained from three samples was reported. [39]

$$\% \text{ Water Absorption} = \left[\frac{\text{Wet weight} - \text{Dry weight}}{\text{Dry weight}} \right] \times 100 \quad (4.2)$$



(a)



(b)

Figure 4.12 (a) The test specimen and (b) Water absorption test.

4.3.3.3 Natural Outdoor Weathering

Outdoor test was examined according to ASTM D1435. The dimension of the test specimen has no specified sizes. The pure HDPE, HDPE/RH composites were mounted on a placed outdoor. The changes of color of the specimens after an exposure of 1 month were evaluated and reported [40]. The natural weathering test is shown in Figure 4.13.



Figure 4.13 Natural weathering test

4.3.4 Interfacial Adhesion

4.3.4.1 Scanning Electron Microscope (SEM)

The dispersion of rice husk filler and the adhesion at interface between rice husk and HDPE matrix were investigated by using a scanning electron microscope (JEOL model JSM 6480LV) as performed in Figure 4.14 at an accelerating voltage at 15 kV. The fractured surface of each composite was mounted on an aluminum stub and sputter coated with a thin layer of gold before microscopic observations on the interfacial adhesion between the RH particles and the HDPE matrix.



Figure 4.14 Scanning electron microscope (SEM)

4.3.4.2 Attenuated Total Reflectance (ATR-IR)

The infrared spectra in the rice husk, HDPE, the HDPE/RH composites and those modified with MA-g-PE were analyzed using a Nexus 870 FTIR spectrophotometer (Model Nicolet 6700) as shown in Figure 4.15. A diamond was used as an ATR crystal. The samples were analyzed over the range of 750–4000 cm^{-1} with a spectrum resolution of 4 cm^{-1} . This analysis of the composites was performed at point-to-point contact with a pressure device.



Figure 4.15 Attenuated total reflectance (ATR-IR)

CHAPTER V

RESULTS AND DISCUSSION

The experimental results from various tests on the untreated HDPE/RH composites and treated composites were illustrated and discussed in this chapter.

5.1 Mechanical Characterization of the HDPE/RH Composites.

5.1.1 Flexural Properties

Figures 5.1 and 5.2 present the effects of rice husk contents and its particle sizes on the flexural modulus and strength of the HDPE/RH composites respectively. The flexural modulus of pure HDPE was 0.52 GPa. All of the plots indicated that the composites exhibited higher flexural modulus than those of unfilled HDPE. The flexural modulus of the HDPE/RH composites increased with increasing RH contents. The flexural modulus of the HDPE/RH composites at 10, 20, 30 and 40% by weight were found to increase by approximately 30%, 42%, 56% and 66% respectively. This because the high silica content makes rice husk a much more stiff and rigid phase than the HDPE matrix. The relationship between RH contents, particle sizes and the flexural strength, as shown in Figure 5.2, which indicated a slightly raised only with rice husk content upto 30% was applied. However at 40% RH, the flexural strength of the HDPE/RH composites was drastically lower than those with less RH content. The reduction in the flexural strength may be due to the agglomeration of the RH filler within the HDPE matrix. This poor interfacial bonding between the large RH agglomerates and the HDPE matrix created partial separation seen as microspaces between the RH and the HDPE matrix. As a consequence, the ability of the RH filler to support the flexural stress transferred from the HDPE matrix was drastically reduced. The existence of numerous agglomerates of the RH was supported by the SEM micrograph as shown in Figure 5.3. Furthermore, the results indicated that the particle sizes of rice husk over the range studied on the flexural

modulus and the flexural strength of the HDPE/RH composites had no significant than the rice husk contents.

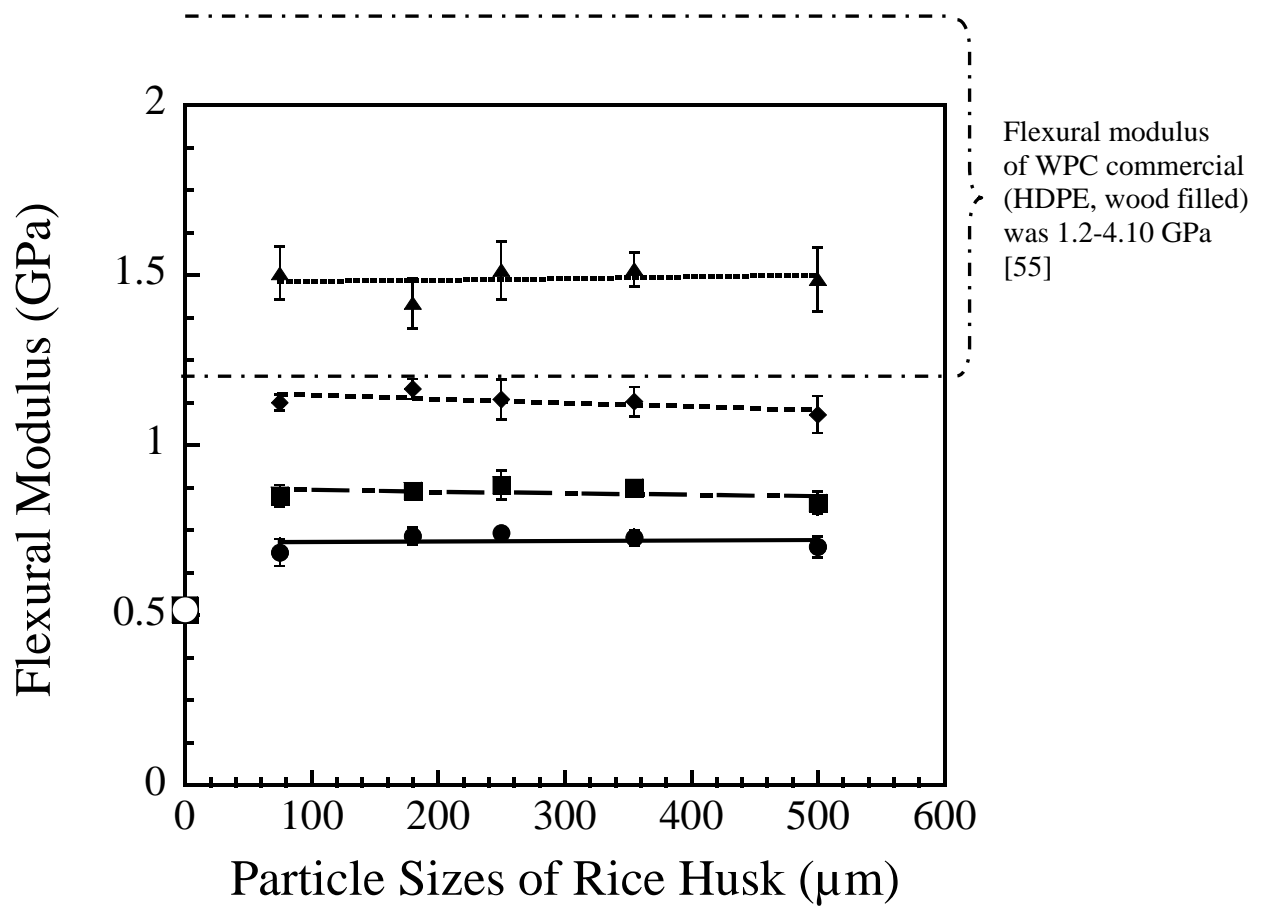


Figure 5.1 The flexural modulus of the HDPE/RH composites filled with different particle sizes of rice husk at 10 (●), 20 (■), 30 (◆) and 40% by weight (▲).

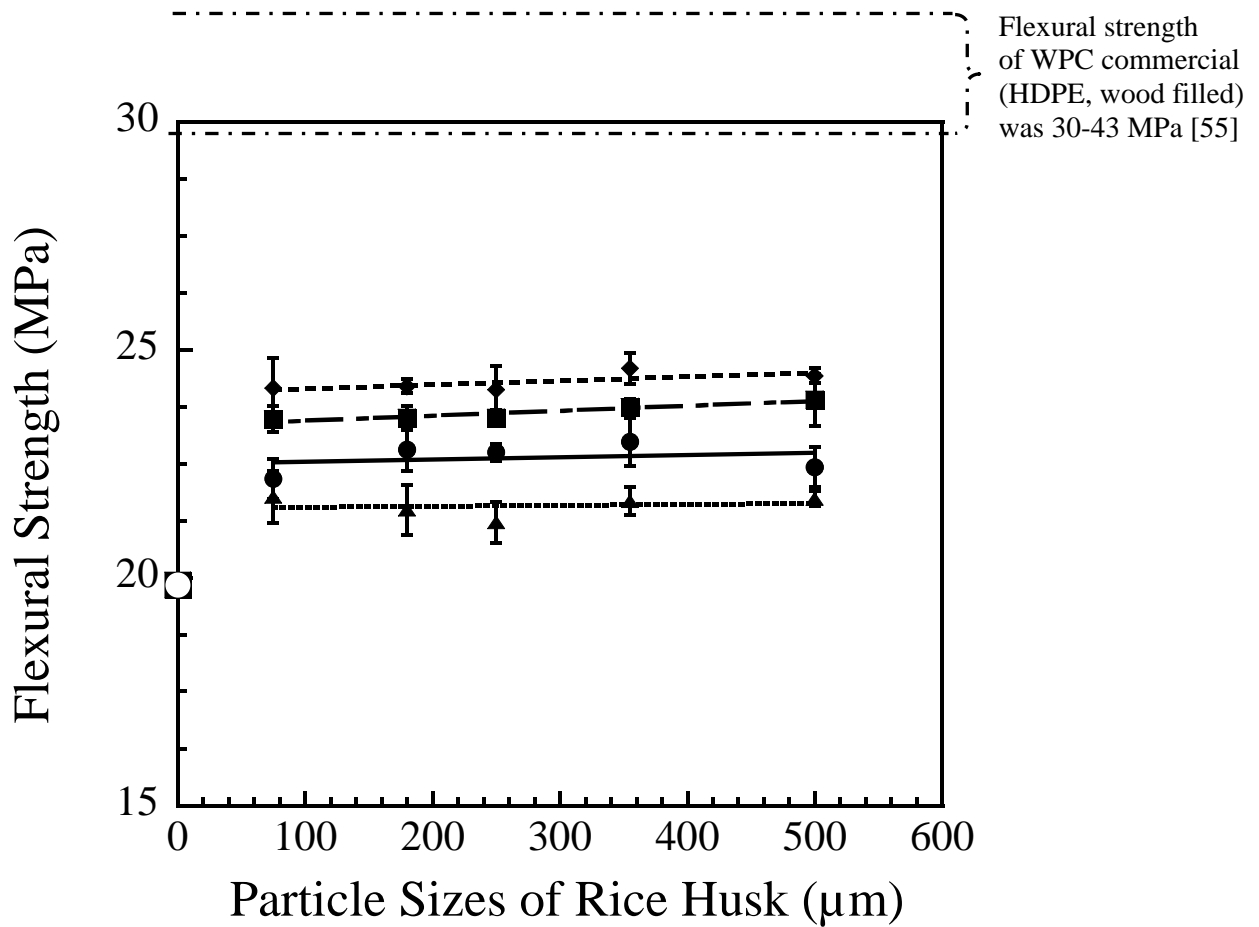


Figure 5.2 The flexural strength of the HDPE/RH composites filled with different particle sizes of rice husk at 10 (●), 20 (■), 30 (◆) and 40% by weight (▲).

Compared with the commercially available WPC, the present WPC with RH content below 40% by weight possessed lower flexural modulus than the commercially available WPC. In fact, all the current WPC with RH exhibited lower flexural strength than commercial ones as well. So, the HDPE/RH composites in the present study can be flexed more easily.

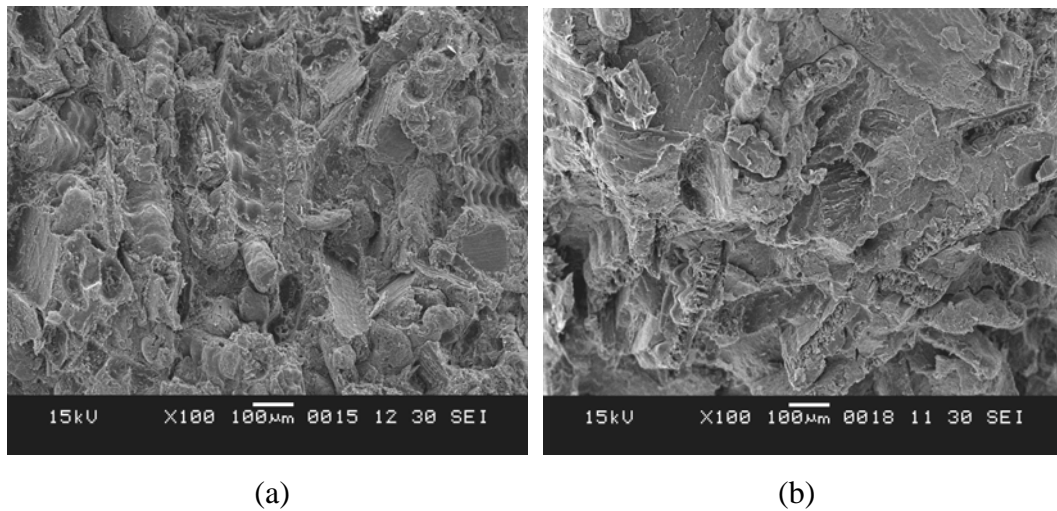


Figure 5.3 The SEM micrograph of the HDPE/RH composites with 40% of rice husk by weight at (a) 180µm and (b) 500µm.

After flexural, tensile and impact characterization of the HDPE/RH composites and comparing to those of WPC commercial, the formulation of the HDPE/RH composite was HDPE 70%, rice husk 30% by weight at 500µm RH particle. Because this composition was in acceptable range of the mechanical property of WPC commercial. This composition was selected for further investigation on the used of MA-g-PE as coupling agent at various contents of 1, 3, 5 and 7% by weight. The flexural modulus and strength of the HDPE/RH composites at 30% by weight of 500µm RH particle treated with MA-g-PE ranging from 0 to 7% by weight was illustrated in Figure 5.4. The flexural modulus and flexural strength of HDPE/RH composites without MA-g-PE were 1.09 GPa and 24.43 MPa respectively. At identical RH content, the treated RH exhibited improvement in the flexural strength compared with those of the untreated ones. The treated HDPE/RH composites showed greater in the flexural strength by 15%, 18%, 20% and 17%. The addition of MA-g-PE in HDPE/RH composites was expected to improve the interfacial adhesion between HDPE and RH by the reaction between the maleic anhydride groups with the hydroxyl groups on the surface of wood fiber to form strong covalent ester linkages, leading to a strong interfacial bonding between the rice husk and the HDPE matrix as confirmed by SEM micrograph in Figure 5.5.

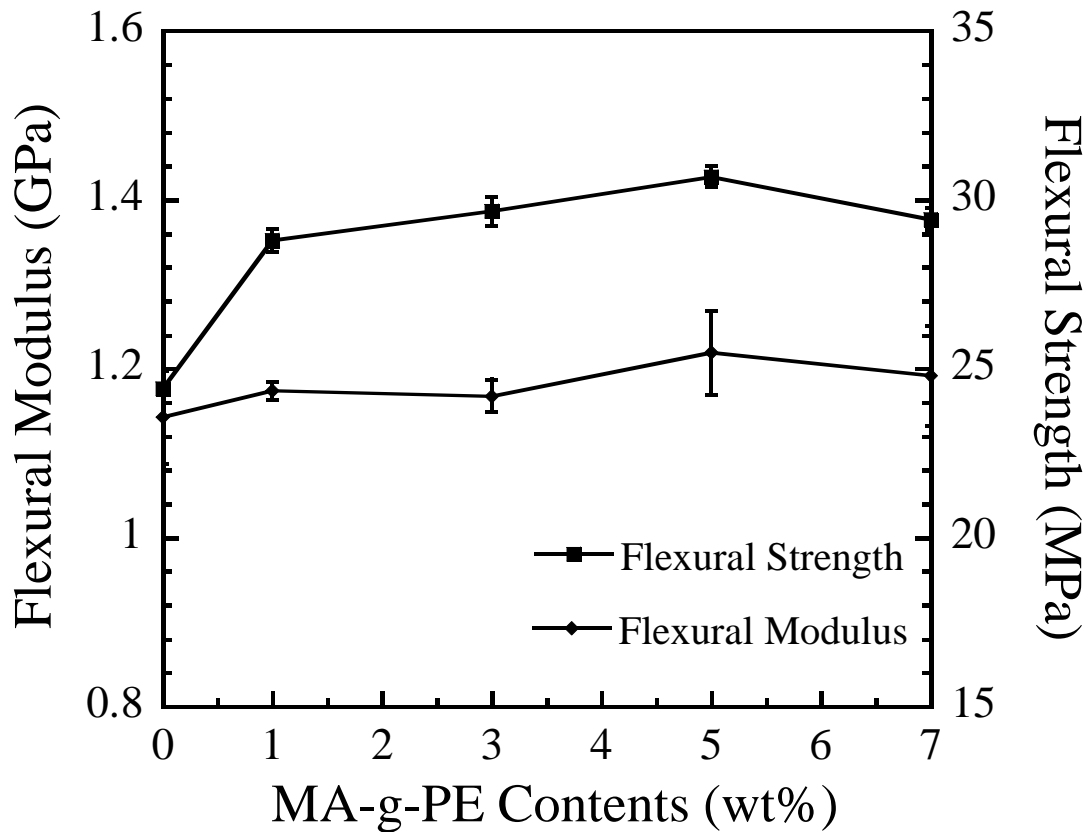


Figure 5.4 The flexural modulus and flexural strength of the HDPE/RH composites at 30% by weight of 500 μ m RH particle treated with MA-g-PE from 1 to 7 % by weight.

Comparison with the other HDPE-based WPC system (Wood flour 60%, 60 mesh pine) treated with 1% by weight of the Fuzabond WPC-576D. The flexural strength of the HDPE-wood composites was 24.47 MPa [57] while those of the HDPE/RH composites treated with the same coupling agent was 24.43 MPa. The flexural strength of the treated HDPE/RH composites with WPC-576D did no differ when compared with those of the treated HDPE-wood composites.

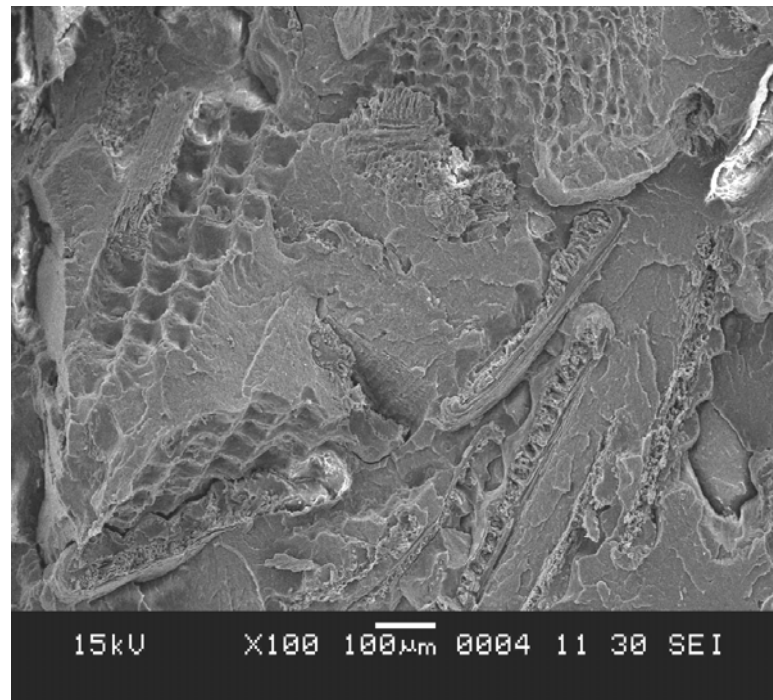


Figure 5.5 The SEM micrograph of the HDPE/RH composites at 30% by weight, 500µm treated with MA-g-PE at 5% by weight.

5.1.2 Tensile Properties

The tensile modulus and tensile strength of the HDPE/RH composites are shown in Figures 5.6 and 5.7. The incorporation of the rigid, silica-rich RH particles in the tough HDPE causes the composite to be stiffer than pure HDPE. The tensile modulus of pure HDPE was 0.75 GPa. The tensile modulus of the HDPE/RH composites at 10, 20, 30 and 40% by weight were found to increase by approximately 21%, 31%, 45% and 53% respectively. While the tensile strength of the HDPE/RH composites decreased with the addition of RH contents as represented in Figure 5.7. The tensile strength of pure HDPE was 24.48 MPa, which lower than that of the pure HDPE approximately 8%, 12%, 15% and 16% respectively. This results can be explained the non-uniform partial separations between the RH and the HDPE matrix as the same reasons as shown in flexural properties of the HDPE/RH composites. It was believed to be the cause of tensile strength reduction. Furthermore, the results indicated that the size of RH had no significant change on the tensile properties of the HDPE/RH composites. For example, the tensile modulus and tensile strength of the

HDPE/RH composites with 40% by weight of 75 μm in size were 1.52 GPa and 20.42 MPa respectively while those of HDPE/RH composites with the same % RH content of 500 μm particle were 1.50 GPa and 20.47 MPa respectively.

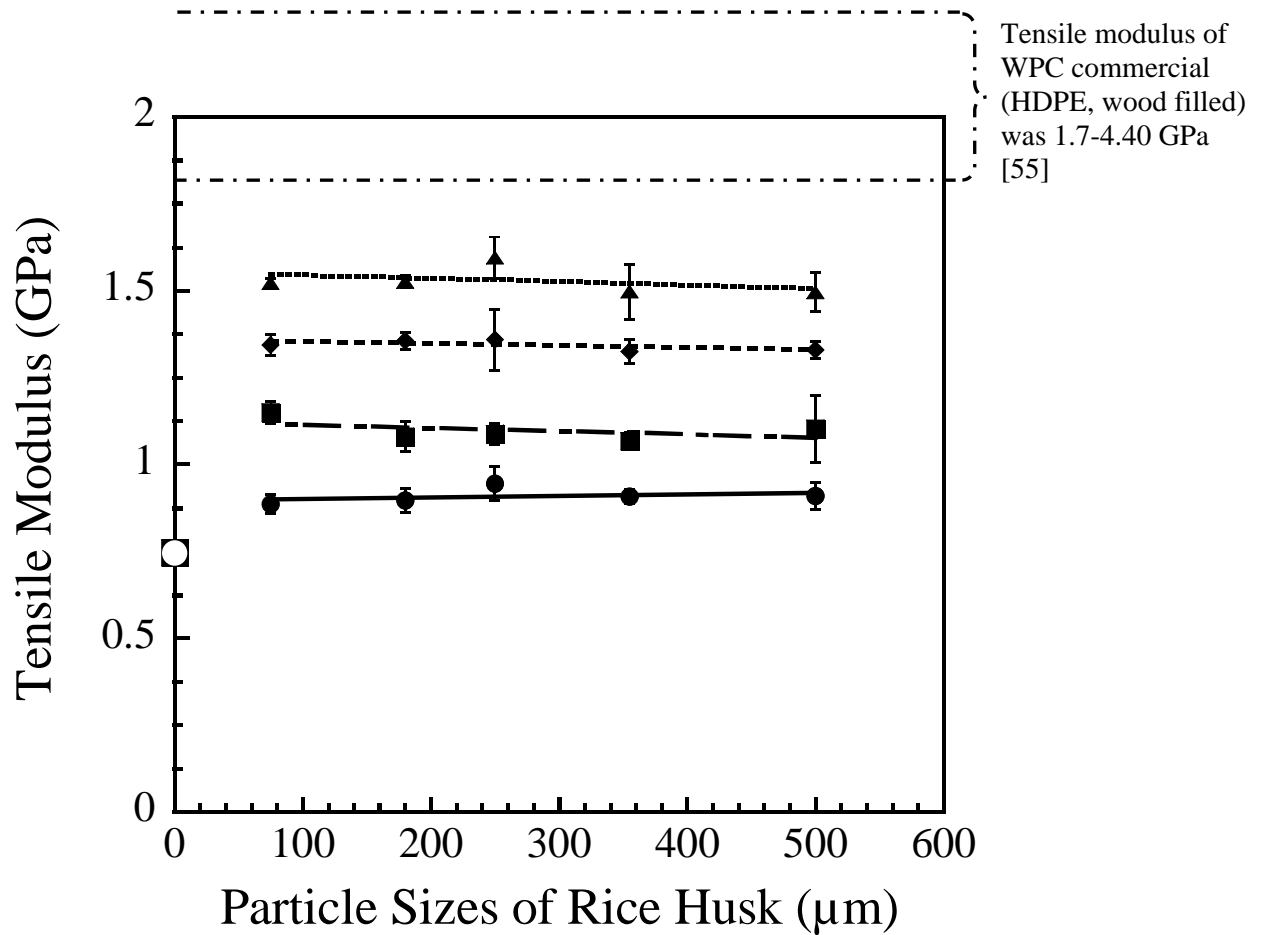


Figure 5.6 The tensile modulus of the HDPE/RH composites filled with different particle sizes of rice husk at 10 (●), 20 (■), 30 (◆) and 40% by weight (▲).

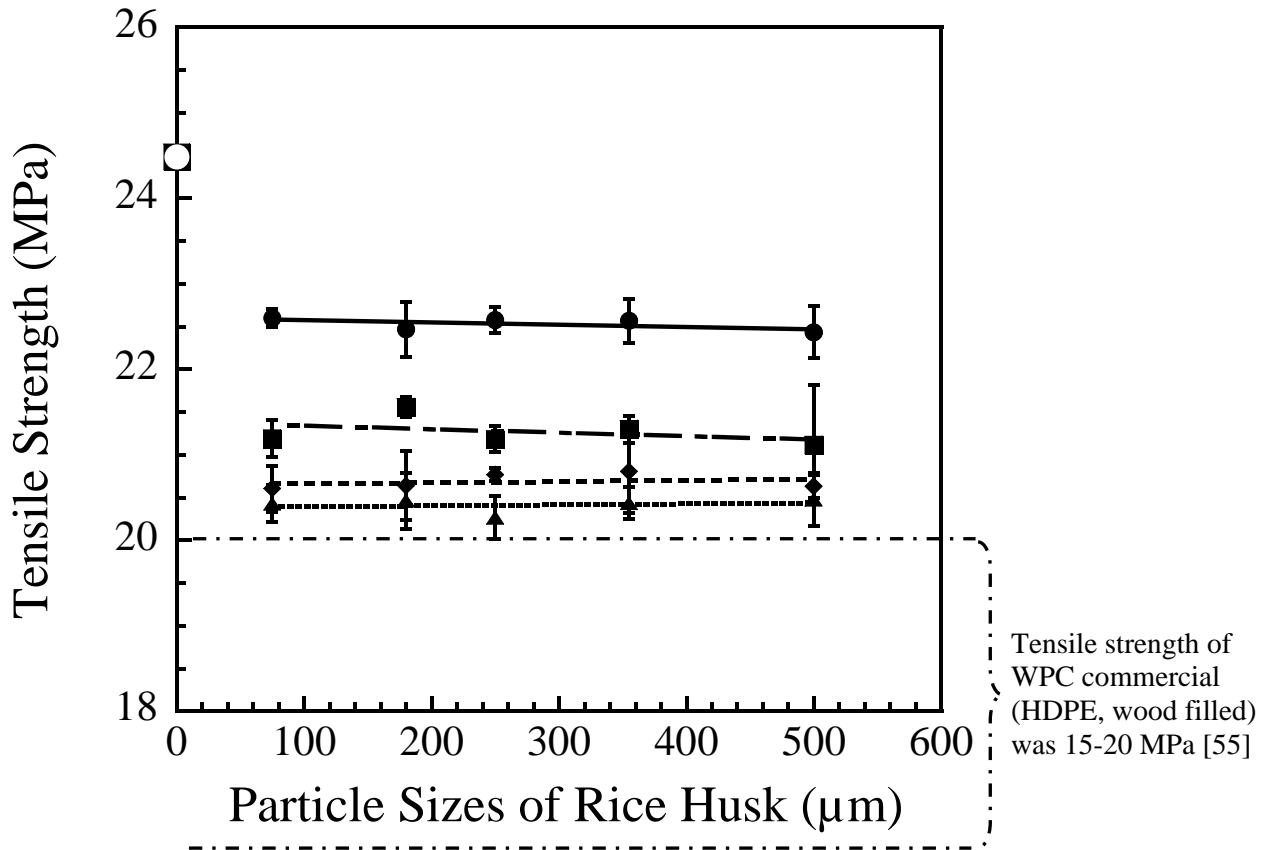


Figure 5.7 The tensile strength of the HDPE/RH composites filled with different particle sizes of rice husk at 10 (●), 20 (■), 30 (◆) and 40% by weight (▲).

Furthermore, in comparison to the commercially available WPC, the HDPE filled with all contents of the RH, i.e. 10, 20, 30 and 40% by weight, exhibit lower tensile modulus than the commercially available WPC. In contrast, all compositions of the HDPE/RH system possessed higher tensile strength than those of the commercially available WPC. Figure 5.8 shows the tensile modulus and strength of the HDPE/RH composites at 30% by weight of 500 μ m RH particle treated with MA-g-PE ranging from 0 to 7% by weight. The tensile modulus and tensile strength of untreated HDPE/RH composites were 1.33 GPa and 20.63 MPa respectively. All the treated composites showed slightly greater in tensile properties, as compared to the untreated ones.

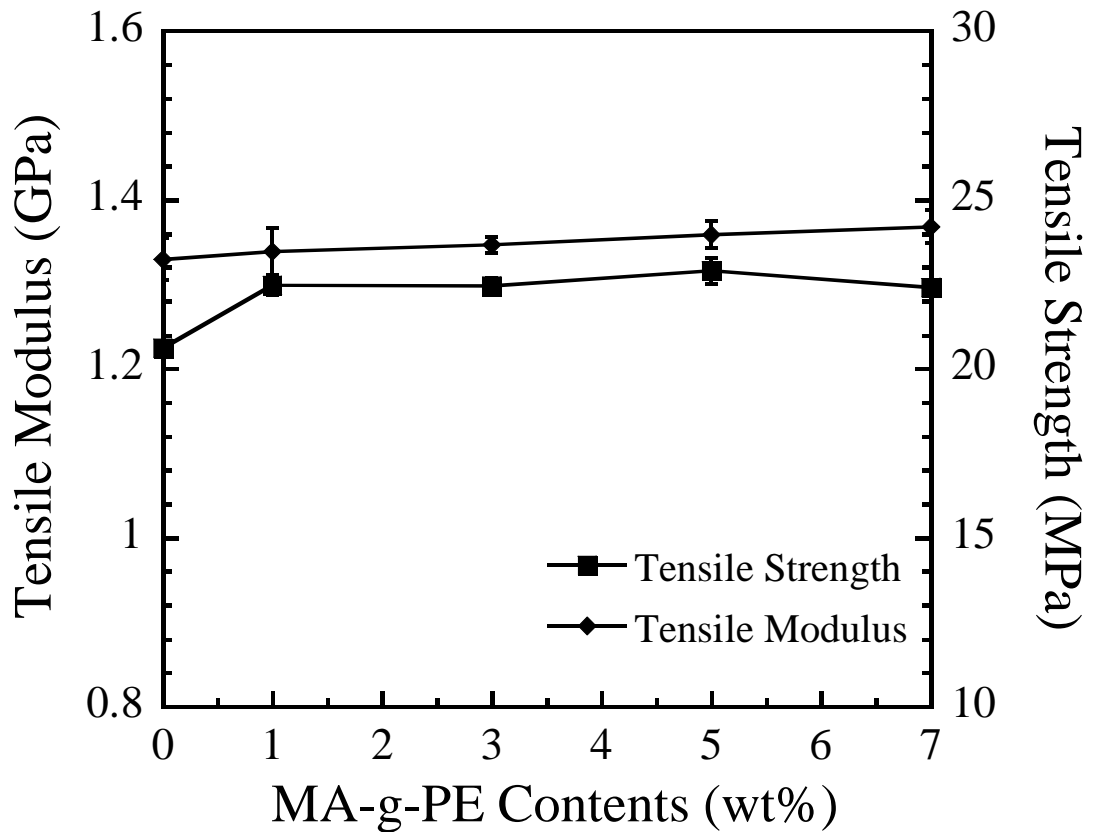


Figure 5.8 The tensile modulus and tensile strength of the HDPE/RH composites at 30% by weight of 500 μ m RH particle treated with MA-g-PE from 1 to 7% by weight.

Compared with the other HDPE-based WPC system (Wood flour 50%, HDPE 50%) treated with 5% by weight of the Fuzabond MB 100D and 226D. Their tensile strength were 22.34 and 23.33 MPa [25] respectively while those of the HDPE/RH composites treated with Fuzabond WPC-576D at the same concentration was 22.90 MPa. This result showed the treated composites with WPC-576D had the tensile strength closed to those of the treated composites with MB 100 MB and 226D.

5.1.3 Impact Properties

Figure 5.9 illustrated the notched Izod impact strength of the HDPE/RH composites. The impact strength of pure HDPE was 15.47 kJ/m². All the plots of impact strength of the HDPE/RH composites were lower than that of pure HDPE. The impact strength declined with further addition of rice husk particles. The

HDPE/RH composites with the highest RH content showed the lowest impact strength. For example, the impact strength of the HDPE/RH composites with 40% by weight of 75 μ m particle was 10.25 kJ/m² while that of the HDPE/RH composites with the same % RH content of 500 μ m particle was 12.23 kJ/m². They were lower than that of the pure HDPE by approximately 34% and 21%. This result was caused from the RH in the matrix causing the composites to be stiffer. Part of the ductile portion of HDPE was reduced, thus decreasing the toughness of the composites. Moreover, it was found that the composites with larger RH particles showed higher strength than those with smaller particles. This is because smaller particles with its larger surface area trends to have more poorly-adhered interfacial sites as indicated in the SEM micrograph in Figure 5.11. The numerous partial separations or voids between the RH and the HDPE phase led to easier crack propagation along the interface upon impact. Figure 5.12 shows the impact strength of the HDPE/RH composites at 30% by weight of 500 μ m RH particles treated with MA-g-PE ranging from 0 to 7% by weight. The impact strength of the HDPE/RH composites without MA-g-PE was 13.01 kJ/m². The HDPE/RH composites treated with MA-g-PE ranging from 0 to 7% by weight exhibited higher impact strength with the untreated composite. This result was found to increase by approximately 14%, 15%, 17% and 15% respectively at MA-g-PE contents of 1, 3, 5 and 7% by weight.

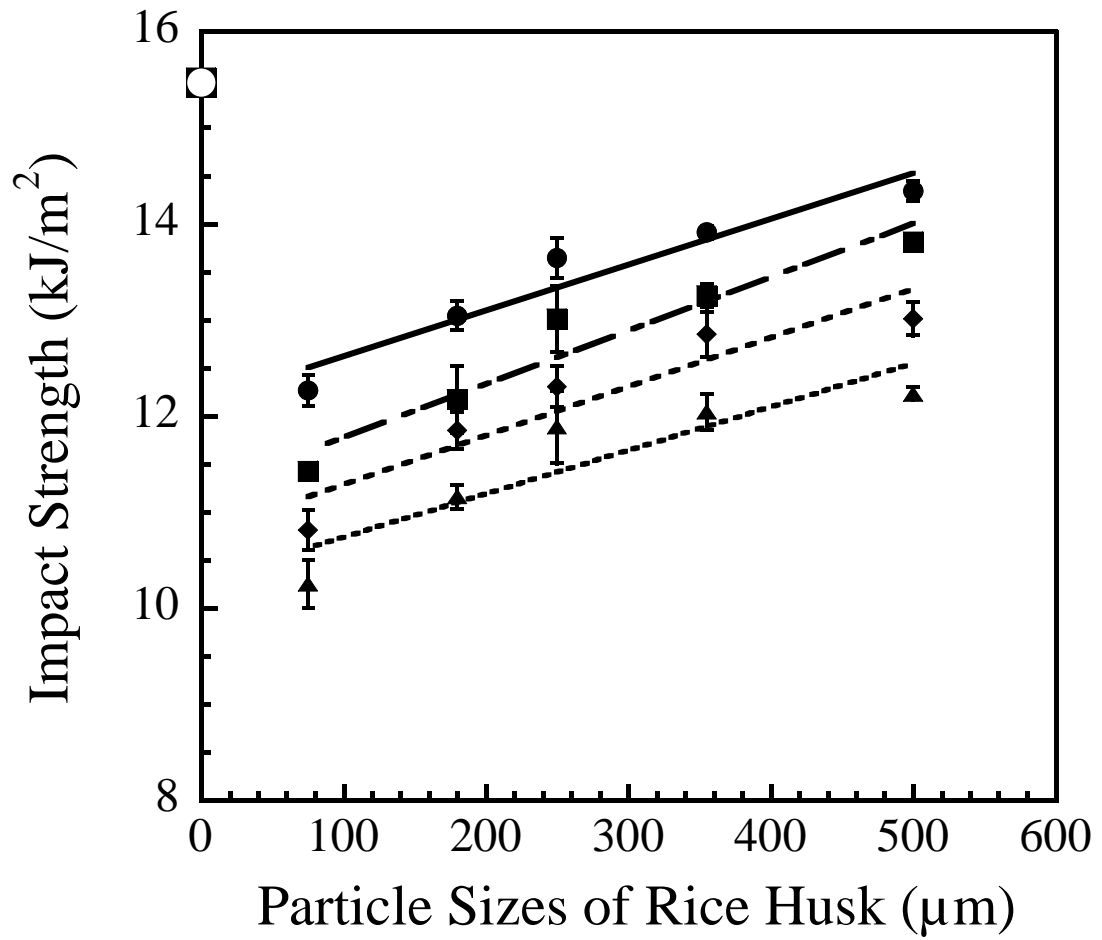


Figure 5.9 The impact strength of the HDPE/RH composites filled with different particle sizes of rice husk at 10 (●), 20 (■), 30 (◆) and 40% by weight (▲).

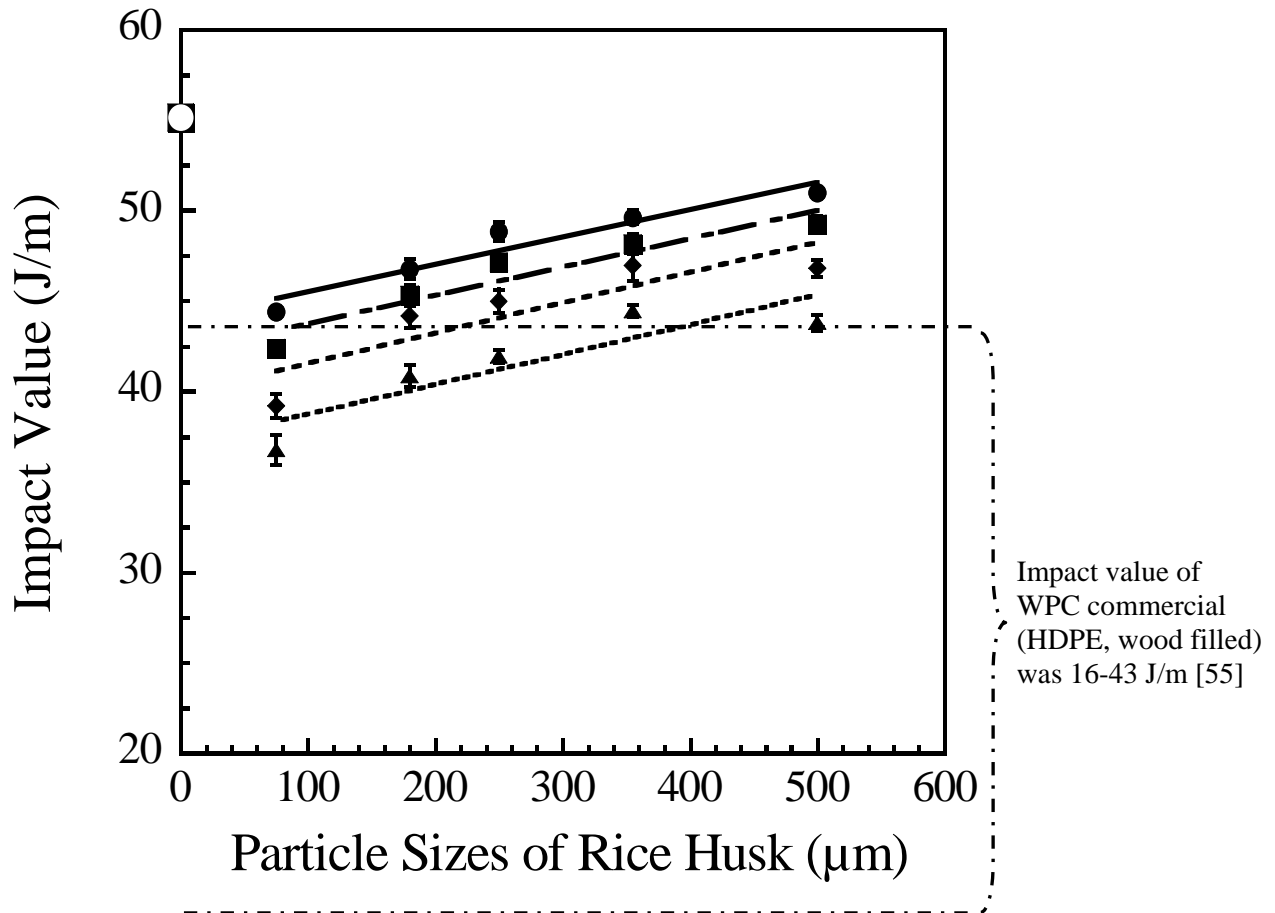
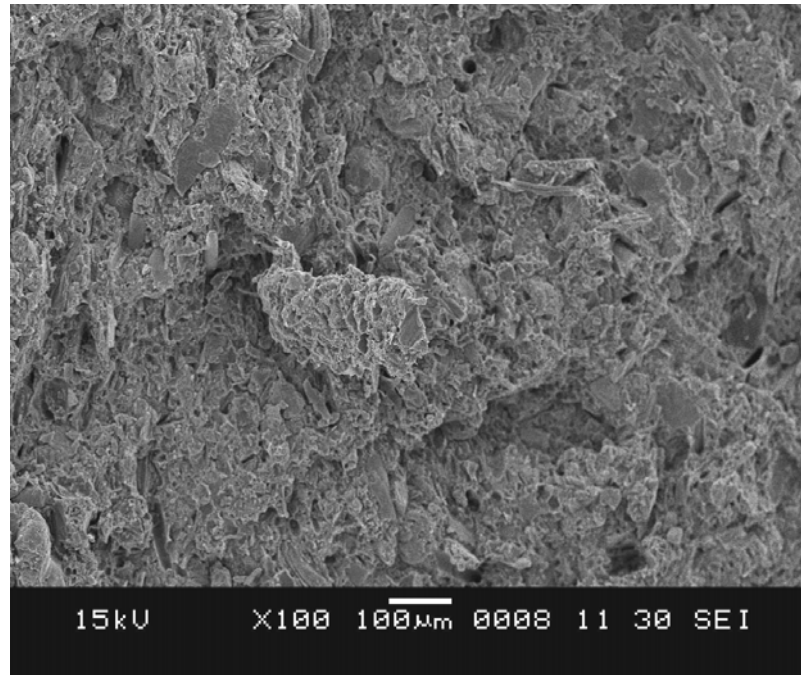
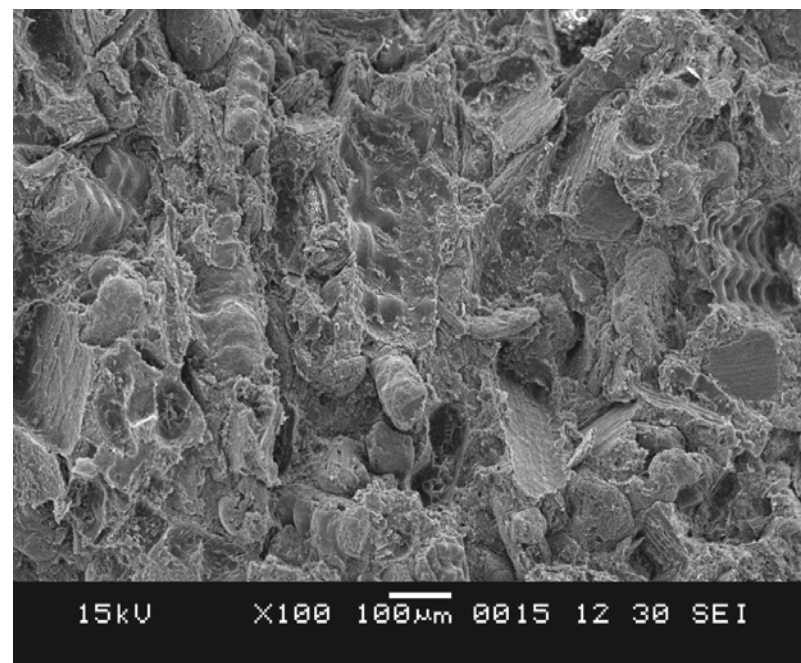


Figure 5.10 The impact value of the HDPE/RH composites filled with different particle sizes of rice husk at 10 (●), 20 (■), 30 (◆) and 40% by weight (▲).

Compared with the commercially available WPC, all of the results displayed that the HDPE/RH composites exhibited in the range of the impact value of the commercially available WPC. So, the HDPE/RH composites in the present study can be used as WPC to replace natural wood in application under impact resistance.



(a)



(b)

Figure 5.11 The SEM micrograph of the HDPE/RH composites with 40% of rice husk by weight at (a) 75µm and (b) 180µm.

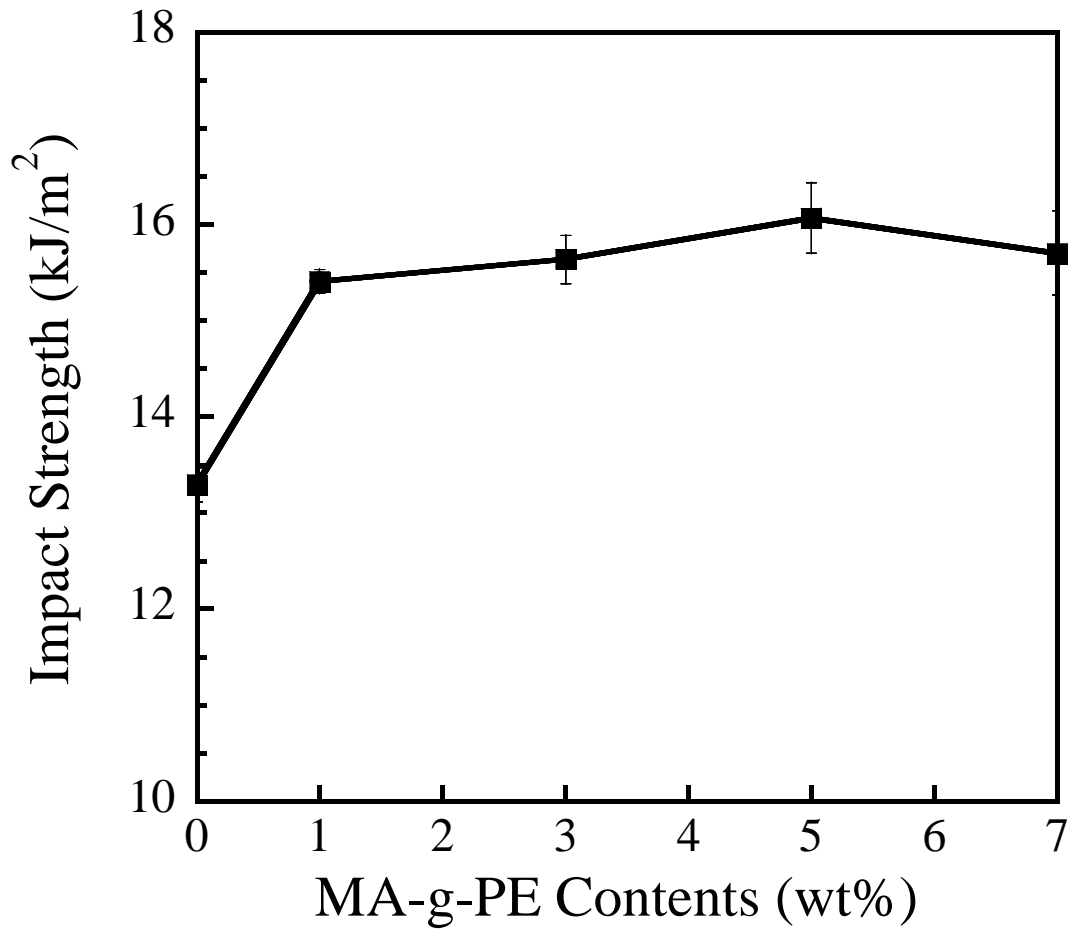


Figure 5.12 The impact strength of the HDPE/RH composites at 30% by weight of 500 μ m RH particle treated with MA-g-PE from 1 to 7% by weight.

5.1.4 Compressive Properties

The results of compressive modulus and compressive strength of the HDPE/RH composites are shown in Figure 5.13 and 5.14. The plots demonstrated clearly the increase of compressive modulus of the HDPE/RH composites with RH filler contents. The compressive modulus of the pure HDPE was 0.39 GPa. While the compressive modulus of the HDPE/RH composites at 10, 20, 30 and 40% by weight were found to increase by approximately 28%, 36%, 48% and 54% respectively. In contrast, the compressive strength of the HDPE/RH composites decreased with the incorporation of RH content as demonstrated in Figure 5.13. The compressive strength of the pure HDPE was 48.11 MPa. Those of the HDPE/RH composites are all lower than that of the pure HDPE by 8%, 11%, 16% and 22% respectively. The reduction was caused by poor dispersion of the RH filler in the HDPE matrix. Moreover, the increment of interfacial defects caused more debonding between the RH and the HDPE matrix. The size of the RH particles did not influence the change of compressive properties of the HDPE/RH composites. Figure 5.15 shows the compressive properties of the HDPE/RH composites treated with MA-g-PE ranging from 0 to 7% by weight. At 30% by weight of 500 μ m RH particle, the compressive modulus and compressive strength of HDPE/RH composites without MA-g-PE were 0.74 GPa and 40.27 MPa respectively. All the treated composites showed slightly higher in compressive strength of the HDPE/RH composites than those of the untreated ones.

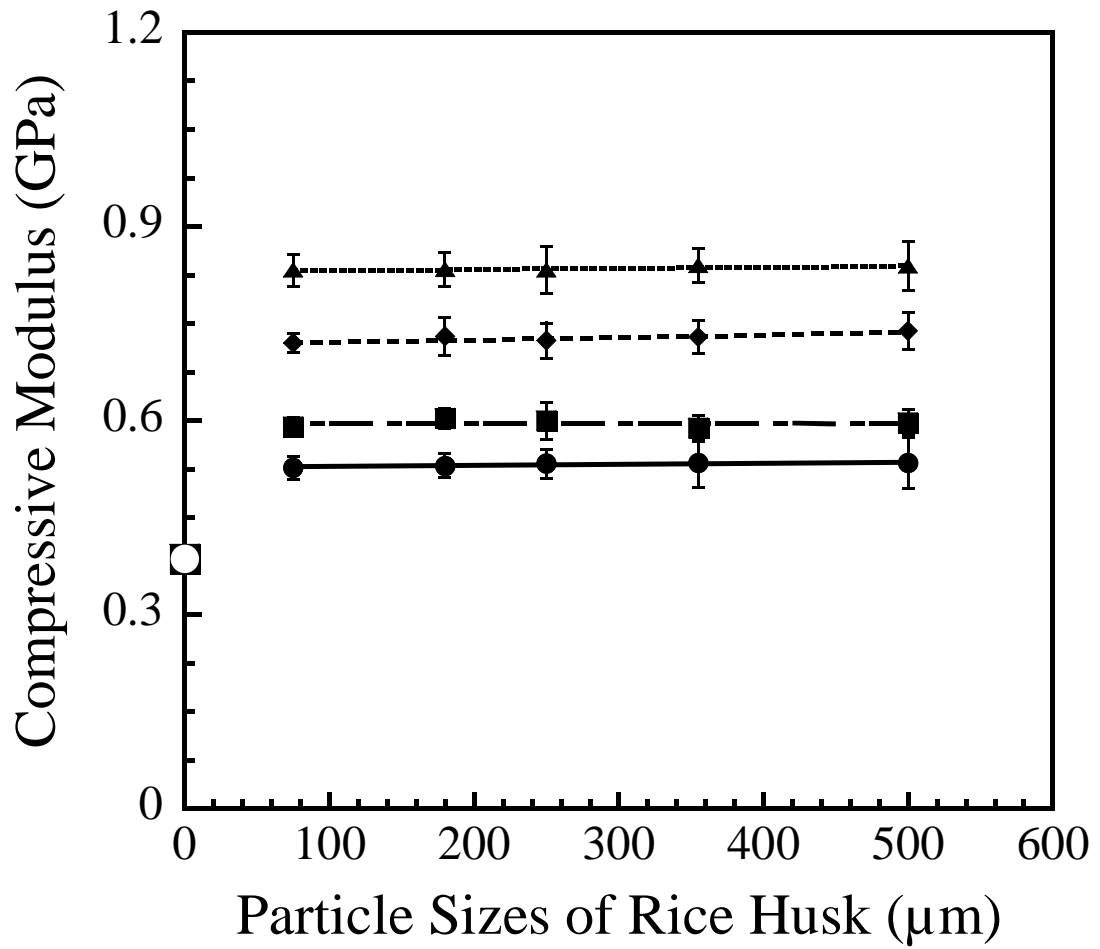


Figure 5.13 The compressive modulus of the HDPE/RH composites filled with different particle sizes of rice husk at 10 (●), 20 (■), 30 (◆) and 40% by weight (▲).

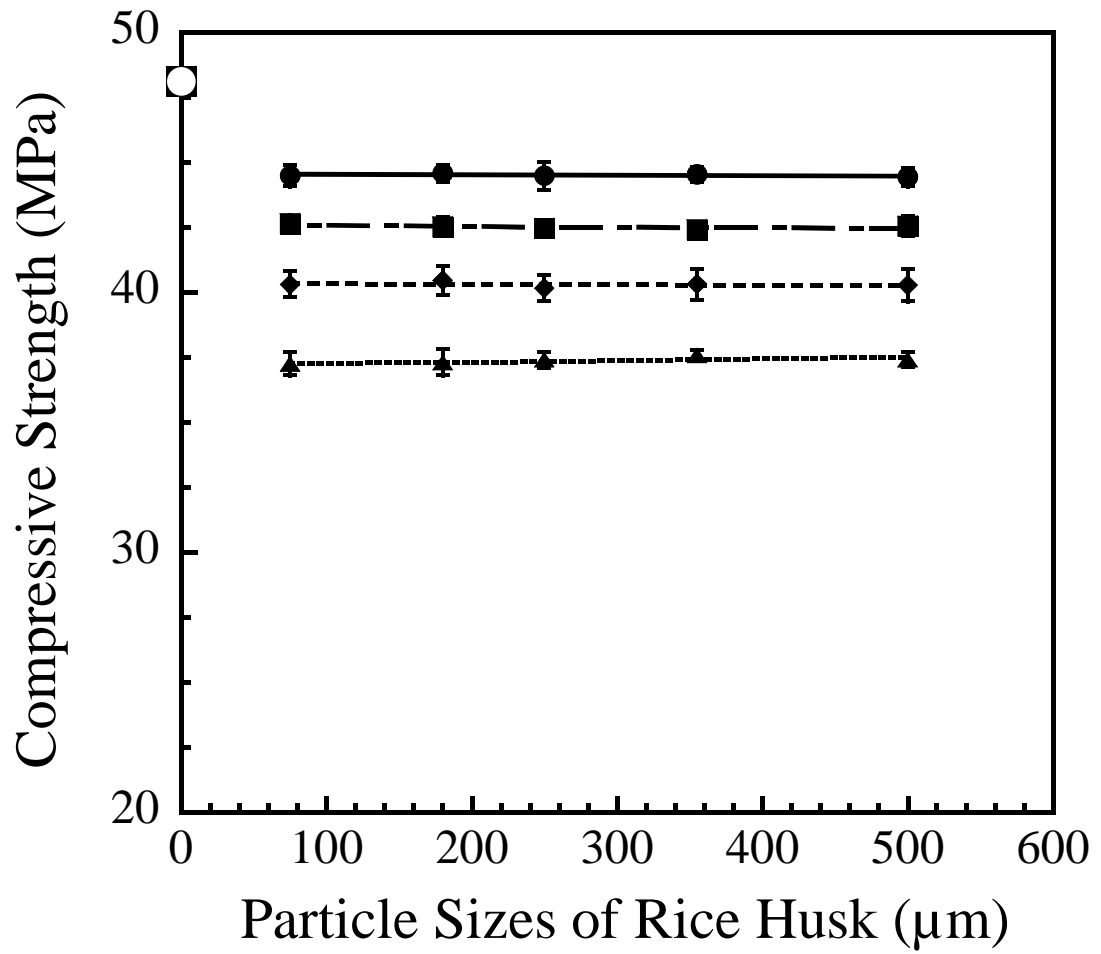


Figure 5.14 The compressive strength of the HDPE/RH composites filled with different particle sizes of rice husk at 10 (●), 20 (■), 30 (◆) and 40% by weight (▲).

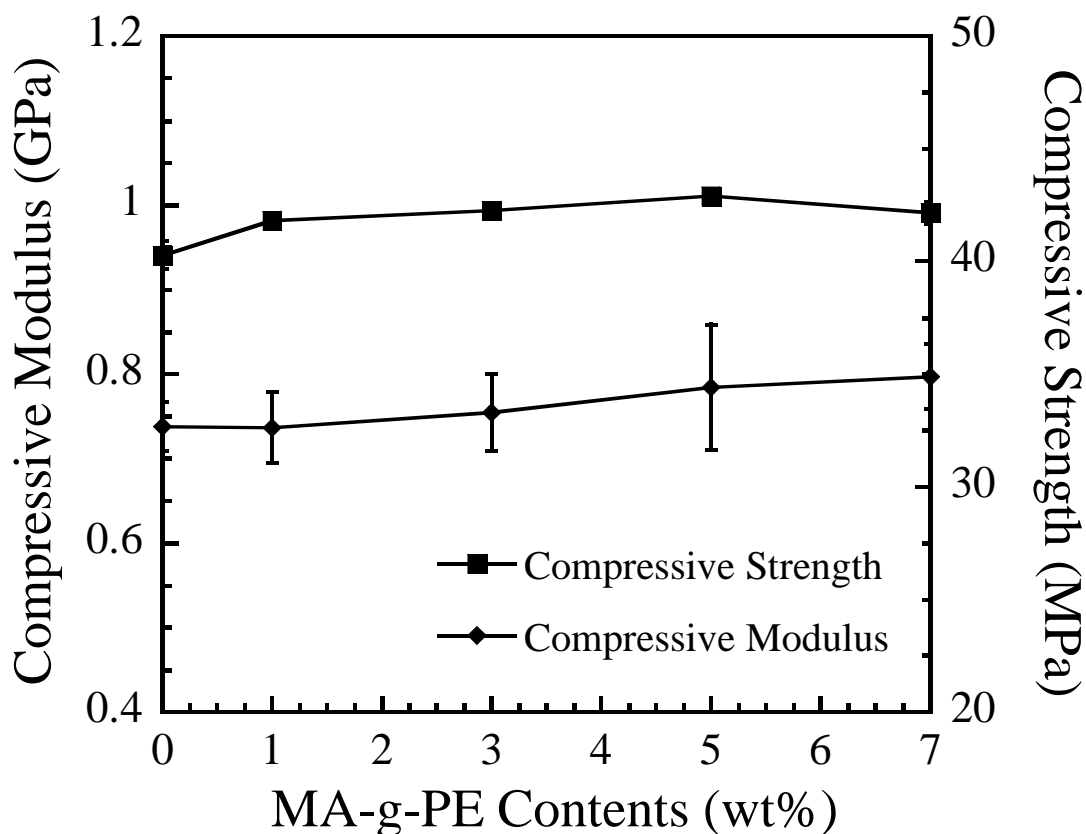


Figure 5.15 The compressive modulus and compressive strength of the HDPE/RH composites at 30% by weight of 500 μ m RH particle treated with MA-g-PE from 1 to 7% by weight.

5.2 Thermal Characterization of the HDPE/RH Composites

5.2.1 Thermogravimetric Analysis (TGA)

Figure 5.16 shows the TGA thermograms of the pure HDPE, RH and the HDPE/RH composites. The TGA curves indicated that the decomposition of RH occurred over the two temperature ranges, 70-100 °C and 250-350 °C. The first thermal degradation corresponded to dehydration whereas the second thermal degradation related to the thermal degradation of the organic compounds within the RH such as cellulose, hemicellulose and lignin, leaving a char yield of 40% by weight. The TGA curve of HDPE illustrated the range of decomposition from 400-470 °C. Above 500 °C, the quantity of the HDPE residue was very small due to the thermal

degradation of the HDPE into gaseous products at higher temperature. The HDPE/RH composites were decomposed at two temperature ranges, i.e. 250-350 °C and 400-470 °C. The first thermal degradation corresponded to the decomposition of the major constituents in the RH whereas the second thermal degradation was the thermal degradation temperature of the pure HDPE. At the first decomposition range, the weight loss of the HDPE/RH composites decreased with greater RH content and the weight loss of the HDPE/RH composites was 10 and 25% by weight at 10 and 40% by weight respectively. This is because HDPE which was decomposed had lower content. Furthermore, the char yield of the HDPE/RH composites increased with increasing RH contents. The char yield of the HDPE/RH composites at 10 and 40% by weight were 18 and 5% by weight respectively. The effects of RH particle sizes had no significant change on the degradation temperature (T_d) of the HDPE/RH composites, but it was found that the smaller particles affect on the decreased char yield of the HDPE/RH composites about 2% when compared with smaller particles. The TGA thermograms of the HDPE/RH composites at 30% by weight of 500 μ m RH particle with treated MA-g-PE ranging from 0 to 7% by weight as shown in Figure 5.17. From graph, the treated composites were decomposed at two temperature ranges, 250-350 °C and 400-470 °C as same as in those of the untreated composites. The thermal stability and degradation temperature of the HDPE/RH composites treated with MA-g-PE were slightly higher than those of untreated composites and were slightly increased with increasing MA-g-PE contents. The improved thermal stability of the treated composites was due to enhanced interfacial bonding.

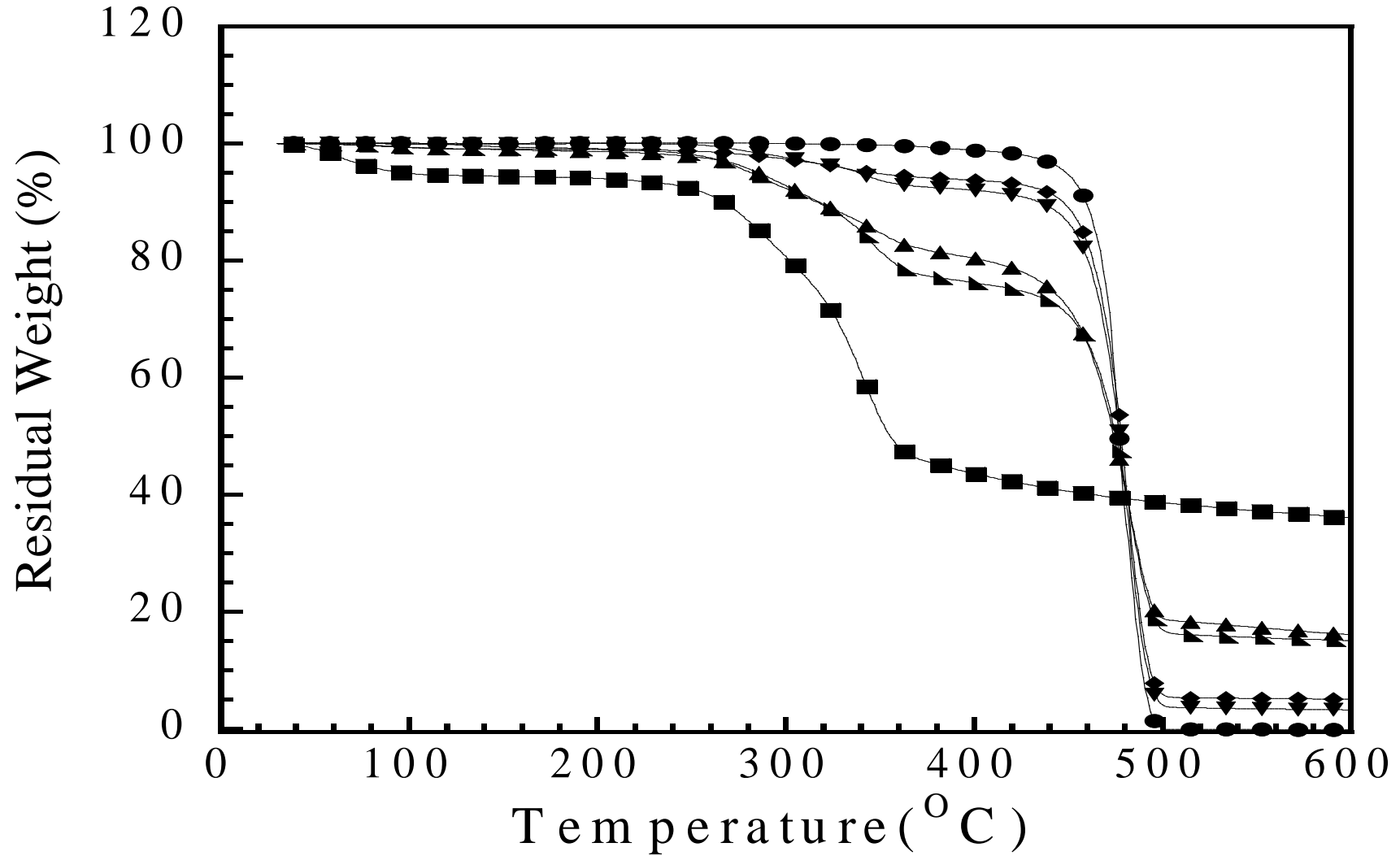


Figure 5.16 TGA thermograms of the pure HDPE (●), RH (■) and the HDPE/RH composites: 10 wt% 75 μm (◆), 40 wt% 75 μm (▲), 10 wt% 500 μm (▼) and 40 wt % 500 μm (▴).

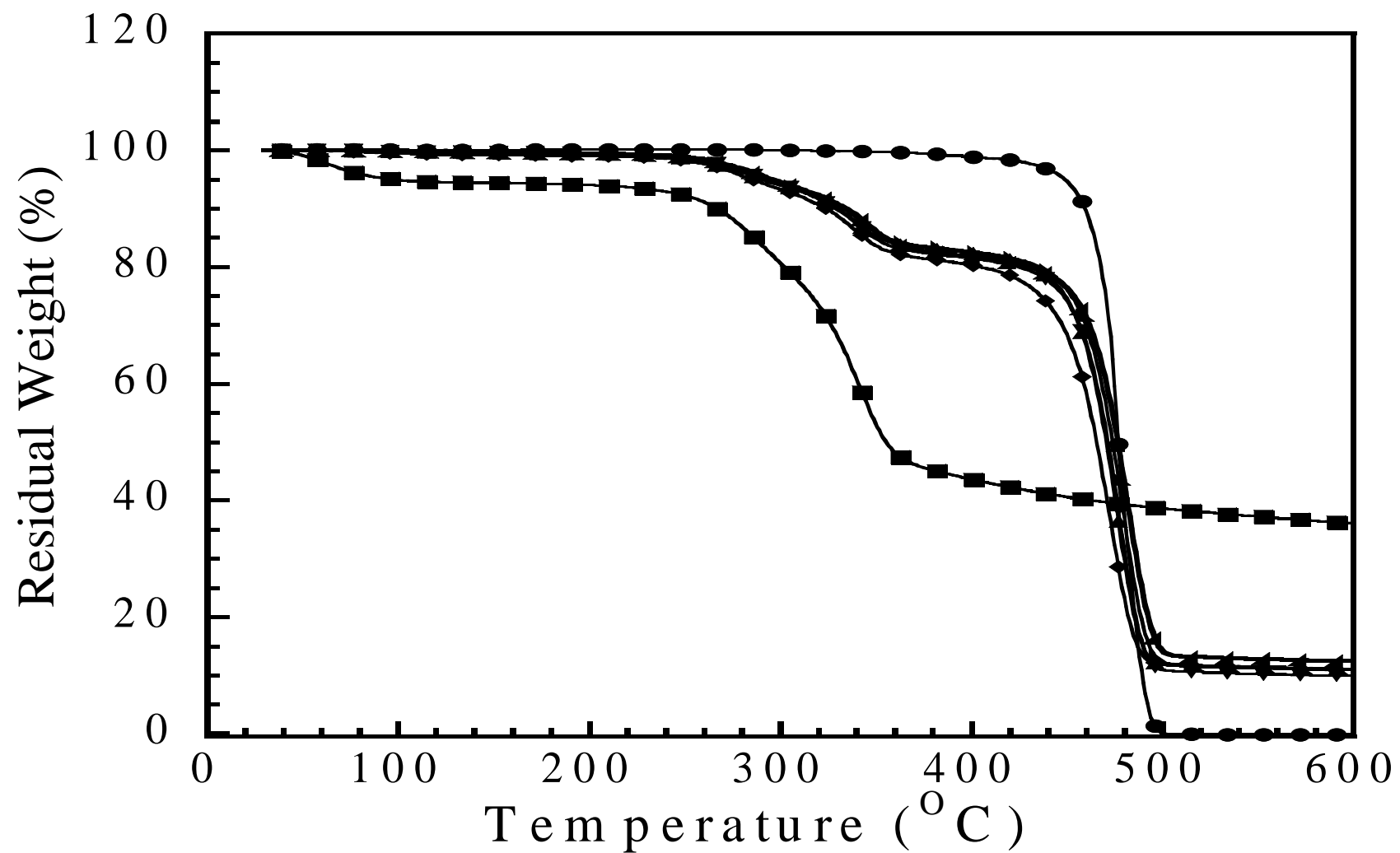


Figure 5.17 TGA thermograms of the pure HDPE (●), RH (■) and the HDPE/RH composites treated with MA-g-PE at 1% (▲), 3% (▼), 5% (◄) and 7% by weight (▲).

5.2.2 Glass Transition Temperature (T_g) and Melting Temperature (T_m) Measurement

The effects of the RH contents and its particle sizes on the glass transition temperature and melting temperature of the HDPE/RH composites were shown in Table 5.1. The T_g and T_m of pure HDPE were $-121.5\text{ }^\circ\text{C}$ and $134\text{ }^\circ\text{C}$ respectively. These results exhibited that the addition of RH in the HDPE matrix led a slightly changed T_m of the HDPE/RH composites compared to that of the pure HDPE. This might imply that the RH filler obstructed the motion of the HDPE chain in this composite. The size of RH did not affect T_g and T_m of the HDPE/RH composites. For example, T_g and T_m of the HDPE/RH composite with 40% by weight of $75\mu\text{m}$ RH particle was $-119.7\text{ }^\circ\text{C}$ and $136\text{ }^\circ\text{C}$ respectively. While T_g and T_m of the HDPE/RH composite with 40% by weight of $500\mu\text{m}$ RH particle was $-119.4\text{ }^\circ\text{C}$ and $136.1\text{ }^\circ\text{C}$ respectively. This effect can be explained that size of RH did not influence the change of the structure of composites. Moreover, it was no significantly changed in T_m and T_g when amount of MA-g-PE increased as illustrated in Table 5.2.

Table 5.1 Glass transition temperature (T_g) and melting temperature (T_m) of the HDPE/RH composites with different RH contents and particle sizes.

Particle size (μm)	Glass transition temperature ($^\circ\text{C}$)		Melting temperature ($^\circ\text{C}$)	
	10 wt%	40 wt%	10 wt%	40 wt%
75	-120.7	-119.7	134.3	136
500	-120.5	-119.4	134.5	136.1

Table 5.2 Glass transition temperature (T_g) and melting temperature (T_m) of the HDPE/RH composites treated with MA-g-PE from 1 to 7% by weight.

PE-g-MA content (wt %)	Glass transition temperature (°C)	Melting temperature (°C)
1	-120.2	134.1
3	-120.3	134.2
5	-120.3	134.5
7	-120.5	134.5

5.2.3 Heat Deflection Temperature (HDT)

Figure 5.18 was used to establish the effects of the RH contents and particle sizes on the heat deflection temperature of the HDPE/RH composites. The deflection temperature of the pure HDPE was achieved by 71.8 °C. All the composites were found to have greater HDT than that of the pure HDPE. The HDPE/RH composites with higher RH content also exhibited greater HDT. This phenomenon is seemed to relate with those having RH which is rigid phase, its presence restricted the mobility of the HDPE molecules, tend to resist heat deflection better than the pure HDPE. Therefore, the more RH content in HDPE matrix is, the better the composites can withstand heat before distortion. Furthermore, it was seen that the HDT increased with increasing RH particle sizes. The HDPE/RH composites with larger RH particle at 500 μ m exhibited a slightly higher deflection temperature than that with smaller RH particle at 75 μ m. The heat deflection temperature of the HDPE/RH composites at 30% by weight of 500 μ m RH particle with treated MA-g-PE ranging 0 to 7% by weight as shown in Figure 5.19. From the figure, it was found that the HDPE/RH composites treated with MA-g-PE ranging from 0 to 7% by weight were higher value of HDT of the HDPE/RH composites compared to the pure HDPE. These results were explained in the term of bonding energy. The bonding energy of the untreated composites, example an O-H bond of cellulose structure in RH was 111 kcal/mole and the C-H bond of the structures of PE backbone was 99 kcal/mole [60],

so the bonding energy of the untreated composites was 210 kcal/mole. While the bonding energy of the treated composites had not only the similar results as those of the untreated composites, but also the addition part of the bonding energy of the used of MA-g-PE as coupling agent, such as the C-O bond, C=O bond (halide) and C-C bond were 85.5, 177 and 83 kcal/mole respectively and the C=O bond (ester) was 179 kcal/mole [60] which occurred from esterification between the RH and the HDPE matrix. So, the bonding energy of the treated composites was 734.5 kcal/mole. The bonding energy of the treated composites had greater than those of the untreated composites because the energy needed to break a particular bond in molecule leading to resist heat before composites form under load.

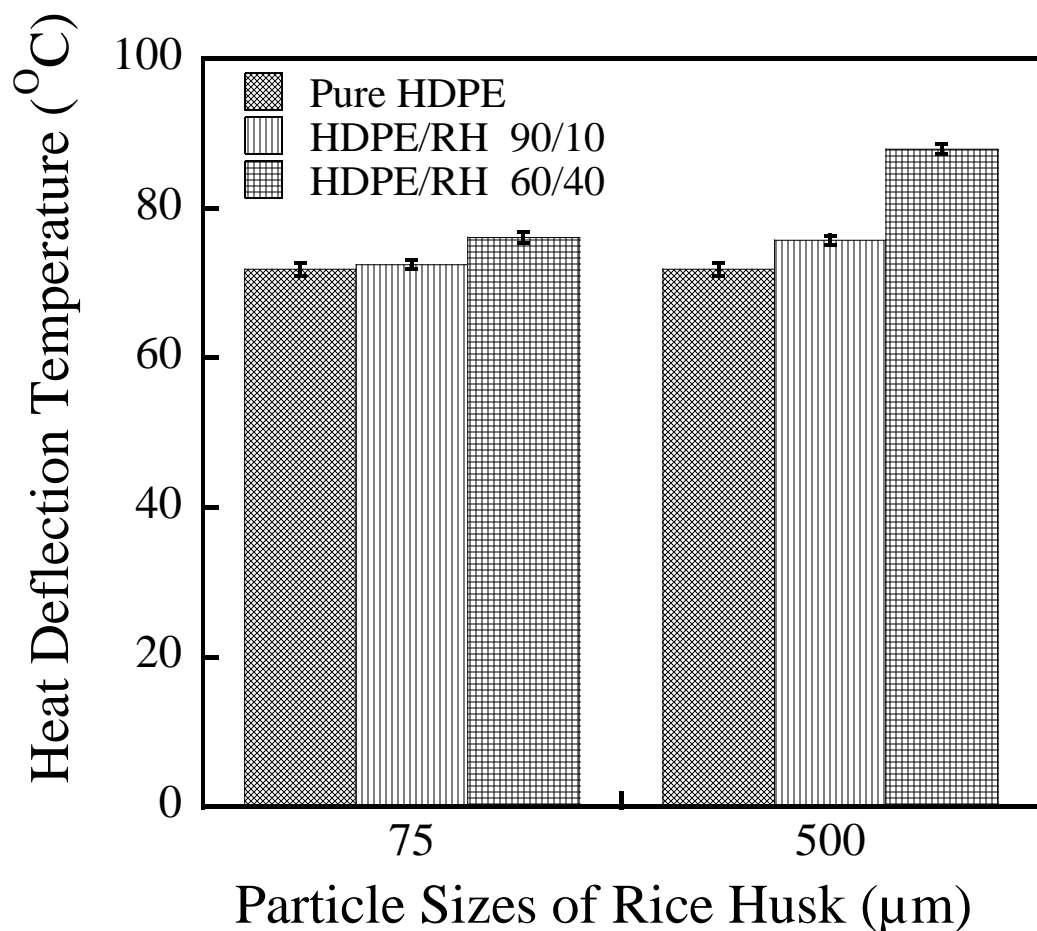


Figure 5.18 The heat of deflection temperature of the pure HDPE, the HDPE/RH composites with different RH contents and particle sizes.

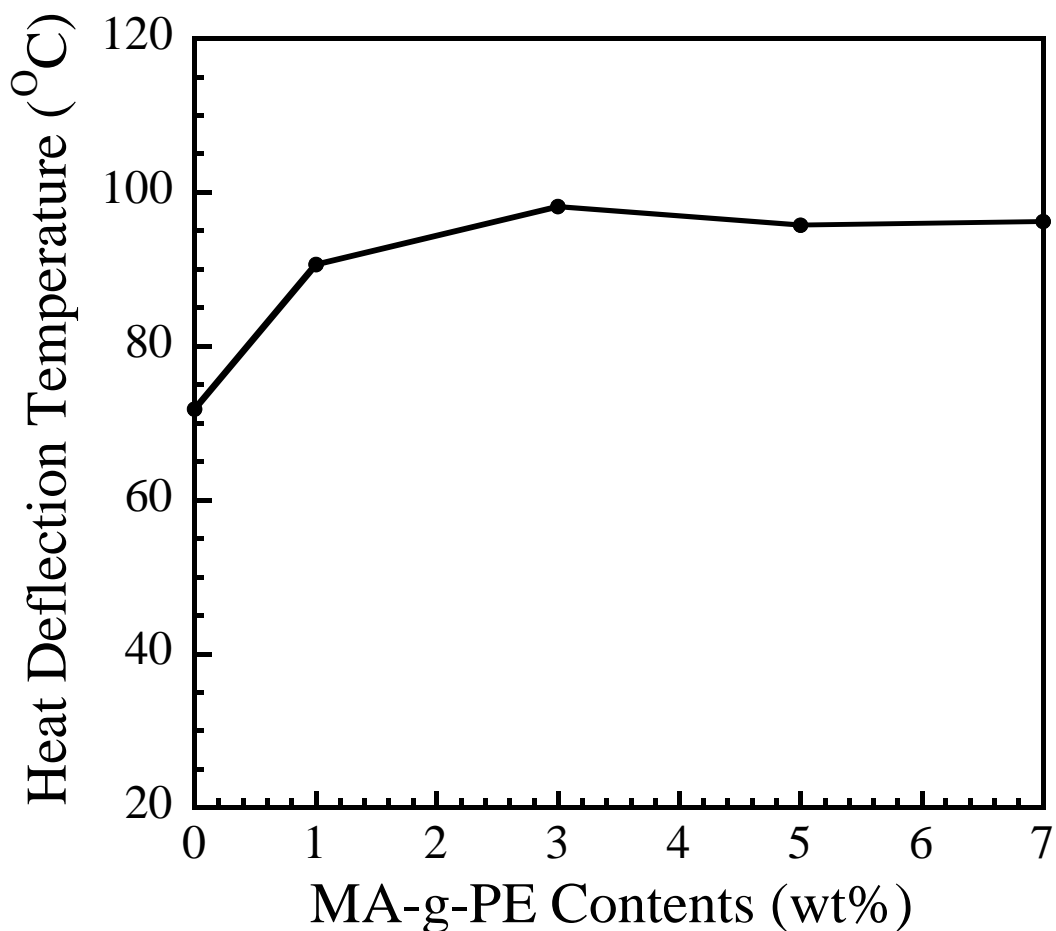


Figure 5.19 The heat deflection temperature of the HDPE/RH composites treated with MA-g-PE at 1 to 7% by weight.

5.3 Physical Characterization of the HDPE/RH Composites

5.3.1 Density Measurement

The density of the HDPE/RH composites was demonstrated in Figure 5.20. The measured density of the pure HDPE at room temperature was 0.95 g/cm^3 whereas density of the rice husk was 1.35 g/cm^3 . The density of all the HDPE/RH composites was clearly increased with increasing rice husk contents. This effect demonstrated that the density rises as a result of the higher density of the rigid rice husk particles with comparing to the pure HDPE. The results indicated that size of RH had no significant change on density of the HDPE/RH composites.

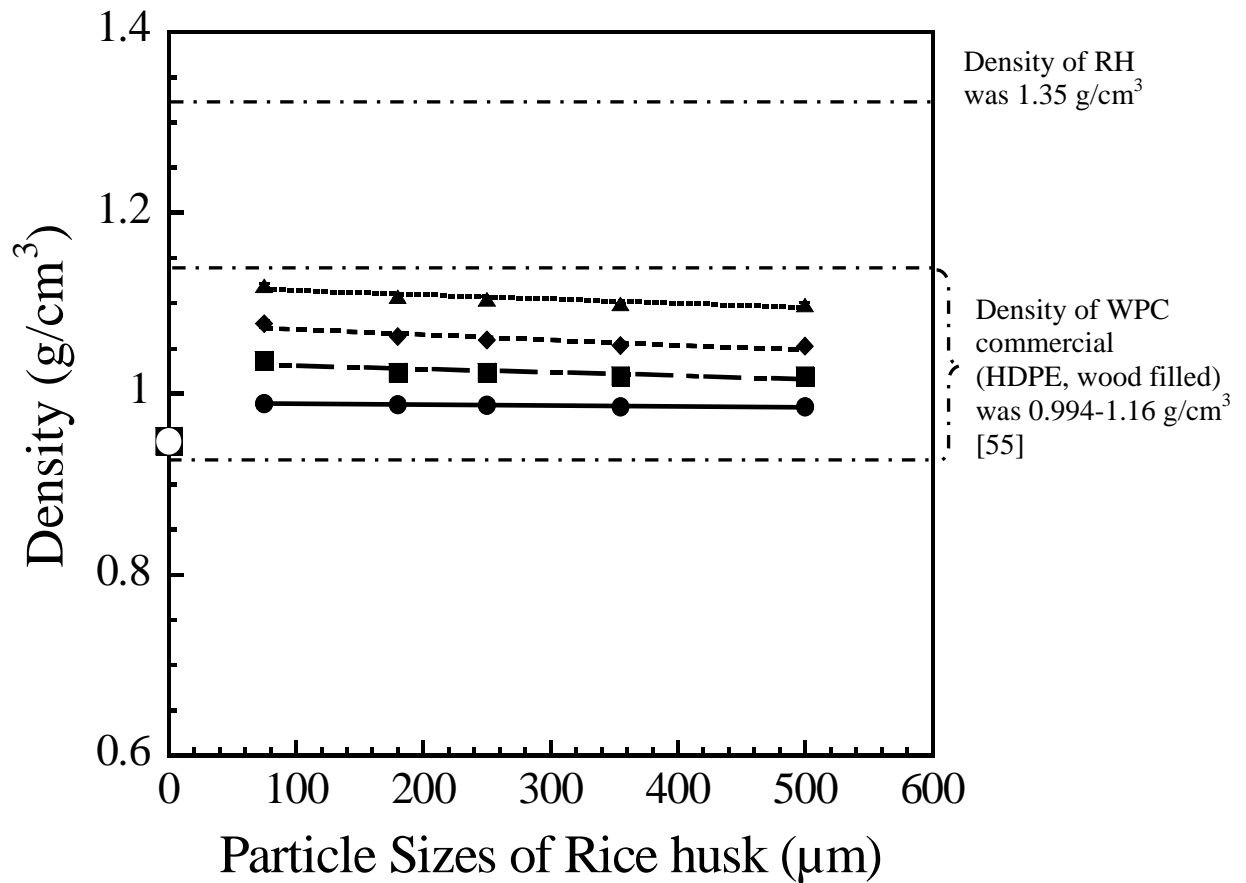
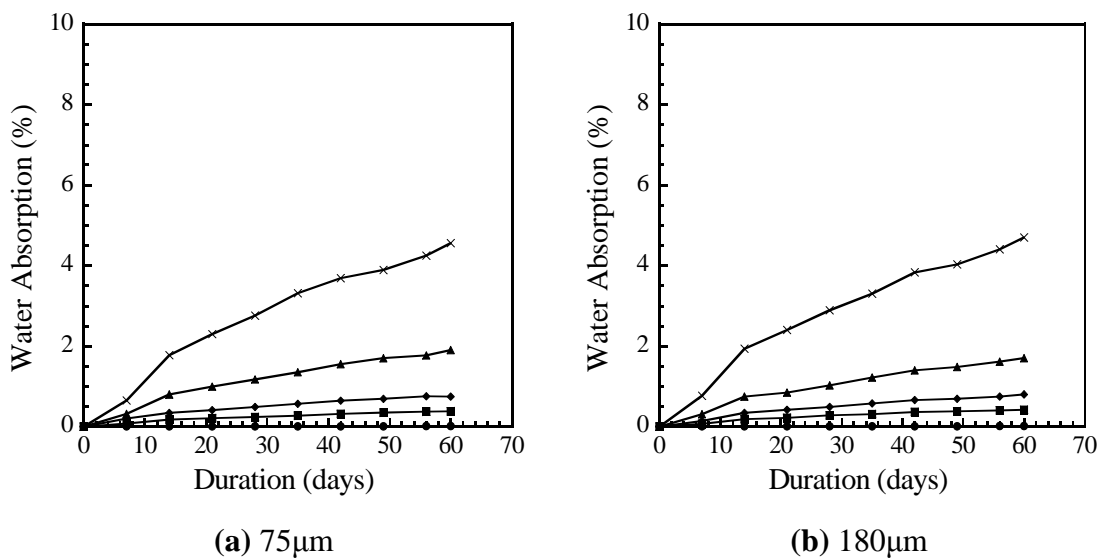


Figure 5.20 The density of the HDPE/RH composites filled with different particle sizes of rice husk at 10 (●), 20 (■), 30 (◆) and 40% by weight (▲).

Compared with the density of the commercially available WPC, the density of the HDPE/RH composites was 0.987-1.117 g/cm³ which was in the density range of the commercially available WPC.

5.3.2 Water Absorption Measurement

Figure 5.21(a)-(e) present the water absorption behaviors of the pure HDPE and the HDPE/RH composites. With greater RH content, the rate of water absorption of the HDPE/RH composites clearly increased. After that, the rate of initial water absorption of the HDPE/RH composites was slowly declined. The water absorption of the HDPE/RH composites at the soaking time of 60 days is demonstrated in Figure 5.22. The water absorption of the pure HDPE was 0.06%. That of the HDPE/RH composites was all higher than that of the pure HDPE. All the HDPE/RH composites showed high uptake of water when greater amount of RH was applied. The water absorption of the HDPE/RH composites was higher with the increment of the RH contents by 22%, 48%, 73% and 101% which corresponded to the RH content of 10, 20, 30 and 40% by weight respectively. The presence of the hydroxyl group of the lignocellulosic constituent of the rice husk filler, was responsible for the absorption of water. Again the size of the RH had no significant influence on the water absorption of the HDPE/RH composites.



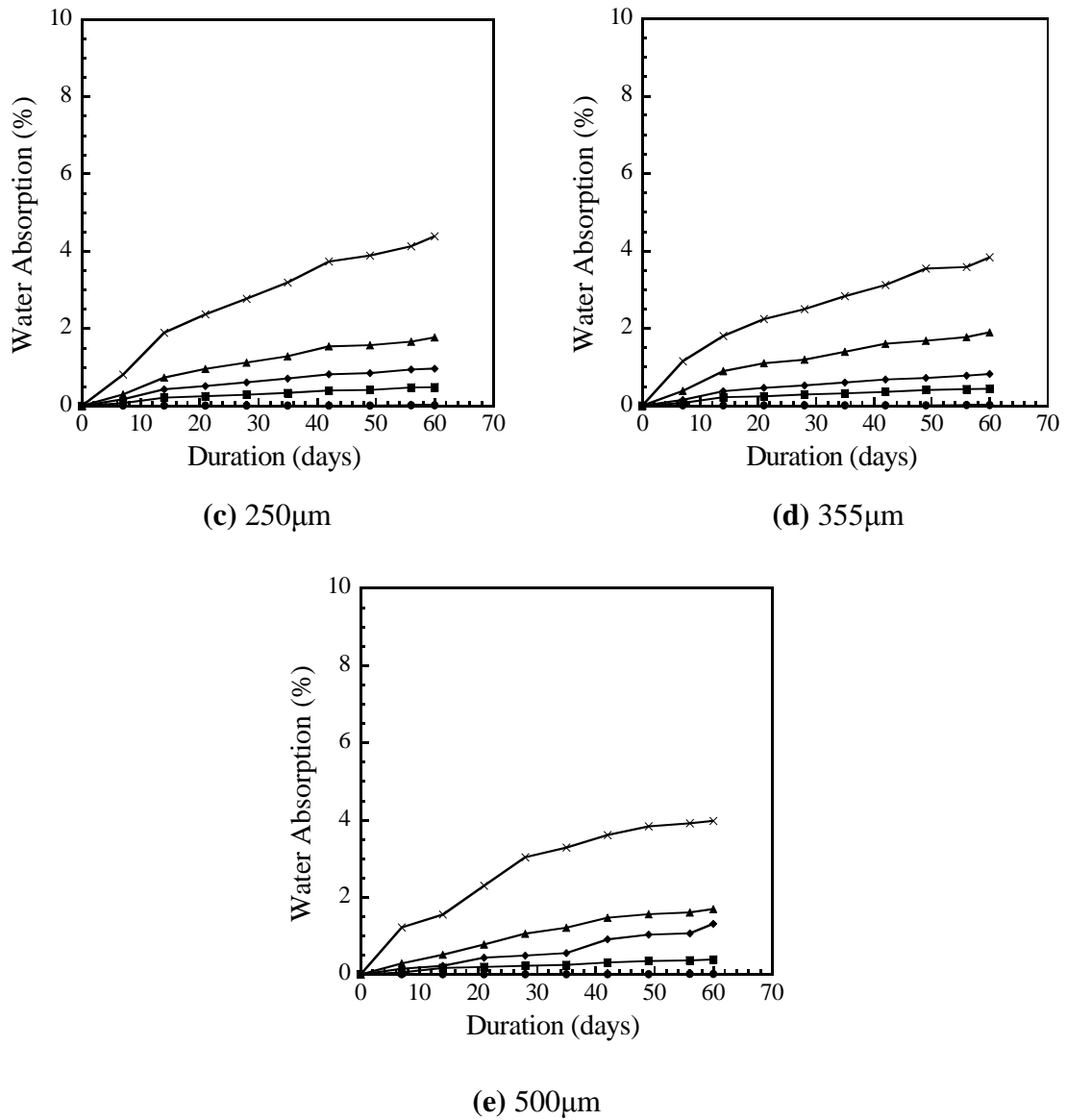


Figure 5.21 The water absorption behavior of the pure HDPE (●) and the HDPE/RH composites filled with different RH contents of 10 wt% (■), 20 wt% (◆), 30 wt% (▲) and 40 wt% (×) at (a) 75 μ m, (b) 180 μ m, (c) 250 μ m, (d) 355 μ m and (e) 500 μ m.

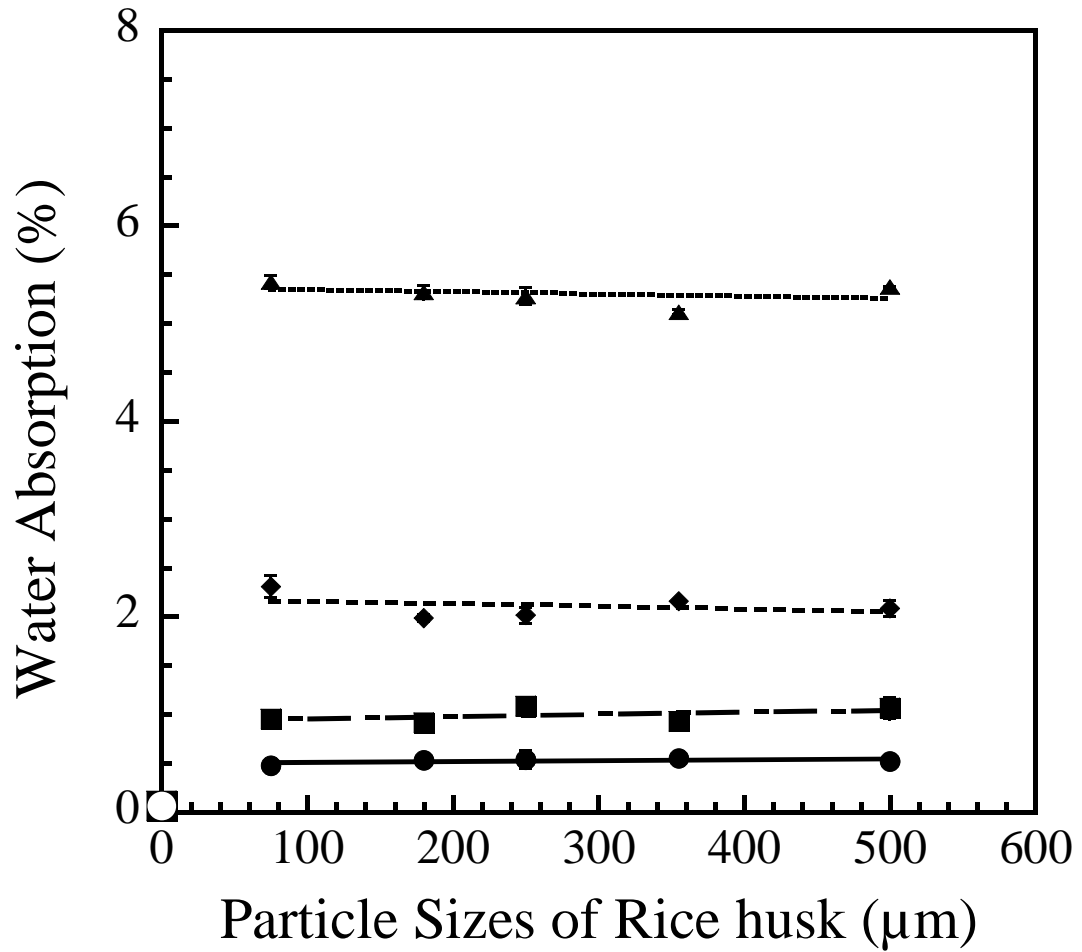


Figure 5.22 The water absorption of the HDPE/RH composites filled with different particle sizes of rice husk at 10 (●), 20 (■), 30 (◆) and 40% by weight (▲) after 60 days of immersion in water.

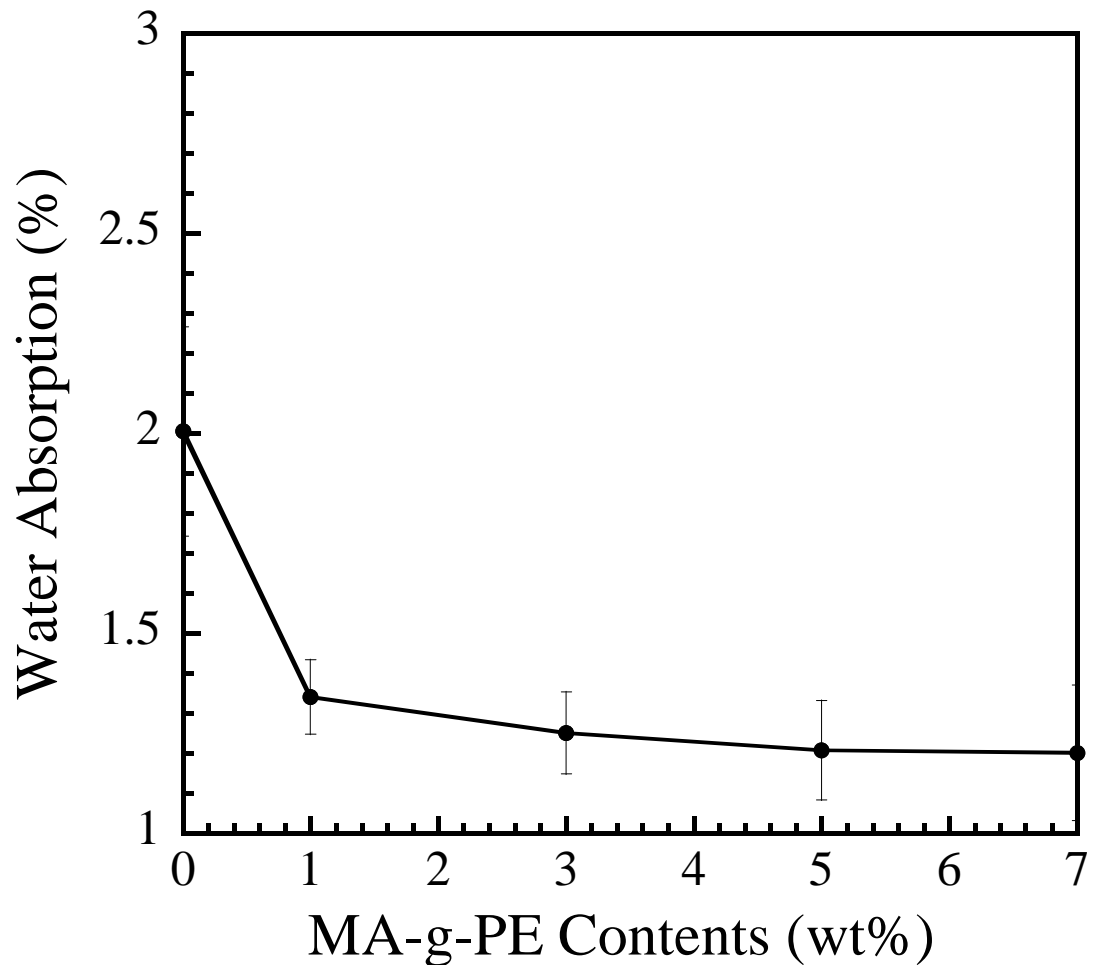


Figure 5.23 The water absorption of the HDPE/RH composites treated with MA-g-PE at (a) 1%, (b) 3%, (c) 5% and (d) 7% by weight.

Figure 5.23 shows the water absorption of the HDPE/RH composites at 30% by weight of 500 μ m RH particle treated with MA-g-PE from 1 to 7% by weight. The addition of the MA-g-PE as coupling agent, the rate of water absorption was clearly decreased. Because the MA-g-PE can enhance the interfacial bonding. These voids cause from the poor adhesion between the RH and the pure HDPE which the filtration of water or moisture was slightly occurred. The treated composites reduced the water absorption by approximately 33%, 38%, 40% and 41% respectively at MA-g-PE contents of 1, 3, 5 and 7% by weight.

5.3.3 Visual Appearance

In terms of appearance, the HDPE/RH composites with smaller rice husk particles appeared homogeneously with dark brown color while those with larger particles have a lighter shade of brown as shown in Figure 5.24. The fine particle size of 75 μm functioned as a pigment in the HDPE/RH composites. The large rice husk particle sizes such as at 355 and 500 μm , showed up as spots on the HDPE matrix. The HDPE/RH composites have the appearance of wood.

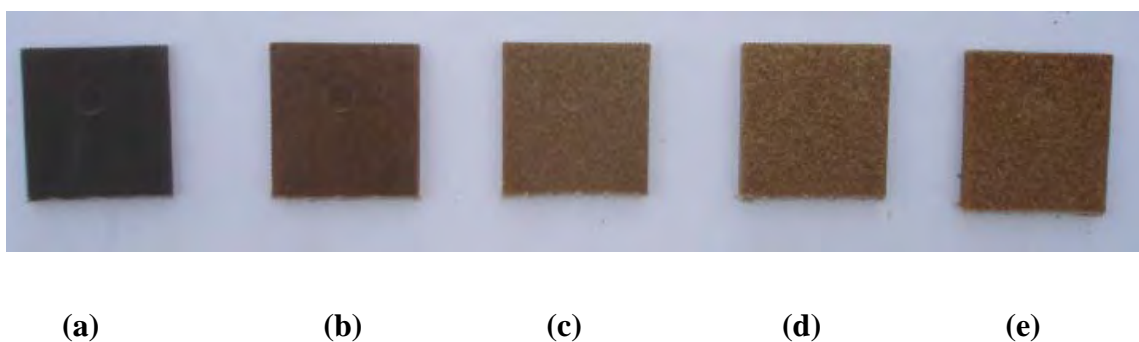


Figure 5.24 The appearance of the HDPE/RH composites at 40% by weight: (a) 75 μm , (b) 180 μm , (c) 250 μm , (d) 355 μm and (e) 500 μm .

5.3.4 Natural Weathering Test

The effect of UV-natural weathering on visual appearances of the HDPE/RH composites was studied by exposing the specimens to natural UV for 60 days since January to February 2008 at the top of a five-story building in Bangkok, Thailand. The exposed HDPE/RH composites are illustrated in Figure 5.25. The pure HDPE exhibited light yellow color after the 60 days UV exposure. The weathered HDPE/RH composite was clearly paler in color than those of non-weathered. Further, the weathered HDPE/RH composite showed more surface roughness comparing to the non-weathered ones.



Figure 5.25 Visual appearances of the HDPE/RH composites at 40% by weight, (a) 75 μm , (b) 180 μm , (c) 250 μm , (d) 355 μm , (e) 500 μm , (f) pure HDPE before and after natural UV-weathering testing for 60 days.

5.4 Interfacial Characterization of the HDPE/RH Composites

5.4.1 Morphological Characteristics

The morphology of the tensile fractured surfaces of untreated composites at different RH contents and particle sizes as illustrated in Figure 5.26. From figure, it was found that the presence of the large amount of gaps means that the poor bonded interfacial area between the RH filler and the HDPE matrix causes the stress was not

well propagated at interface in the composite. At RH content of 10% by weight (Fig 5.26(a), (c)), slightly increased amounts of spaces where RH particles was pulled out. At RH content of 40% by weight (Fig 5.26(b), (d)), it was found that more agglomeration of the RH particles were seen rather than the HDPE matrix. Moreover, the HDPE/RH composites with larger particle sizes showed numerous partial separations between phases, as compared to that with smaller particles as shown in Figure 5.27. On the contrary, the HDPE/RH composite treated with MA-g-PE improved RH matrix adhesion. As implied from Figure 5.27 (a)-(d), from figure, a few traces where RH particles was pulled out. It was also observed that the treated RH was uniformly coated by layers of the HDPE matrix that reduced the interfacial between them. This phenomenon indicated that the improved interfacial adhesion resulted in the RH filler to support stresses well transferred from the HDPE matrix led to increasing of modulus and strength of the HDPE/RH composites.

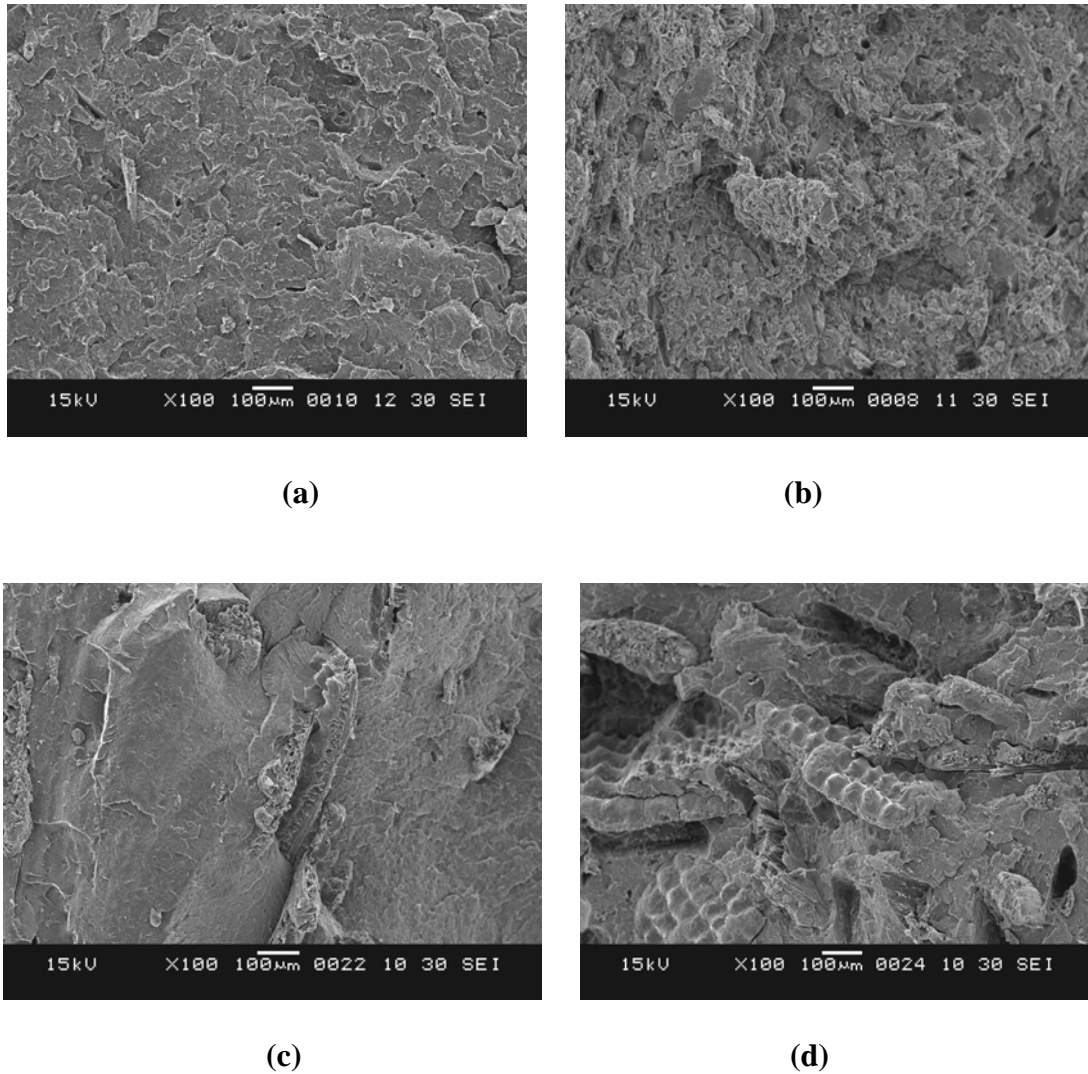


Figure 5.26 The SEM micrograph of the HDPE/RH composites filled with different RH contents and particle sizes: (a) 10 wt%, 75 μm (b) 40 wt%, 75 μm (c) 10 wt%, 500 μm (d) 40 wt%, 500 μm.

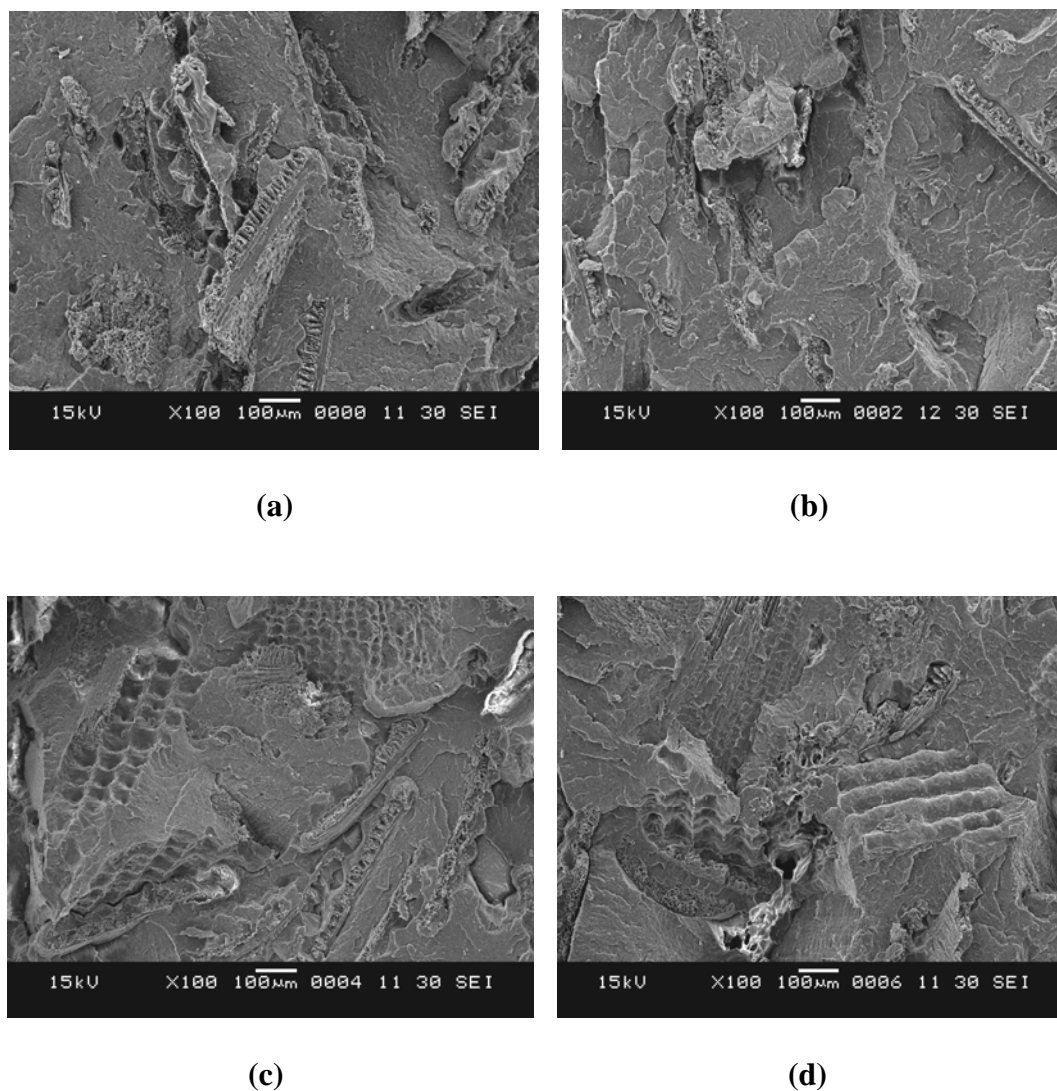


Figure 5.27 The SEM micrograph of the HDPE/RH composites treated with MA-g-PE at (a) 1%, (b) 3%, (c) 5% and (d) 7% by weight.

5.4.2 Attenuated Total Reflectance (ATR-IR) Analysis

Results obtained from the analysis of the HDPE/RH composites and those modified with 7% MA-g-PE (30% by weight of 500 μm in RH size) using attenuated total reflectance (ATR-IR) are shown in Figure 5.28. From the spectrum of the pure HDPE, strong peaks at 2850 cm^{-1} (CH stretching) and 1470 cm^{-1} (CH_2 deformation) are observed respectively. These peaks are the characteristic signals of the structures of PE backbone. The spectrum of MA-g-PE exhibited not only the same peaks as those of the HDPE matrix, but also the characteristic peak at 1700 cm^{-1} , which were assigned to symmetric C=O stretching of MA functions grafted on PE.

For the untreated HDPE/RH composites, the peaks around 3300 cm^{-1} were observed. This result indicated OH functional group of rice husk. For the HDPE/RH composites treated with MA-g-PE, the peak at 1730 cm^{-1} was observed. That relates to the stretching vibration of the ester groups (C=O stretching) which is resulted from esterification reaction between the hydroxyl groups of rice husk and the carbonyl groups of MA-g-PE to form covalent bonding. This phenomenon related to the property improvement of the HDPE/RH composites.

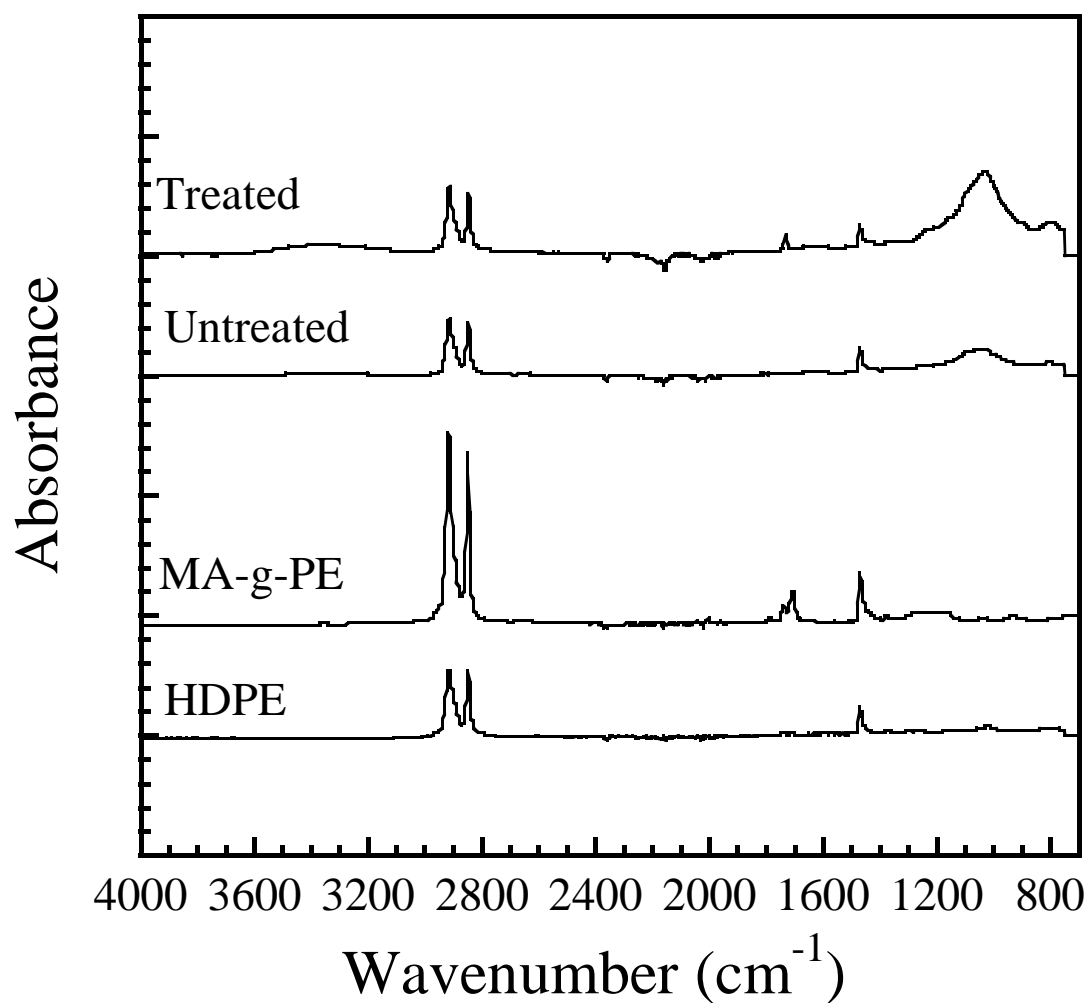


Figure 5.28 The ATR-IR spectra of the pure HDPE, MA-g-PE, untreated and treated HDPE/RH composites with 7% by weight (30% by weight of 500 μm in RH size).

5.5 Cost Analysis of the HDPE/RH Composites

The cost analysis of the HDPE/RH composites is based on the raw materials cost as calculated in Table 5.3. The costs of the HDPE resin and the RH were 53.50 and 1 Baht/kg respectively. [58, 59] The production cost of the HDPE/RH composites clearly decreased with increasing RH contents. The increment of RH contents at 20, 30 and 40% by weight, the production cost of the HDPE/RH composites was found to decrease by approximately 10.88%, 21.76% and 32.64% respectively.

Table 5.3 The raw materials cost of the HDPE/RH composites.

Materials	Price (Baht/kg)	Weight (kg)			
		10 wt%	20 wt%	30 wt%	40 wt%
HDPE Resin	53.5	0.9	0.8	0.7	0.6
Rice husk	1	0.1	0.2	0.3	0.4
Cost (Baht/Kg)		48.25	43.00	37.75	32.50

CHAPTER VI

CONCLUSIONS AND RECOMMENDATIONS

6.1 Conclusions

6.1.1 The addition of the rice husk into HDPE matrix can enhance the wood composite's properties by

- With increasing RH content led to increase the flexural, tensile and compressive modulus due to the RH provided higher stiffness and modulus than HDPE matrix. But the tensile, flexural, compressive and impact strength were lowered because the poor interfacial bonding between HDPE and RH. Furthermore, the glass transition temperature (T_g), melting temperature (T_m) and heat deflection temperature (HDT) increased slightly. The increment of both density and water absorption by raising the RH content. The water absorption of the HDPE/RH composites induced the darker color to the WPC.
- The RH particle sizes did not influence the tensile, flexural and compressive properties, but it was found that the larger RH particles provided better impact strength than the smaller ones. The RH particle sizes did not influence glass transition temperature (T_g), melting temperature (T_m), heat deflection temperature (HDT) and degradation temperature (T_d) of the HDPE/RH composites. The HDPE/RH composites with smaller RH appeared the darker color than the larger ones.
- After outdoor weather exposure for 60 days, the weathered HDPE/RH composite was clearly paler in color than those of non-weathered

6.1.2 The addition of the MA-g-PE as coupling agent can enhance the wood composite's properties by

- The utilization of coupling agent improved the interfacial adhesion between HDPE and RH led a higher mechanical properties and thermal stability of the HDPE/RH composites. These results can be confirmed by SEM micrograph. With increasing in MA-g-PE contents, affected on the mechanical properties, the melting temperature, the heat deflection temperature and the degradation temperature of the HDPE/RH composites increased slightly, but it did not affect on the glass transition temperature. In addition, the rate of water absorption clearly decreased when the MA-g-PE contents increased.
- The FTIR spectra of the treated and untreated HDPE/RH composites were also studied to confirm the existence of type of interfacial bonds.

6.2 Recommendations for Future Study

- i) Comparison with other coupling agents for the HDPE/RH composites to enhance interfacial bonding.
- ii) Investigation of the effects of environment such as chemical resistance, exposure to UV and weathering on the mechanical properties.
- iii) Incorporation of blowing agents to produce the HDPE/RH foamed composites.

REFERENCES

- (1) Clemons C. Wood-plastic composites in the United States. The interfacing of two Industries. Forest Prod J. 52(2002) : 10-20.
- (2) A.K. Mohanty. ; M. Misra. ; and L.T. Drzal. Natural Fibers, Biopolymers, and Biocomposites. New York : CRC Press, 2005.
- (3) Jennifer Markarian. Wood-plastic composites: current trends in materials and processing. Plastics, Additives and Compounding. September-October 7(2005) : 20-26.
- (4) Nicholas P. Cheremisinoff. Handbook of Polymer Science and Technology. New York and Basel : MARCEL DEKKER, INC.
- (5) John Z. Lu.; Qinglin Wu.; and Ioan I. Negulescu. Wood-Fiber/High-Density-Polyethylene Composites: Coupling Agent Performance. Journal of Applied Polymer Science 96(2005) : 93–102.
- (6) L. Chotirat.; K. Chaochanchaikul.; and N. Sombatsompop. On adhesion mechanisms and interfacial strength in acrylonitrile–butadiene–styrene/wood sawdust composites. International Journal of Adhesion & Adhesives 27(2007) : 669–678.
- (7) H. Jiang.; and D. P. Kamdem. J. Vinyl. Additive Technology. 10 (2004).
- (8) Reinhart, T.J.; and Clements, L.L. Engineered Material Handbook. Ohio : ASTM International, 1989.
- (9) Peter C. Powell. Engineering with fibre-polymer laminates. London. Chapman & Hall, 1994.
- (10) I S Miles.; and S Rostami. Multicomponent Polymer Systems. New York : Longman Publishers, 1994.
- (11) Gachter, R.; and Muller H. Plastics Additives Handbook. New York : Hanser Gardner Publications, 1987.
- (12) Hull, D. An Introduction to Composite Materials. Cambridge : Great Britain at the University Press, 1990.
- (13) Kenneth G. Budinski. Engineering Materials Properties and Selection. Prentice-Hall International, Inc. 1992.
- (14) Manas C.; and Salil K. Roy. Plastic Technology Handbook. 1987.

- (15) Fried, J.R. Polymer Science and Technology. New Jersey : Prentice-Hall International, Inc., 1995
- (16) J.A. Brydson. Plastics Materials. Butterworth Heinemann, 1995.
- (17) Kishi, H.; M. Yoshioka.; A. Yamanoi.; and N. Shiraishi. Composites of wood and polypropylenes I. Mokuzai Gakkaishi 34 (1988) : 133-139.
- (18) Filex, J. M.; and P. Gatenholm. The nature of adhesion in composites of modified cellulose fibers and polypropylene. J. Appl. Polym. Sci. 42(1991) : 609-620.
- (19) L.M. Matuana.; K. Carlborn. Process for the Preparation of Maleated Polyolefin Modified Wood Particles in Composites and Products. US Patent, (Pending since July 30, 2005).
- (20) Hee-Soo Kim.; Byoung-Ho Lee.; Seung-Woo Choi.; Sumin Kim.; and Hyun-Joong Kim. The effect of types of maleic anhydride-grafted polypropylene(MAPP) on the interfacial adhesion properties of bio-flour-filled polypropylene composites. Composites: Part A 38 (2007) : 1473–1482.
- (21) Han-Seung Yang a.; Michael P. Wolcott a.; Hee-Soo Kim b.; Sumin Kim b.; and Hyun-Joong Kim. Effect of different compatibilizing agents on the mechanical properties of lignocellulosic material filled polyethylene bio-composites. Composite Structures (2006).
- (22) Mohd Suzeren Jamil.; Ishak Ahmad.; and Ibrahim Abdullah. Effects of Rice Husk Filler on the Mechanical and Thermal Properties of Liquid Natural Rubber Compatibilized High-Density Polyethylene/Natural Rubber Blends. Journal of Polymer Research 13 (2006) : 315-321.
- (23) Smita Mohanty.; Sushil K. Verma.; and Sanjay K. Nayak. Dynamic mechanical and thermal properties of MAPE treated jute/HDPE composites. Composites Science and Technology 66 (2006) : 538–547.
- (24) H.C. Chen.; T.Y. Chen.; C.H. Hsu. Effects of Wood Particle Size and Mixing Ratios of HDPE on the Properties of the Composites. Holz als Roh-und Werkstoff 64 (2006) : 172–177.
- (25) John Z. Lu.; Qinglin Wu.; and Ioan I. Negulescu. Wood-Fiber/High-Density-Polyethylene Composites: Coupling Agent Performance. Journal of Applied Polymer Science 96 (2005): 93–102.

- (26) Han-Seung Yang.; Hyun-Joong Kim.; Hee-Jun Park.; Bum-Jae Lee.; and Taek-Sung Hwang. Effect of compatibilizing agents on rice-husk flour reinforced polypropylene composites. Composite Structures 77 (2005) : 45–55.
- (27) John Z.; Lu, Q. Wu.; and I. I. Negulescu. Wood-Fiber/High-Density-Polyethylene Composites: Compounding Process. Journal of Applied Polymer Science 93 (2004):2570-2578.
- (28) X. Colom.; F. Carrasco.; P. Pages.; and J. Canavate. Effects of different treatments on the interface of HDPE/lignocellulosic fiber composites. Composites Science and Technology 63 (2003): 161–169.
- (29) อธิพิพล แจ่มชัด.; ธีรพัฒน์ อุณหโชค.; พจนีย์ ศรธรรมดี.; และวราธรรม คุณจิตติชัย. “การศึกษาไม้เทียมพอลิเมอร์คอมโพสิตจากเส้นใยผักตบชวาและพอลิเอทิลีนความหนาแน่นต่ำที่ใช้พอลิเอทิลีน-กราฟท์-มาลิกแอนไฮไดรด์เป็นสารช่วยผสม”.การประชุมการป่าไม้ประจำปี 2545 ด้านวัสดุทดแทนไม้, วันที่ 18-20 กันยายน 2545, หน้า 29-45.
- (30) S. Panthapulakkal.; S. LAW.; AND M. SAIN. Enhancement of Processability of Rice Husk Filled High-density Polyethylene. Journal of Thermoplastic Composite Materials 18 (2005) : 445.
- (31) M.N. Ichazo.; C. Albano.; J. Gonzalez.; R. Perera.; M.V. Candal. Polypropylene/wood flour composites: treatments and properties. Composite Structure 54 (2001) : 207-214.
- (32) Y. Breton.; and J. J. Robin. Reinforcement of recycled polyethylene with heat treated wood fibers. Journal of Reinforced Plastics and Composites 20 (2001): 1253-1262.
- (33) ASTM D 638 – 03 Standard Test Method for Tensile Properties of Plastics, 2003.
- (34) ASTM D 790 – 03 Standard Test Methods for Flexural Properties of Unreinforced and Reinforced Plastics and Electrical Insulating Materials, 2003.
- (35) ASTM D 256 – 05 Standard Test Methods for Determining the Izod Pendulum Impact Resistance of Plastics, 2005.
- (36) ASTM D 695 – 02a Standard Test Method for Compressive Properties of Rigid Plastics, 2002.

- (37) ASTM D 648 – 04 Standard Test Method for Deflection Temperature of Plastics Under Flexural Load in the Edgewise Position, 2004.
- (38) ASTM D 792 – 00 Standard Test Method for Density and Specific Gravity (Relative Density) of Plastics by Displacement, 2000.
- (39) ASTM D 570-98 Standard Test Method for Water Absorption of Plastics, 1998.
- (40) Michael L. Berins. Plastic Engineering Handbook of the Society of the Plastics Industry. New York : VAN NOSTRAND REINHOLD Inc, 1991.
- (41) Tensile Testing [Online], Available:
http://www.instron.co.th/wa/applications/test_types/tension.aspx
[11 March 2008].
- (42) Flexural Testing [Online], Available:
http://www.instron.co.th/wa/applications/test_types/flexure.aspx
[11 March 2008].
- (43) Compression Testing [Online], Available:
http://www.instron.co.th/wa/applications/test_types/compression.aspx
[11 March 2008].
- (44) Izod Impact Testing [Online], Available:
<http://www.ptli.com/testlopedia/tests/izod-d256-ISO180.asp>
[11 March 2008].
- (45) Izod Impact Testing [Online], Available:
<http://www.matweb.com/reference/izod-impact.aspx> [11 March 2008].
- (46) Classification of composites [Online], Available:
http://www.substech.com/dokuwiki/doku.php?id=classification_of_composites
[13 March 2008].
- (47) Differential scanning calorimetry [Online], Available:
http://en.wikipedia.org/wiki/Differential_scanning_calorimetry
[13 March 2008].
- (48) Dynamic mechanical analysis [Online], Available:
http://en.wikipedia.org/wiki/Dynamic_mechanical_analysis [13 March 2008].
- (49) Thermogravimetric analysis [Online], Available:
http://en.wikipedia.org/wiki/Thermogravimetric_analysis [13 March 2008].
- (50) Heat deflection temperature [Online], Available:
http://en.wikipedia.org/wiki/Heat_deflection_temperature [14 March 2008].

- (51) Scanning Electron Microscope [Online], Available:
http://en.wikipedia.org/wiki/Scanning_Electron_Microscope
[14 March 2008].
- (52) Scanning Electron Microscope [Online], Available:
http://www.sciencedaily.com/articles/s/scanning_electron_microscope.htm
[14 March 2008].
- (53) Scanning Electron Microscope [Online], Available:
<http://www.abdn.ac.uk/emunit/sem.htm> [14 March 2008].
- (54) Attenuated total reflectance [Online], Available:
http://en.wikipedia.org/wiki/Attenuated_total_reflectance [14 March 2008].
- (55) Overview of Materials for High Density Polyethylene (HDPE), Wood Filled
[Online], Available:
<http://www.matweb.com/search/DataSheet.aspx?MatID=78289&ckck=1>
[14 March 2008].
- (56) Hernandez, R. J.; Selke, S. E. M.; and Culter, J. D. Plastics Packaging. Hanser Gardner Publications, 2000.
- (57) Anatole A. Klysov. Wood-Plastic Composites. Wiley Interscience, Inc., 2007 :
95.
- (58) Sookchareon Rice Mill, Ayutthaya, Thailand
- (59) PTT Polymer Marketing Company Limited (PTTPM)
- (60) Bonding energy [Online], Available:
<http://www.cem.msu.edu/~reusch/OrgPage/bndenrgy.htm> [1 May 2008].

APPENDICES

Appendix A

Mechanical Characterizations

Appendix A-1 The tensile modulus of the HDPE/RH composites.

Particle size (μm)	Tensile modulus (GPa)			
	10 %wt	20 %wt	30 %wt	40 %wt
75	0.89 \pm 0.027	1.15 \pm 0.031	1.34 \pm 0.030	1.52 \pm 0.015
180	0.90 \pm 0.034	1.08 \pm 0.044	1.36 \pm 0.024	1.53 \pm 0.017
250	0.94 \pm 0.049	1.09 \pm 0.029	1.36 \pm 0.088	1.59 \pm 0.061
355	0.91 \pm 0.020	1.07 \pm 0.024	1.32 \pm 0.034	1.50 \pm 0.079
500	0.91 \pm 0.039	1.10 \pm 0.097	1.33 \pm 0.025	1.50 \pm 0.057

Tensile modulus of the pure HDPE is 0.75 \pm 0.024 GPa.

Appendix A-2 The tensile strength of the HDPE/RH composites.

Particle size (μm)	Tensile strength (MPa)			
	10 %wt	20 %wt	30 %wt	40 %wt
75	22.60 \pm 0.110	21.19 \pm 0.216	20.60 \pm 0.269	20.42 \pm 0.221
180	22.46 \pm 0.322	21.56 \pm 0.113	20.64 \pm 0.408	20.46 \pm 0.331
250	22.58 \pm 0.154	21.18 \pm 0.149	20.76 \pm 0.080	20.26 \pm 0.249
355	22.56 \pm 0.260	21.30 \pm 0.156	20.80 \pm 0.482	20.43 \pm 0.188
500	22.43 \pm 0.301	21.11 \pm 0.696	20.63 \pm 0.141	20.47 \pm 0.314

Tensile strength of the pure HDPE is 24.48 \pm 0.329 MPa.

Appendix A-3 The flexural modulus of the HDPE/RH composites.

Particle size (μm)	Flexural modulus (GPa)			
	10 %wt	20 %wt	30 %wt	40 %wt
75	0.684 \pm 0.041	0.85 \pm 0.032	1.12 \pm 0.024	1.51 \pm 0.077
180	0.73 \pm 0.026	0.87 \pm 0.024	1.16 \pm 0.030	1.42 \pm 0.074
250	0.74 \pm 0.018	0.88 \pm 0.044	1.13 \pm 0.057	1.51 \pm 0.085
355	0.73 \pm 0.023	0.87 \pm 0.012	1.13 \pm 0.043	1.52 \pm 0.049
500	0.70 \pm 0.030	0.83 \pm 0.032	1.09 \pm 0.054	1.49 \pm 0.094

Flexural modulus of the pure HDPE is 0.52 \pm 0.005 GPa.

Appendix A-4 The flexural strength of the HDPE/RH composites.

Particle size (μm)	Flexural strength (MPa)			
	10 %wt	20 %wt	30 %wt	40 %wt
75	22.17 \pm 0.438	23.47 \pm 0.280	24.16 \pm 0.647	21.77 \pm 0.572
180	22.80 \pm 0.463	23.50 \pm 0.270	24.20 \pm 0.157	21.49 \pm 0.548
250	22.75 \pm 0.179	23.51 \pm 0.177	24.13 \pm 0.504	21.22 \pm 0.450
355	22.98 \pm 0.520	23.74 \pm 0.168	24.58 \pm 0.349	21.67 \pm 0.315
500	22.42 \pm 0.440	23.89 \pm 0.562	24.43 \pm 0.168	21.72 \pm 0.172

Flexural strength of the pure HDPE is 19.83 \pm 0.155 MPa.

Appendix A-5 The compressive modulus of the HDPE/RH composites.

Particle size (μm)	Impact strength (kJ/m^2)			
	10 %wt	20 %wt	30 %wt	40 %wt
75	0.53 \pm 0.018	0.59 \pm 0.014	0.72 \pm 0.015	0.84 \pm 0.025
180	0.53 \pm 0.018	0.60 \pm 0.016	0.73 \pm 0.029	0.83 \pm 0.026
250	0.53 \pm 0.022	0.60 \pm 0.029	0.72 \pm 0.027	0.83 \pm 0.036
355	0.53 \pm 0.037	0.59 \pm 0.020	0.73 \pm 0.025	0.84 \pm 0.027
500	0.53 \pm 0.039	0.60 \pm 0.020	0.74 \pm 0.029	0.84 \pm 0.038

Compressive modulus of the pure HDPE is 0.34 \pm 0.759 GPa.

Appendix A-6 The compressive strength of the HDPE/RH composites.

Particle size (μm)	Impact strength (kJ/m^2)			
	10 %wt	20 %wt	30 %wt	40 %wt
75	44.49 \pm 0.423	42.64 \pm 0.299	40.30 \pm 0.502	37.24 \pm 0.451
180	44.57 \pm 0.322	42.52 \pm 0.376	40.45 \pm 0.558	37.29 \pm 0.503
250	44.47 \pm 0.519	42.46 \pm 0.250	40.15 \pm 0.492	37.39 \pm 0.293
355	44.53 \pm 0.274	42.42 \pm 0.288	40.31 \pm 0.595	37.56 \pm 0.219
500	44.43 \pm 0.350	42.54 \pm 0.375	40.27 \pm 0.636	37.39 \pm 0.282

Compressive strength of the pure HDPE is 48.11 \pm 0.023 MPa.

Appendix A-7 The notched Izod impact strength of the HDPE/RH composites.

Particle size (μm)	Impact strength (kJ/m^2)			
	10 %wt	20 %wt	30 %wt	40 %wt
75	12.27 \pm 0.155	11.43 \pm 0.079	10.81 \pm 0.205	10.25 \pm 0.252
180	13.05 \pm 0.151	12.17 \pm 0.350	11.85 \pm 0.187	11.16 \pm 0.127
250	13.65 \pm 0.208	13.01 \pm 0.343	12.31 \pm 0.210	11.89 \pm 0.376
355	13.91 \pm 0.064	13.26 \pm 0.119	12.85 \pm 0.237	12.04 \pm 0.186
500	14.34 \pm 0.100	13.82 \pm 0.073	13.01 \pm 0.176	12.23 \pm 0.062

Notched Izod impact strength of the pure HDPE is 15.47 \pm 0.243 kJ/m^2 .

Appendix A-8 The tensile modulus and tensile strength of the HDPE/RH composites at 30% by weight of 500 μm RH particle treated with PE-g-MA from 0 to 7% by weight.

PE-g-MA Content (wt %)	Tensile modulus (GPa)	Tensile strength (MPa)
1	1.34 \pm 0.028	22.47 \pm 0.276
3	1.35 \pm 0.009	22.46 \pm 0.236
5	1.36 \pm 0.016	22.90 \pm 0.394
7	1.37 \pm 0.020	22.41 \pm 0.168

Appendix A-9 The flexural modulus and flexural strength of the HDPE/RH composites at 30% by weight of 500 μm RH particle treated with PE-g-MA from 0 to 7% by weight.

PE-g-MA Content (wt %)	Flexural modulus (GPa)	Flexural strength (MPa)
1	1.17 \pm 0.011	28.81 \pm 0.350
3	1.17 \pm 0.019	29.67 \pm 0.428
5	1.22 \pm 0.049	30.69 \pm 0.299
7	1.19 \pm 0.059	29.42 \pm 0.321

Appendix A-10 The compressive modulus and compressive strength of the HDPE/RH composites at 30% by weight of 500 μm RH particle treated with PE-g-MA from 0 to 7% by weight.

PE-g-MA Content (wt %)	Compressive modulus (GPa)	Compressive strength (MPa)
1	0.74 \pm 0.042	41.80 \pm 0.186
3	0.75 \pm 0.046	42.25 \pm 0.176
5	0.78 \pm 0.074	42.91 \pm 0.317
7	0.79 \pm 0.039	42.16 \pm 0.497

Appendix A-11 The impact strength of the HDPE/RH composites at 30% by weight of 500 μm RH particle treated with PE-g-MA from 0 to 7% by weight.

PE-g-MA Content (wt %)	impact strength (kJ/m²)
1	15.41 \pm 0.124
3	15.63 \pm 0.249
5	16.06 \pm 0.364
7	15.70 \pm 0.438

Appendix B

Physical Characterizations

Appendix B-1 The density of the HDPE/RH composites.

Particle size (μm)	Density (kg/m^3)			
	10 %wt	20 %wt	30 %wt	40 %wt
75	0.989 \pm 0.002	1.036 \pm 0.001	1.077 \pm 0.004	1.119 \pm 0.002
180	0.988 \pm 0.001	1.023 \pm 0.001	1.063 \pm 0.002	1.107 \pm 0.002
250	0.987 \pm 0.001	1.023 \pm 0.001	1.059 \pm 0.001	1.104 \pm 0.003
355	0.985 \pm 0.003	1.019 \pm 0.001	1.053 \pm 0.001	1.099 \pm 0.000
500	0.985 \pm 0.002	1.019 \pm 0.002	1.052 \pm 0.002	1.098 \pm 0.002

Density of the pure HDPE is 0.947 \pm 0.0008 kg/m^3 .

Appendix B-2 The water absorption of the HDPE/RH composites.

Particle size (μm)	Water absorption (%)			
	10 %wt	20 %wt	30 %wt	40 %wt
75	0.474 \pm 0.010	0.950 \pm 0.028	2.305 \pm 0.112	5.423 \pm 0.067
180	0.528 \pm 0.002	0.915 \pm 0.048	1.985 \pm 0.040	5.319 \pm 0.007
250	0.535 \pm 0.091	1.082 \pm 0.095	2.011 \pm 0.008	5.278 \pm 0.087
355	0.548 \pm 0.025	0.925 \pm 0.091	2.153 \pm 0.015	5.113 \pm 0.026
500	0.513 \pm 0.018	1.062 \pm 0.113	2.081 \pm 0.079	5.371 \pm 0.007

% Water absorption of the pure HDPE is 0.061 \pm 0.027.

VITA

Mr. Sirapat Chanakul was born in Krabi, Thailand on April 07, 1983. He graduated at high school level from Phuket Wittayalai School in 2001 and received Bachelor degree from the Department of Chemical Engineering, Faculty of Engineering, Prince of Songkhla University, Thailand in 2005. He continued his study for a Master's Degree in Chemical Engineering at the Department of Chemical Engineering, Faculty of Engineering, Chulalongkorn University.